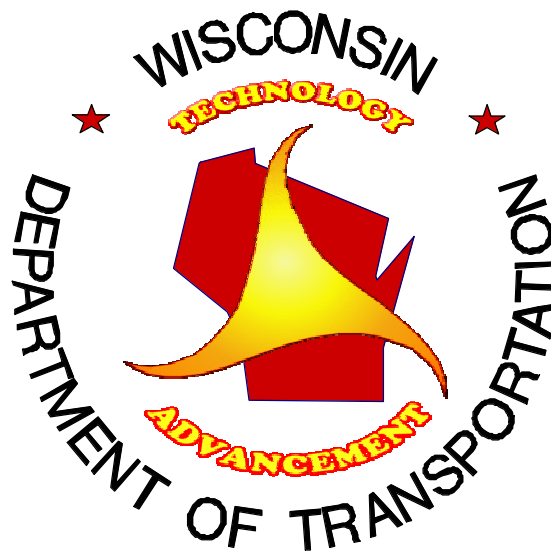


REPORT NUMBER: WI/SPR-07-01

CHARACTERIZATION OF SIMPLE AND COMPLEX CRUMB RUBBER MODIFIED BINDERS

FINAL REPORT



JULY 2000

1. Report No. WI/SPR-07-01	2. Government Accession No.	3. Recipients Catalog No.	
4. Title and Subtitle Characterization of Simple and Complex Crumb Rubber Modified Binders		5. Report Date July 2000	
		6. Performing Organization Code	
7. Author(s) Ssu-Wei Loh, Research Assistant Sohee Kim, Research Assistant H.U. Bahia, Assistant Professor		8. Performing Organization Report No.	
9. Performing Organization Name and Address University of Wisconsin - Madison Department of Civil and Environmental Engineering 1415 Engineering Drive, Madison, WI 53706-1490		10. Work Unit No. (TRAIS)	
		11. Contract or Grant No. # 0687-45-14	
12. Sponsoring Agency Name and Address Wisconsin Department of Transportation Division of Transportation Infrastructure Development Bureau of Highway Construction Technology Advancement Unit 3502 Kinsman Blvd., Madison, WI 53704-2507		13. Type of Report and Period Covered Final Report; 1998-2000	
		14. Sponsoring Agency Code WisDOT Study # 98-06	
15. Supplementary Notes			
16. Abstract <p>This research focused on the evaluation of using crumb rubber modifier (CRM) in asphalt binders. The increasing usage of CRM in asphalt pavements requires a better understanding of the physical, chemical, and rheological properties of CRM so that its performance in the field can be more accurately predicted. The existing literature regarding CRM in asphalt binders has been focused on using either conventional binder testing procedures or the Superpave binder testing protocol. It is believed that Superpave binder specifications cannot be extended to all modified binders, since certain simplifications are used in the current specification that cannot estimate their contribution to pavement performance under different traffic and pavement structure conditions. Therefore the benefits of using crumb rubber for modification of asphalt needs more detailed evaluation using an extended set of testing methods.</p> <p>This report shows the results of the binder testing and analysis of these results to quantify the effects of size and concentration of CRM on critical binder properties related to construction and performance of HMA in pavements. The evaluation was conducted by measuring the change in performance-related properties of the selected asphalt binders as a result of mixing various levels of CRM content and particle with asphalts. Testing was conducted at different temperatures, testing frequencies, and strain conditions using methods recently developed as part of the NCHRP 9-10 project (Superpave Protocols for Asphalt Binders). Statistical analysis was used to develop models that predict the nature of effects on the performance-related properties of asphalts and that can quantify the role of different variables.</p> <p>The results of the research indicate that the inclusion of crumb rubber does affect some of the properties of the asphalt binder, and that the effects differ based on the size and concentration of crumb rubber added. It was found that the viscosity of asphalt binders increase when there is an increased concentration of crumb rubber, and when the size of the crumb rubber used is decreased. It was also found that crumb rubber modified asphalt binders have increased dependency on mechanical working, higher strain dependency, increased strain at failure, and increased stress at failure. On the mixture end, it was found that the belief that crumb rubber modification of asphalt binders would results in a rebound effect, or increase in mix volume, was unfounded. The presence of crumb rubber modifier did affect the amount of air voids and the frictional resistance of a mixture. The effects were, however, dependent on the stage of densification, and were also influenced by other material characteristics in some cases.</p>			
17. Key Words Crumb rubber, crumb rubber modifier, CRM, asphalt binders, crumb rubber binders, crumb rubber mixtures		18. Distribution Statement	
19. Security Classif. (of this report)	19. Security Classif. (of this page)	21. No. of Pages	22. Price

CHARACTERIZATION OF SIMPLE AND COMPLEX CRUMB RUBBER MODIFIED BINDERS

FINAL REPORT WI/SPR-07-01
WisDOT Highway Research Study # 98-06
SPR # 0687-45-14

by

Ssu-Wei Loh, Research Assistant
Sohee Kim, Research Assistant
H. U. Bahia, Assistant Professor

University of Wisconsin – Madison
Department of Civil and Environmental Engineering
1415 Engineering Drive, Madison, WI 53706-1490

for

WISCONSIN DEPARTMENT OF TRANSPORTATION
DIVISION OF TRANSPORTATION INFRASTRUCTURE DEVELOPMENT
BUREAU OF HIGHWAY CONSTRUCTION
TECHNOLOGY ADVANCEMENT UNIT
3502 KINSMAN BLVD., MADISON, WI 53704-2507

Study Manager
Deb Bischoff, Technology Advancement Engineer

JULY 2000

The Technology Advancement Unit of the Division of Transportation Infrastructure Development, Bureau of Highway Construction, conducts and manages the highway technology advancement program of the Wisconsin Department of Transportation. The Federal Highway Administration provides financial and technical assistance for these activities, including review and approval of publications. This publication does not endorse or approve any commercial product even though trade names may be cited, does not necessarily reflect official views or policies of the agency, and does not constitute a standard, specification or regulation.

TABLE OF CONTENTS

CHAPTER 1: INTRODUCTION	1
1.1 Background.....	1
1.2 Problem Statement	2
1.3 Organization of Report	3

PART I: CRUMB RUBBER BINDERS

CHAPTER 2: BINDER TESTS	4
2.1 Study Objectives	4
2.2 Experimental Matrix	4
2.3 Methods of Statistical Analysis	6
 CHAPTER 3: LABORATORY EVALUATION	 8
3.1. Rheological Measurements	8
3.2. Analysis of Results	10
3.2.1. Effect of Size and Concentration on Results of Particulate Additive Test (PAT)	10
3.2.2. Viscosity-Temperature Relationship	11
3.2.3. Statistical Analysis for Viscosity Tests	16
3.2.4. Statistical Analysis for Critical Temperature for Viscosity	20
3.3. Mechanical Working Dependency Evaluation	22
3.3.1. Statistical Analysis for Mechanical Working Dependency	27
3.4. Strain Dependency Evaluation.....	35

3.4.1. Effect of Strain Dependency and Geometry Dependency on Rheological Properties.....	37
3.4.2. Statistical Analysis for Strain Dependency.....	39
3.5. Effect of Testing Frequency at High, Intermediate, and Low Temperature, and Loading Time.....	47
3.5.1. Statistical Analysis for Frequency Sweep.....	53
3.5.2. Low Temperature Failure Properties of CRM Binders	63
3.6. Laboratory Asphalt Stability Test (LAST).....	68
3.6.1. Analysis of Separation Results	69
3.6.2. Analysis of the Degradation Results	73
CHAPTER 4: SUMMARY OF FINDINGS OF PART I	76
4.1 Summary of Findings.....	76
4.1.1 Viscosity Results.....	76
4.1.2 Particulate Additive Test Results.....	77
4.1.3 Mechanical Working Dependency Results	78
4.1.4 Strain Dependency Results	78
4.1.5 Frequency Testing at High and Intermediate Temperatures.....	79
4.1.6 Creep and Direct Tension Testing at Low Temperature	80
4.1.7 Storage Stability Test Results	82
4.2 Summary for Construction Applications	83
4.3 Limitations of Current Research and Suggested Future Work.....	83

PART II: CRUMB RUBBER MIXTURES

CHAPTER 5: MIXTURE TESTING	85
5.1 Study Objectives	85
5.2 Experimental Testing Plan	86
 CHAPTER 6: TEST PROCEDURES	 90
6.1 Mixing and Compaction	90
6.2 Rebound Effects of Crumb Rubber Modified Mixtures	90
6.3 Frictional Resistance Measured Using a Gyratory Load-Cell Plate Assembly (GLPA)	94
 CHAPTER 7: ANALYSIS OF RESULTS AND DISCUSSION	 97
7.1 Results of Volume Change	97
 CHAPTER 8: ANALYSIS OF DENSIFICATION CURVES.....	 103
8.1 Initial Packing of Mixtures	104
8.2 Air Voids at Ninitial (N=8)	106
8.3 Air Voids at Ndesign (N=100)	107
8.4 Air Voids at Nmaximum (N=160)	109
8.5 Terminal Density of Mixtures	111
8.6 Summary of the Effect of CRM on Air Void Content.....	112
8.7 Statistical Analysis of Air Void Results	113

CHAPTER 9: ANALYSIS OF FRICTIONAL RESISTANCE 120

9.1 Initial Resistance to Deformation.....	122
9.2 Frictional Resistance of Mixes at Nini (N=8)	125
9.3 Statistical Analysis of Construction Stage of Compaction.....	128
9.4 Frictional Resistance at Ndesign (N=100).....	131
9.5 Frictional Resistance at Nmaximum (N=160).....	134
9.6 Statistical Analysis of Performance Stage of Compaction.....	137
9.7 Frictional Resistance at N=600	140
9.8 Maximum Frictional Resistance.....	143
9.9 Statistical Analysis of Failure Stage of Compaction	146
9.10Summary of the Effect of Crumb Rubber on Frictional Resistance	148

CHAPTER 10: SUMMARY OF FINDINGS OF PART II..... 150

10.1Rebound Effects of Crumb Rubber Modified Mixes.....	150
10.2Crumb Rubber Effects on Densification Characteristics of Asphalt Mixtures	151
10.2.1 During the Construction Stage.....	151
10.2.2 During the Performance Stage of the Pavement Life	152
10.2.3 During the Terminal Stage of Pavement Life	152
10.3Crumb Rubber Effects on the Frictional Resistance of Mixtures	153
10.3.1 During the Construction Stage.....	153
10.3.2 During the Performance Stage	153
10.3.3 During the Failure Stage of the Pavement's Service Life.....	154
10.4Limitations of Research and Suggested Future Work	154

CHAPTER 11: SUMMARY OF PROJECT	156
11.1Overall Summary	156
11.1Summary of Construction Applications	158
 REFERENCES.....	 160

LIST OF TABLES

Table 2.2.1: Experimental Matrix for Binding Test	5
Table 3.2.1: Results of Particulate Additives Test	10
Table 3.2.2 : Analysis of Variance : Log (Viscosity)	18
Table 3.3.1 : Statistical Models for Estimation of the normalized G^*_n ratio for Mechanical Working Dependency.....	30
Table 3.3.2 : Statistical Models for Estimation of the Normalized δ_n Ratio for the Mechanical Working Dependency.....	34
Table 3.4.1: Statistical Models for Estimation of the Normalized G^*_n Ratio for Strain Dependency.....	43
Table 3.4.2: Statistical Models for Estimation of the normalized δ_n ratio for Strain Dependency	46
Table 3.5.1: Statistical Models for Estimation of the G^* ratio for Frequency sweep	57
Table 3.5.2: Statistical Models for Estimation of the δ ratio for Frequency sweep	62
Table 3.5.3: Results of Direct Tension Test	64
Table 3.6.1: LAST Test Results - Separation	70
Table 3.6.2: LAST Test Results - Degradation	73
Table 5.2.1 Mixture Control Variables	86
Table 5.2.2 Mix Design.....	87
Table 5.2.3 Mixture Compaction Test Matrix	88
Table 8.0.1 Air Void Content of Specimen During Compaction.....	104

Table 8.7.1 Statistical Model for Air Voids at N=2	114
Table 8.7.2 Statistical Model for Air Voids at N=8	115
Table 8.7.3 Statistical Model for Air Voids at N=100	117
Table 8.7.4 Statistical Model for Air Voids at N=160	118
Table 8.7.5 Statistical Model for Air Voids at N=600	119
Table 9.0.1 Frictional Resistance (units are kPa) of Specimens During Compaction	122
Table 9.3.1 Statistical Model for Frictional Resistance at N=2	128
Table 9.3.2 Statistical Model for Frictional Resistance at N=8	129
Table 9.6.1 Statistical Model for Frictional Resistance at N=100.....	138
Table 9.6.2 Statistical Model for Frictional Resistance at N=160.....	139
Table 9.9.1 Statistical Model for Frictional Resistance at N=600.....	146
Table 9.9.2 Statistical Model for Frictional Resistance when FR is Maximum.....	147

LIST OF FIGURES

Figure 3.2.1: Comparison of Viscosity-Shear Rates	13
Figure 3.2.2: Critical Temperature and Viscosity Ratio Versus binder Type	14
Figure 3.2.3: Comparison of Viscosity-Shear Rates for Binders with Reacted Rubber	15
Figure 3.2.4: Critical Temperature and Viscosity Ratio Versus Binder Type for Binders with Reacted Rubber	15
Figure 3.2.5: Box plots for concentration, temperature, RPM, binder, and size vs log (viscosity)	17
Figure 3.2.6: Interaction among binder types, concentration and shear rate vs log (viscosity)	19
Figure 3.2.7: Box plots for sheer rate, binder, size and concentration vs critical temperature for viscosity	21
Figure 3.3.1: Effect of repeated loading at 10% & 42% Strain on G^* and δ ratio at HT	24
Figure 3.3.2: Effect of repeated loading at 1% & 10% Strain on G^* and δ ratio at IT	25
Figure 3.3.3: Time sweep with different strain levels for AC 10 and AC 20	26
Figure 3.3.4: The box plots for G^*_n ratio ($G^*_{\text{rubber 50/5000}}/G^*_{\text{unmodified 50/5000}}$) vs binder, size, concentration, and strain	28
Figure 3.3.5: Interaction effects when G^* ratio (50/5000) is selected as a response variable	31
Figure 3.3.6: The box plots for δ_n ratio ($\delta_{\text{rubber 50/5000}}/\delta_{\text{unmodified 50/5000}}$) vs binder, size, concentration, and strain	32
Figure 3.4.1: G^* and δ ratios (%) measured from strain sweeps at HT & IT	36
Figure 3.4.2: Effect of the plates for PG 70-22 with Different Concentrations of CRM	38

Figure 3.4.3: The box plots for G^* ratio ($G^*_{\text{rubber ratio}}/G^*_{\text{unmodified ratio}}$) vs plate, binder, size, concentration, replicate, and temperature	41
Figure 3.4.4: Interaction effects when the normalized G^*_n ratio is selected as a response variable	44
Figure 3.4.5: The box plots for δ ratio ($\delta_{\text{rubber ratio}}/\delta_{\text{unmodified ratio}}$) vs plate, binder, size, concentration, replicate, and temperature	45
Figure 3.5.1: Effect of Crumb Rubber Particle Size and Concentration on Variation of Critical Temperature with Testing Frequency	50
Figure 3.5.2: Effect of Crumb Rubber Particle Size and Concentration on Variation of Critical Temperature for $S(t)$ with Loading Time (sec)	51
Figure 3.5.3: Effect of Crumb Rubber Particle Size and Concentration on Variation of Critical Temperature for m-value with Loading Time (sec)	52
Figure 3.5.4: The box plots for the G^* ratio ($G^*_{\text{rubber}}/G^*_{\text{unmodified}}$) vs temperature, frequency, binder, size, concentration and aging	55
Figure 3.5.5: Interaction effects when the G^* ratio is selected as a response variable	58
Figure 3.5.6: The box plots for δ ratio ($\delta_{\text{rubber}}/\delta_{\text{unmodified}}$) vs temperature, frequency, binder, size, concentration and aging	61
Figure 3.5.7(a): Effect of Temperature	66
Figure 3.5.7(b): Failure strain at -12 °C with the rate of 3%/min strain	66
Figure 3.5.7(c) : Failure stress at -12 °C with the rate of 3%/min strain	66
Figure 3.5.8(a) : Effect of cooling rate on stress	67
Figure 3.5.8(b) : Effect of cooling rate on strain	67

Figure 3.6.1: The box plots for the external without agitation (separation ratio) at HT vs frequency, binder, size, and concentration.....	72
Figure 5.2.1 Aggregate Gradation on 0.45 Power Chart.....	87
Figure 6.2.1 Modified Calipers for Dimension Measurements	91
Figure 6.2.2 Jaw of Calipers Attached with Metal Plates	91
Figure 6.2.3 Locations Where Measurements are Taken are Marked on the Compacted Specimen	92
Figure 6.2.4 Measurement of Diameter Taken Using the Modified Calipers	93
Figure 6.3.1 Sketch of Gyrotory Load Cell Plate Assembly.....	94
Figure 6.3.2 Varying Frictional Resistance for Different Mix Types	95
Figure 7.1.1 (a) Volume Change – Coarse Gradation Gravel Specimens	99
Figure 7.1.1 (b) Volume Change – Fine Gradation Gravel Specimens	99
Figure 7.1.1 (c) Volume Change – Coarse Gradation Crushed Aggregate Specimens.....	100
Figure 7.1.1 (d) Volume Change – Fine Gradation Crushed Aggregate Specimens	100
Figure 7.1.2 Boxplots of Volume Change	102
Figure 8.1.1 Differential Air Voids of Mixes at N=2.....	105
Figure 8.2.1 Differential Air Voids of Mixes at Nini.....	107
Figure 8.3.1 Differential Air Voids of Mixes at N=100 (Ndes).....	109
Figure 8.4.1 Differential Air Voids of Mixes at N=160 (Nmax).....	110
Figure 8.5.1 Differential Air Voids of Mixtures at N=600.....	112
Figure 9.0.1 Typical Chart Generated from Gyrotory Load Cell Plate Assembly	121
Figure 9.1.1 Frictional Resistance of Mixes at N=2.....	123
Figure 9.1.2 Boxplots of Frictional Resistance at N=2	124

Figure 9.2.1 Frictional Resistance of Mixes at Nini (N=8)	125
Figure 9.2.2 Boxplots of Frictional Resistance at N=8	126
Figure 9.4.1 Frictional Resistance of Mixes at Ndes (N=100)	132
Figure 9.4.2 Boxplots of Frictional Resistance at N=100	133
Figure 9.5.1 Frictional Resistance of Mixes at Nmax (N=160)	134
Figures 9.5.2 Boxplots of Frictional Resistance at N=160	136
Figure 9.7.1 Frictional Resistance in Mixes at N=600	141
Figure 9.7.2 Boxplots of Frictional Resistance at N=600	142
Figure 9.8.1 Maximum Frictional Resistance	144
Figure 9.8.2 Boxplots of Maximum Frictional Resistance	145

CHAPTER 1 : INTRODUCTION

1.1 Background

Crumb Rubber is recycled rubber that is obtained by mechanical shearing or grinding tires into small particle sizes less than 6.3mm (1/4"). It is one of the modifiers researched by pavement engineers for many years. The Federal Highway Administration (FHWA) has been involved in research related to Crumb Rubber Modifier (CRM) since the beginning of the 1970's, and CRM was first introduced into hot-mix asphalt concrete (HMAC) in 1975. Increasing interests in the use of recycled materials has led to a broadened use of CRM in asphalt mixtures. Increasing interests has also encouraged an expansion in the asphalt rubber industry. The Intermodal Surface Transportation Efficiency Act (ISTEA) included a mandate of recycling used tires in 1991. However due to a lack of data to evaluate the use of CRM in asphalt pavements, the pavement industry and State agencies are still raising questions as to what types of CRM to use, how to use them and how to construct pavements utilizing CRM.

A few studies on the effects of CRM in asphalt pavements have shown that the method of production of CRM has significant effects on the properties of rubber asphalts. Research indicates that the size, shape and texture of CRM are key factors that may affect the pavement performance. The suitability of crumb rubber modifier in asphalt pavement has been determined by the improvement of performance over conventional additives and its economic assessment. Previous research has shown that increasing the amount of crumb rubber content increases the viscosity of the modified asphalt binder. In addition, some studies indicate that the use of CRM in asphalt would result in improved resistance to permanent deformation, fatigue failure, and thermal cracking. Although significant research

regarding the use of CRM has been performed and some of these CRM modified mixtures indicated outstanding improvement over conventional mixes, the improvement in mechanical properties of CRM modified mixes have not been clearly proven.

The increasing usage of CRM binders in asphalt pavements requires a better understanding of their effects on the physical, chemical, and rheological properties of CRM so that its performance in the field can be more accurately predicted. This study is conducted to allow a determination of the effect of particle size and content on the low, intermediate and high temperature properties of CRM binders, as well as some mixture properties, using the methods recently developed as part of the NCHRP 9-10 project. The objective of the NCHRP 9-10 project, sponsored by the National Cooperative for Highway Research Program, was to evaluate the suitability of using the Superpave binder and mixture test systems for modified asphalt binders. These methods represent an extension of the methods originally developed for the Superpave system and also include methods for evaluation of storage stability.

The focus in this research is asphalt binder modified with varying grades of crumb rubber, which was excluded in the NCHRP 9-10 research. This report is prepared to represent the results of binder testing and analysis of these results to quantify the effects of size and concentration of CRM on critical binder properties related to construction and performance of HMA in pavements.

1.2 Problem Statement

The existing literature regarding CRM in asphalt binders has been focused on using either conventional binder testing procedures or the existing Superpave binder testing

protocol. These procedures were developed for simple binders that do not include solid additives like crumb rubber. CRM binders can be rheologically complex. It is believed that Superpave binder specifications cannot be extended to all modified binders, since there are certain simplifications used in the current specification that cannot estimate their contribution to pavement performance under different traffic and pavement structure conditions.

Because of this complexity, the benefits of using crumb rubber for modification of asphalt binders are uncertain and needs more detailed evaluation using an extended set of testing methods.

1.3 Organization of Report

This research covers both binder and mixture tests, and the report is made up of two parts. Part one discusses the tests performed, the results obtained, and the analysis of CRM binders. Part two discusses the tests, results, and analysis of CRM mixtures.

CHAPTER 2 : BINDER TESTS

2.1 Study Objectives

The main objectives of this research are to determine the properties of CRM asphalt produced with different CRM size and concentration as related to the following characteristics:

1. Workability at production and construction temperatures
2. Storage stability under field-simulated conditions
3. Strain dependency and effect of mechanical working at selected conditions
4. Rheological and damage behavior at high, intermediate and low pavement temperatures.

2.2 Experimental Matrix

There are two phases to the binder testing plan. The first is to qualify the modified binders as either simple or complex systems. This phase includes determining the volume of particulate material larger than 0.075 mm and evaluating the storage stability, and measuring the strain dependency and the thixotropy of the binders. The results were used to quantify the relative importance of the size and concentration on these properties under various conditions of testing. Phase two includes the rheological and failure characterization of the binder before and after short term and long term aging. These aging conditions involve Rolling Thin Film Oven (RTFO) aging and Pressure Aging Vessel (PAV) aging of the modified binders. The measurement were collected using the dynamic shear rheometer to conduct frequency sweep tests at the unaged, RTFO-aged, and PAV-aged conditions of the

binder at high and intermediate temperatures. The bending beam rheometer and the direct tension test were used to measure properties at low pavement temperature.

The study was broken into a matrix of three gradations of rubber, two concentrations of rubber and two sources of base asphalt. Crumb rubber was mixed with two base asphalts of performance grades PG 70-22 and PG 64-22. The PG 70-22 binder came from a Boscan source while the PG 64-22 came from a West Texas Blend source. Varying grades of asphalt binders resulted from the blending of these 2 base asphalt binders with 3 grades of crumb rubber modifier at 2 rubber contents. In addition to these binders, 2 binders modified with reacted crumb rubber using a patented process were received from FHWA and also tested in the study. These FHWA samples were not included in the statistical analysis. Table 2.2.1 shows the experimental matrix and resulting PG grades of the binders obtained. The GF number represents the nominal maximum sieve size of the rubber.

Table 2.2.1 Experimental Matrix for Binder Test

Base Asphalt	GF 40		GF 80		GF 200		FHWA binders
	8% CRM	12% CRM	8% CRM	12% CRM	8% CRM	12% CRM	6% CRM
PG 70-22	PG 76-22 (1B4L)	PG 82-22 (1B4H)	PG 76-22 (1B8L)	PG 82-22 (1B8H)	PG 76-22 (1B2L)	PG 82-22 (1B2H)	AC 20
PG 64-22	PG 76-22 (2T4L)	PG 82-22 (2T4H)	PG 76-22 (2T8L)	PG 82-22 (2T8H)	PG 76-22 (2T2L)	PG 82-22 (2T2H)	AC 10

Note: 1B = Boscan 70-22; 2T = Texas Blend 64-22
 4 = 40 mesh size; 8 = 80 mesh size; 2 = 200 mesh size
 L = low concentration; H = high concentration

The following are the control variables chosen for the testing plan:

- Asphalt source : 2 levels (Boscan, West Texas Blend)
- Crumb rubber particle size : 3 levels (GF 200, 40 and 80)

- Crumb content : 2 levels (8%, 12%)
- Sample geometry : 2 level (parallel, cone plate)
- Strain level : Test at 2 % and 50 % at high temperature

Test at 0.2 % and 20 % at intermediate temperature

- Mechanical working : Conduct time sweeps for 5000 cycles
- Frequency of loading : Conduct frequency sweep from 0.15 Hz to 30 Hz
- Aging Condition : 2 level ; MRTFO, PAV
- Storage stability : sample top and bottom and test at 0, 12, 24 Hrs
- Viscosity : Test at 105 °C, 135 °C, and 165 °C, at each temperature, shear rate
5, 20, 50, and 100 rpm is applied
- Number of replicate measurements : 2 replicates for each measurement

2.3 Methods of Statistical Analysis

Conventional analysis of results (ANOVA) techniques were used to evaluate whether any of the independent variables had an effect on the response variables. The following model was used to apply the ANOVA technique to a table of test results:

$$X_{ijk} = \mathbf{m} + \mathbf{a}_i + \mathbf{b}_j + (\mathbf{ab})_{ij} + \mathbf{e}_{ijk} \quad \mathbf{e}_{ijk} \sim N(0, \mathbf{s}^2)$$

X_{ijk} = k-th observation of the I-th row of the j-th column for all replicates

\mathbf{m} = the overall or grand mean of X_{ijk} values for all rows and columns in the analysis

\mathbf{a}_i = row effect of i-th row

\mathbf{b}_j = column effect j-th column

$(\mathbf{ab})_{ij}$ = interaction between i-th row and j-th column

\mathbf{e}_{ijk} = the experimental chance error in the k-th observation in the i-th row and the j-th column

Two way ANOVA was performed using the following hypothesis tests:

For row means :

$H_0 : \mathbf{a}_i = 0$ for all rows,

$H_a : \mathbf{a}_i$ are not equal to zero,

For column means :

$H_0 : \mathbf{b}_j = 0$ for all rows,

$H_a : \mathbf{b}_j$ are not equal to zero,

For interaction between rows and columns :

$H_0 : (\mathbf{ab})_{ij} = 0$ for all rows and columns,

$H_a : (\mathbf{ab})_{ij}$ are not equal for rows and columns.

In these tests, H_0 is the null hypothesis to be accepted or rejected. If H_0 is rejected, then H_a is accepted.

CHAPTER 3 : LABORATORY EVALUATION

3.1 Rheological Measurements

The effects of crumb rubber on rheological properties of asphalt materials were investigated using different types of rheological measurements. The tests are briefly discussed as follows.

1) Dynamic Shear Rheometer (DSR)

The Dynamic Shear Rheometer is used to characterize the rheological properties of the binders before and after the addition of CRM. It was used to characterize the binders under three aging conditions: in their original stage, after aging in the rolling thin film oven (RTFO) and after aging in the pressure aging vessel (PAV). The DSR was used for testing at high and intermediate temperatures. There are three different geometries used for the binder's evaluation : 25-mm diameter parallel plates, 8-mm diameter parallel plates, and 25-mm cone-plate geometry. The DSR was used to conduct frequency sweeps, strain sweeps and time sweeps. These test procedures are described in appendix A.

2) Bending Beam Rheometer (BBR)

The bending beam rheometer was used for measuring creep behavior at low pavement temperatures. The bending beam rheometer was used to measure creep stiffness $S(t)$ and creep rate $m(t)$ for 8 and 240-second loading intervals. The test was conducted at two aging condition, after aging in the RTFO and after aging the PAV. The test was conducted in duplicate and the average was calculated from the two values.

3) Brookfield Rotational Viscometer

Viscosities of the modified binders were obtained by using the Brookfield Rotational Viscometer at three different temperatures (105 °C, 135°C, and 165°). At each temperature, shear rates of 5, 20, 50, and 100 RPM were applied.

4) Direct Tension Tester (DTT)

The direct tension test measures the low temperature ultimate tensile strain and stress to failure of an asphalt binder. The test was performed at temperatures ranging from –6 °C to –18 °C. The temperatures were chosen such that the range was within which asphalt exhibited brittle behavior. The levels of strain rate were chosen at 0.3%/min and 3%/min, following current recommendation associated with using this device.

5) Particulate Additives Test (PAT)

The test measures the separation of and the determination of the effective packed volume of particulate additives in asphalt binders. This test allows separation of particles with maximum dimension equal to or greater than 75 µm after dissolving the binder in an organic fluid.

6) Storage Stability Test (LAST)

This test measures the separation and degradation of modified binders during storage at 165°C in the laboratory under inert conditions. The test is conducted under static conditions and agitated conditions for 48 hours. This separation and/or degradation is measured using the DSR at selected frequency and temperature conditions.

3.2 Analysis of Results

3.2.1 Effect of Size and Concentration on Results of the Particulate Additives Test

(PAT)

The purpose of the PAT is to determine the volume of particle material greater than 75 μm present in the asphalt. A sample is dissolved in hot organic solvent, then filtered, and the residue is oven-dried and the packed volume determined. The concern is that a high volume of particle additives in the asphalt binder needs to be detected because it may affect the mixture performance when used.

PAT has been performed on the PG 70-22 binders using Toluene and Octane as solvents.

Table 3.2.1: Results of Particulate Additives Test

Binder	Crumb Rubber	Toluene	Octane
PG 70-22	8% GF 40	6.5 %	9.7 %
PG 70-22	8% GF 80	8.6 %	26.5 %
PG 70-22	8% GF 200	9.8 %	21.6 %
PG 70-22	12 % GF 40	13.5 %	24.1 %
PG 70-22	12 % GF 80	10.8 %	13.9 %
PG 70-22	12 % GF 200	12.3 %	15.5 %

The results show that Toluene is more effective in measuring the volume concentration of the crumb rubber. The results obtained using Octane is questionable because of the high values obtained in many occasions. The high values are believed to be caused by perception of the asphaltenes with the rubber during the test. It is also observed that results are dependent on the rubber size. The variation between volume extracted and assumed is expected due to possible variability during sampling of modified binders. Based

on these results, it is concluded that all CRM modified binders contain a relatively large amount of particulate rubber that can interfere with mixture performance. It is hypothesized that rubber particles undergo certain amounts of swelling and this results in a large volume of residue. The rubber is not dissolving in asphalt. The results clearly indicate that the PAT test can detect the rubber particles and gives adequate evidence of the use of rubber.

3.2.2 Viscosity-Temperature Relationship

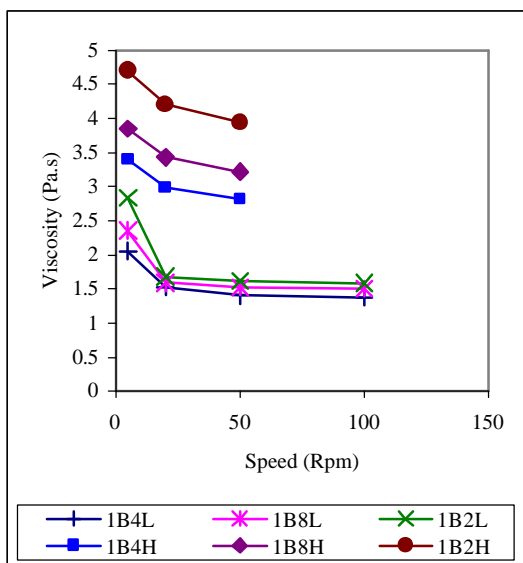
Viscosities of the modified binders were obtained using the Brookfield Rotational Viscometer, measured at temperatures of 105 °C, 135 °C, and 165 °C. At each temperature, shear rates of 5, 20, 50, and 100 rpm were applied. Figures 3.2.1 and 3.2.2 summarize the results from the tests performed at 135 °C and 165 °C. The results from the tests performed at 105 °C could not be charted as testing at shear rates of 100 rpm and occasionally 50 rpm resulted in immeasurable values. Figure 3.2.1 shows the comparison of viscosity-shear rates with different combination of concentration, size, and binder. From this figure, we can determine that there is an obvious effect caused by the different concentration of crumb rubber. It is also observed that temperature and binder source have important effect on viscosity. The general trends observed are as follows:

- All binders are shear rate dependent. Higher rubber concentrations result in higher shear dependency. At the higher concentration, the size of the rubber affects viscosity significantly.
- In all cases the smaller the size of the rubber the higher the viscosity. The relative difference in viscosity is higher for the higher concentration.

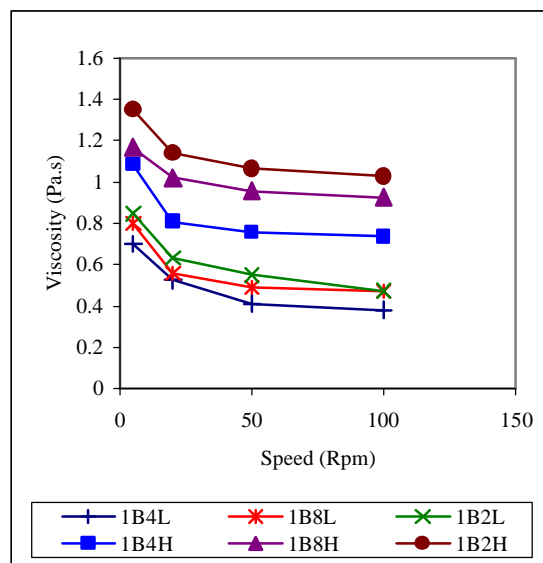
- In all cases the viscosity of the PG 70-22 (1B) mixed with rubber shows higher viscosity values compared to the PG 64-22 (2T) at equal temperatures and same shear rates.
- At 135°C the PG 70-22 mixed with CRM does not satisfy the specification requirement of a maximum value of 3.0 pa-s when the 200 mesh rubber is used at all shear rates and when the 80 mesh rubber is used at low shear rates (<10 RPM). The trend is also true for the PG 64-22.

The detailed analysis of the viscosity test will be accounted for in the following section using statistical analysis procedures.

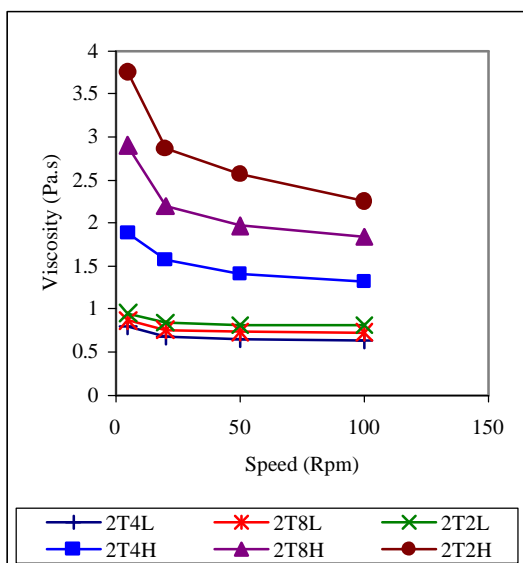
The critical temperature is the temperature at which the viscosity of the binder at 20 Rpm is equal to 3.0 Pa-s. Superpave specifies that the viscosity of any binder at the specified temperature should not exceed 3.0 Pa-s when tested at 135 °C and 20 Rpm. By determining the critical temperature, one would be able to know the range for achieving reasonable workability. To quantify the shear rate dependency of viscosity the viscosity ratio is used. This ratio is calculated by dividing the viscosity value at 5 rpm by the viscosity value at 100 rpm. Critical temperature and viscosity ratio versus binder type is illustrated in Figure 3.2.2. The data shows that as the size of crumb rubber decreases, the critical temperature increases regardless of the type of binder. When the concentration of crumb rubber is tested at 12%, the value of critical temperature is higher than that of 8%. The viscosity ratio value also appears to vary according to crumb rubber size and contents (Figure 3.2.2). This ratio would indicate whether the binder in question is truly a Newtonian fluid or if it was actually dependent on shear rate. It can be seen that viscosity of CRM is highly dependent on the shear rate, size, and concentration of crumb rubber. The non-newtonian behavior is also observed for the binders with reacted rubber, as shown in Figures 3.2.3 and 3.2.4. These



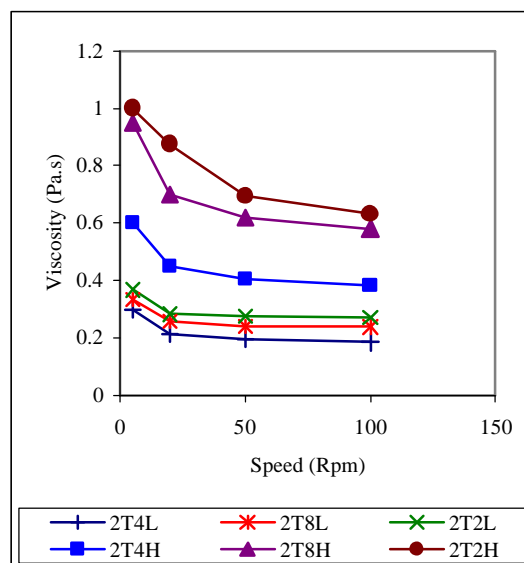
PG70-22 at 135 °C



PG70-22 at 165 °C



PG64-22 at 135 °C



PG64-22 at 165 °C

Figure 3.2.1 Comparison of Viscosity-Shear Rates

Legend : 1B : Boscan 70-22, 2T : Texas blend 64-22
 4 : 40 mesh size, 8 : 80 mesh size, 2 : 200 mesh size
 L : Low concentration, H : High concentration

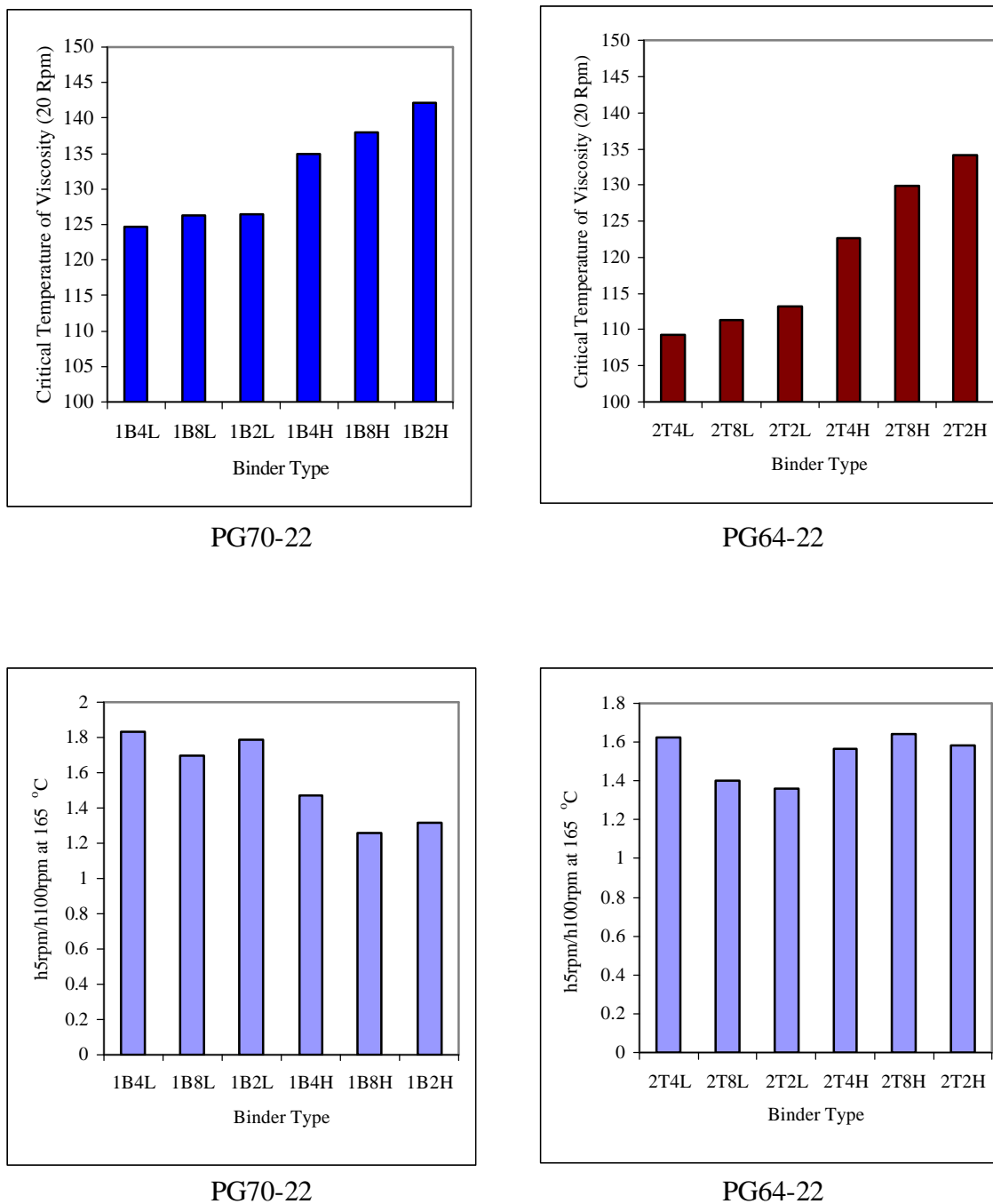


Figure 3.2.2 Critical Temperature and Viscosity Ratio Versus Binder Type

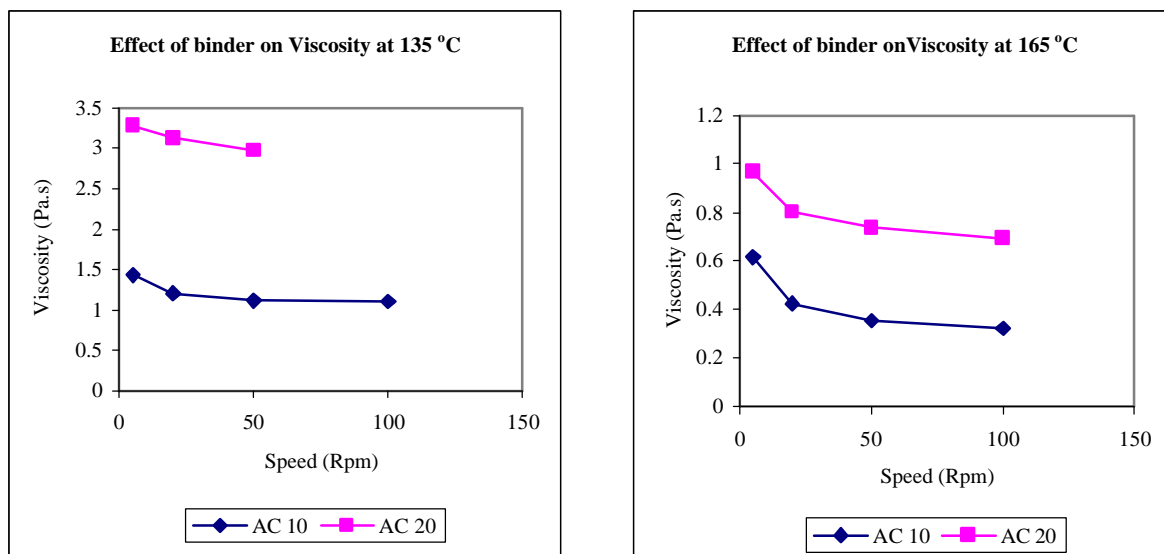


Figure 3.2.3 Comparison of Viscosity-Shear Rates for Binders with Reacted Rubber

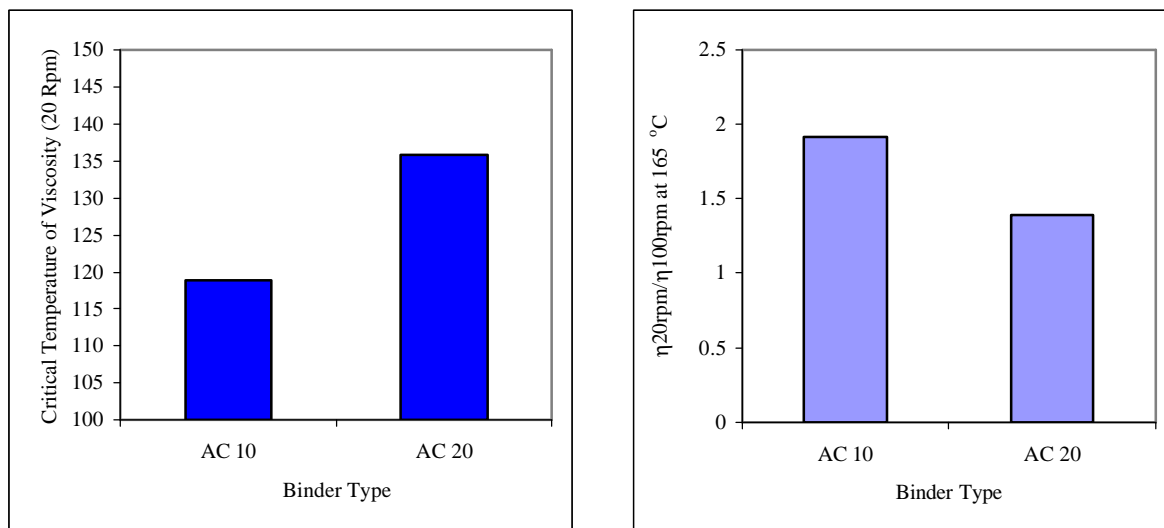


Figure 3.2.4 Critical Temperature and Viscosity Ratio Versus Binder Type

figures show the comparison of viscosity-shear rates with 2 binders containing reacted crumb rubber from FHWA. The results shown indicate that there is a great difference in the critical temperatures implying a difference in workability of those two binders (Figure 3.2.4). The binder of the AC-20 grade shows a higher value of viscosity compared to that of a binder produced from AC-10. The results, however, show that the binders meet the requirement of maximum viscosity of 3 Pa-s at all conditions.

3.2.3 Statistical Analysis for Viscosity Test

The response variable in this experiment is log (viscosity) values. Based on log (viscosity) as the response variable, the box plots for the concentration of crumb rubber, temperatures, shear rate (rpm), types of binders, and the effect of size were obtained and are shown in Figure 3.2.5. These box plots indicate the marginal effects of binders without adjusting for other factors. When a crumb rubber concentration is 12%, the value of log (viscosity) is higher than 8% concentration of crumb rubber, Figure 3.2.5(a). In this plot, we can see that the marginal effects of temperature and shear rate (rpm) are more obvious than other effects. As the temperature increases, the log (viscosity) decreases, as in Figure 3.2.5(b). It can be observed that the log (viscosity) decreases as shear rate (rpm) increases, therefore viscosity of CRM is highly dependant on the shear rate, Figure 3.2.5(c). The value of log (viscosity) is higher for the binder of PG 70-22 than that for the binder of PG 64-22, Figure 3.2.5(d). The effect of size, Figure 3.2.5(e), is not clearly obvious.

The result of fitting the model and the analysis of variance using the log-transformed viscosity as the response variable is summarized in Table 3.2.2. Compared to other variables, the effects of binder source, concentration of crumb rubber, and temperature are

significant. The R-square value for this model is 0.999, which means that this fitted model explains the data very well. The coefficient of variation (C.V) is 13.762.

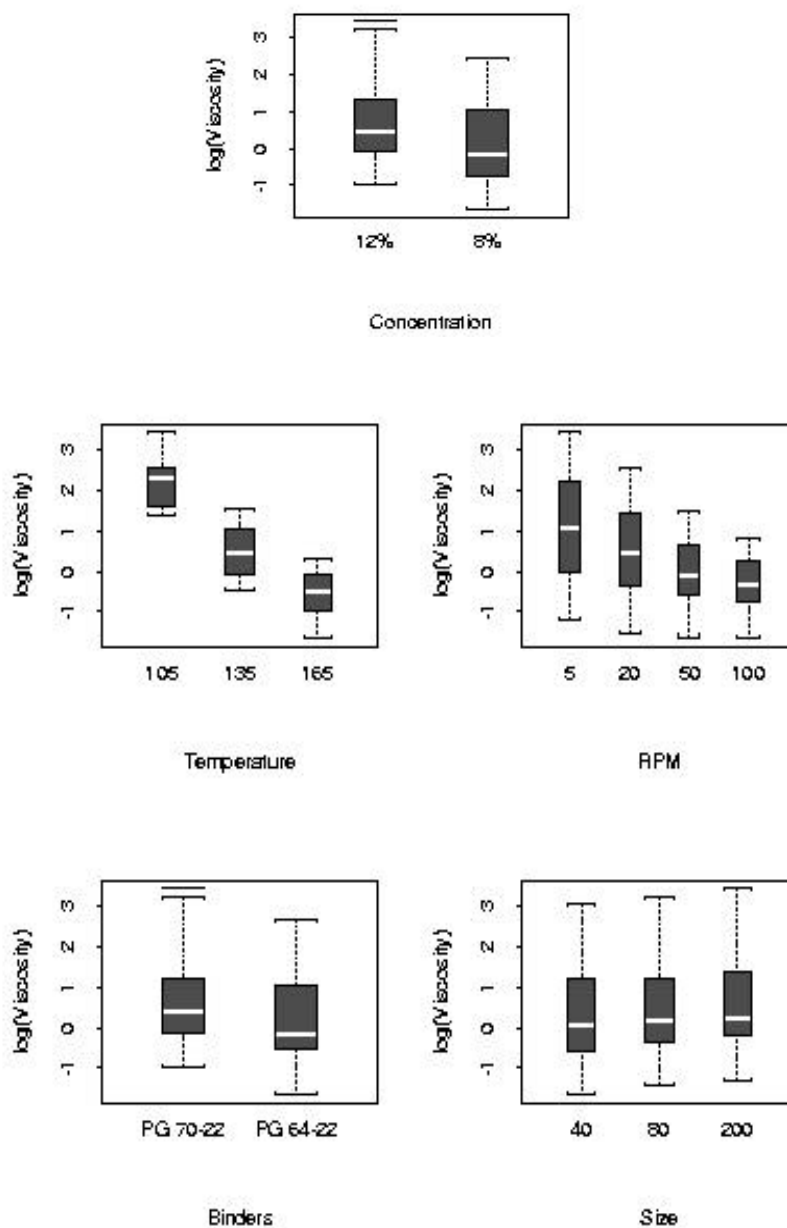


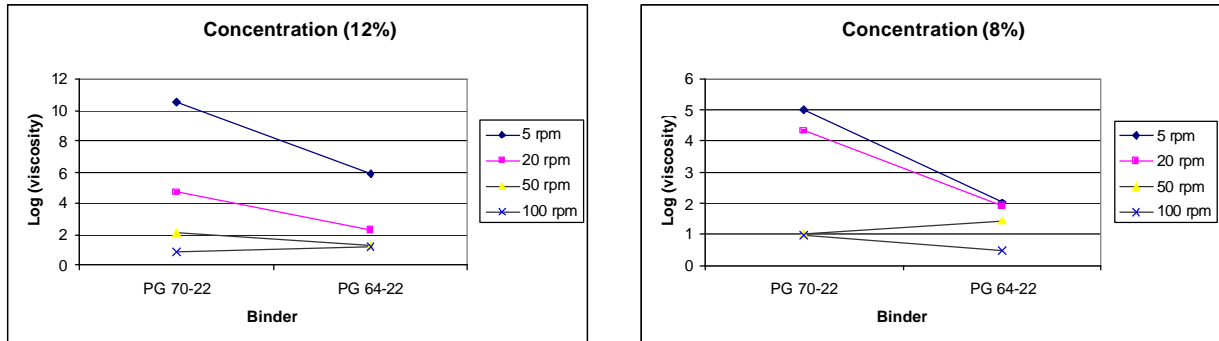
Figure 3.2.5 Box plots for concentration, temperature, RPM, binder, and size vs log (viscosity)

Table 3.2.2 : Analysis of Variance : Log (Viscosity)

Source	DF	Type III SS	Mean Square	F Value	Pr > F
TEMPERATURE	2	73.6127	36.8063	12062.60	0.0001
RPM	3	1.3046	0.4349	142.52	0.0001
BINDER	1	9.3394	9.3394	3060.81	0.0001
SIZE	2	1.4882	0.7441	243.86	0.0001
CON	1	11.5883	11.5883	3797.86	0.0001
TEMP*BINDER	2	0.1399	0.0699	22.92	0.0001
TEMP*SIZE	4	0.0436	0.01092	3.58	0.0114
TEMP*CON	2	0.2039	0.1019	33.41	0.0001
TEMP*RPM	5	0.3015	0.0603	19.76	0.0001
BINDER*SIZE	2	0.0851	0.0426	13.95	0.0001
BINDER*CON	1	0.0622	0.0622	20.38	0.0001
RPM*BINDER	3	0.009	0.0032	1.03	0.3853
SIZE*CON	2	0.3789	0.1894	62.08	0.0001
RPM*SIZE	6	0.0718	0.0120	3.92	0.0024
RPM*CON	3	0.0919	0.0306	10.04	0.0001
TEMP*BINDER*SIZE	4	0.0404	0.0101	3.31	0.0166
TEMP*BINDER*CON	2	0.2803	0.1402	45.94	0.0001
TEMP*RPM*BINDER	4	0.0682	0.0170	5.59	0.0007
RPM*BINDER*SIZE	6	0.0501	0.0083	2.74	0.0211
RPM*BINDER*CON	3	0.3255	0.1085	35.55	0.0001

Figure 3.2.6 indicates the interaction effects of the concentration of crumb rubber and shear rate (rpm) on each binder. From this figure, we can infer that there is an obvious effect caused by the different concentrations of crumb rubber. When the concentration of crumb rubber is 12% , Figure 3.2.6(a), as shear rate increases, the value of log (viscosity) decreases. The effect of shear rate on log viscosity with a CRM concentration of 12% is more significant than that of 8%. There is a large decrease in log (viscosity) when shear rate

changes from 5 rpm to 20 rpm for both PG 70-22 and PG 64-22. There are clear indications of significant interaction effects between binder and shear rate at each concentration level.



a) Concentration of CRM (12%)

(b) Concentration of CRM (8%)

Figure 3.2.6 : Interaction among binder types, concentration and shear rate vs log (viscosity)

The following findings could be drawn from the statistical analysis:

- Temperature, concentration of CRM, and type of binder have significant effect on log (viscosity).
- As the temperature increases, the log (viscosity) decreases.
- The value of log (viscosity) is higher for PG 70-22 than that of for PG 64-22 regardless of temperature.
- An increase in the size of the crumb rubber leads to a decrease of log (viscosity), while an increase in particle concentration results in an increase in the viscosity.
- The size effect is more significant in a binder with a concentration of 12% crumb rubber, therefore an increase in the size of the crumb rubber shows a sharper decrease in log (viscosity) than a binder with a particle concentration of 8%.

- The viscosity ratio calculated for each binder indicates that most of the modified binders display a dependency on the shear rate.
- Based on the viscosity data at 165 °C, to meet the viscosity requirements of 0.17 Pa-s for mixing and 0.280 Pa-s for compaction, only limited number of binders, ones with very low concentration of crumb rubber modifier, could satisfy these requirements.

3.2.4 The Statistical Analysis of Critical Temperature of Viscosity

The critical temperature is the temperature at which the viscosity of the binder at 20 Rpm is equal to 3.0 Pa-s. The response variable in this analysis is the critical temperature. The box plot (Figure 3.2.7) shows each of the main effects, shear stress, type of binder, size, and the concentration of CRM when the response variable is the critical temperature. The findings are as follows:

- It appears that critical temperature decreases as shear rate (rpm) increases, Figure 3.2.7(a). This can be explained by the shear thinning behavior known for such binders
- The variation in critical temperature is greater in the binders produced from PG 70-22 base asphalt compared to those produced from PG 64-22 binders. This could be attributed to a difference in the composition of the crude source, Figure 3.2.7(b). The two asphalts used are very different in chemical composition.
- The size effect on the critical temperature indicates more gradual increase in temperature as the size decreases, Figure 3.2.7(c). The effect is, however, small and could be considered negligible.
- There is a significant effect of concentration on the critical temperatures, indicating a wide variation in workability of the resulting binders. When the crumb rubber

concentration is 12%, the critical temperature is significantly higher than for 8% concentration of crumb rubber as shown in Figure 3.2.7(d).

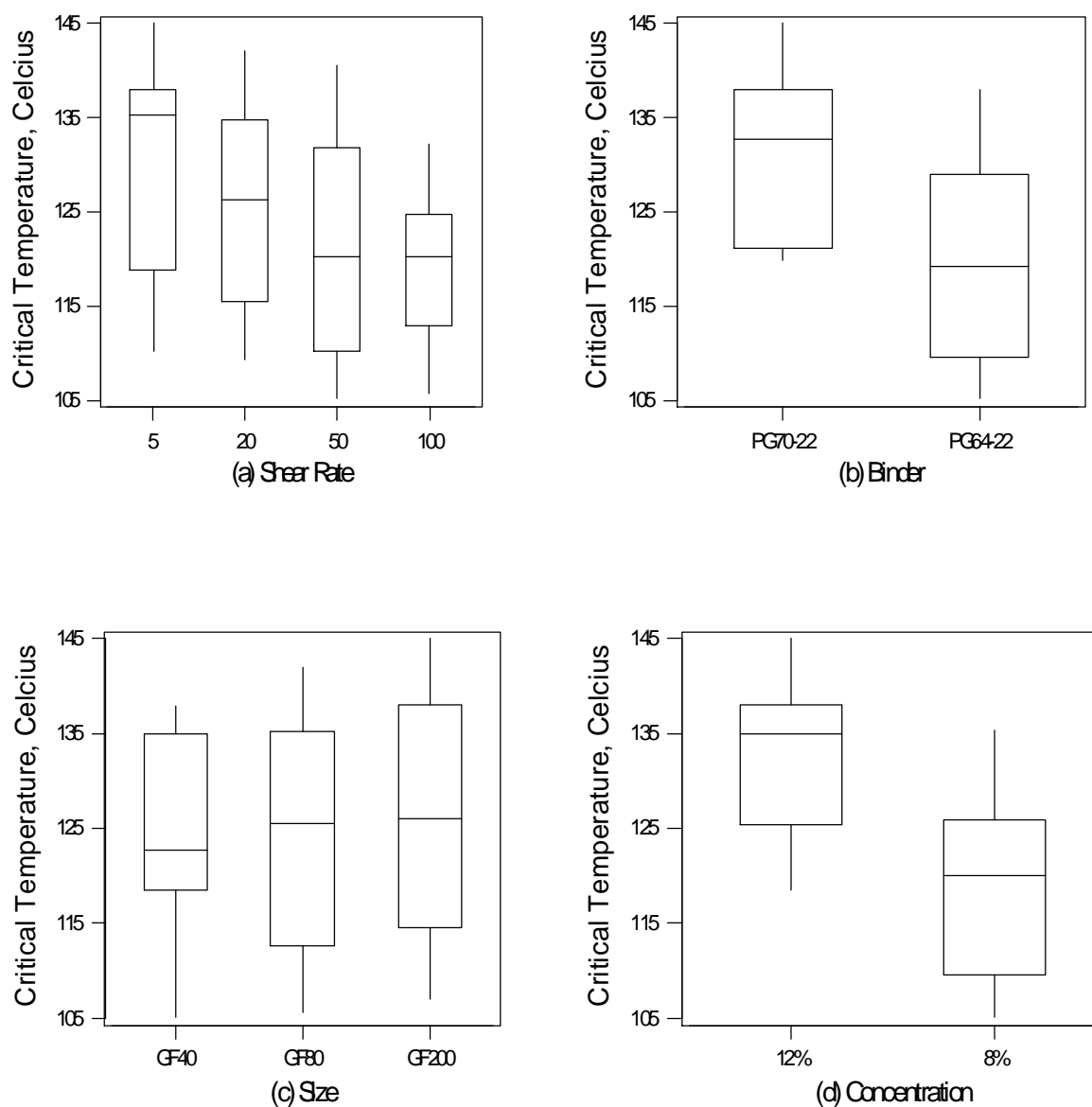


Figure 3.2.7 Box plots for sheer rate, binder, size and concentration vs critical temperature for viscosity

3.3 Mechanical Working Dependency Evaluation

This test was performed using the Dynamic Shear Rheometer (DSR) which provides a means for measuring the complex shear modulus (G^*) and phase angle (δ) of asphalt binder. G^* represents the total resistance to deformation under load, and δ represents the relative distribution of this total response between the elastic component and the viscous component [6]. Each binder was tested for its behavior under repeated cyclic loading to evaluate the effects of mechanical working. The effects were measured at the high temperature (HT) and the intermediate temperature (IT) at a selected frequency (1.59Hz). The temperatures used for testing were based on the resulting grade of the crumb rubber modified binders. For PG 70-22, the high testing temperatures selected were 82°C for high concentration (12%) of crumb rubber, and 76°C for low concentration (8%) of crumb rubber. The PG 64-22 binder was tested at 70°C regardless of crumb rubber concentration. For the intermediate temperature tests, 31°C was used for PG 70-22 and 28°C for PG 64-22.

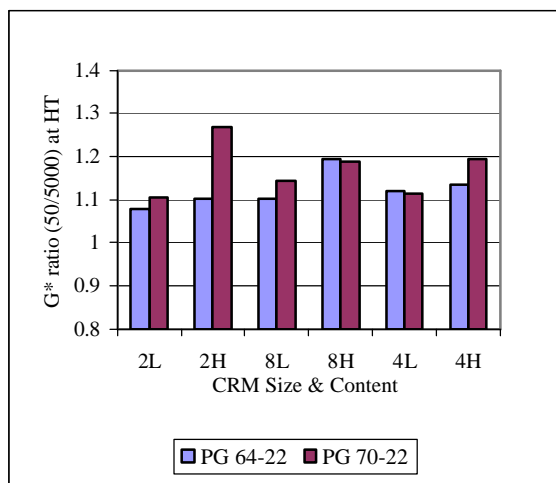
The properties at two numbers of cycles, 50 and 5000, were compared. Since the observations at the exact cycle could not be measured due to the different measurements of time by DSR, an interpolation method was used to obtain the measurements at the above cycles under the assumption that the material follows a linear trend. The strain amplitude levels of 10% and 42% at high temperature and 1% and 10% at intermediate temperature were considered. Asphalt binders were tested using three geometries including parallel plate with 1-mm gap, parallel plate with 2mm gap, and a cone-plate geometry. The test was performed with two aging conditions (unaged and PAV aged).

The value of ratio of G^* and δ calculated by the ratio of value at 50 to 5000 cycles, measured at high temperatures are shown in Figure 3.3.1. Figure 3.3.1 and 3.3.2 are prepared

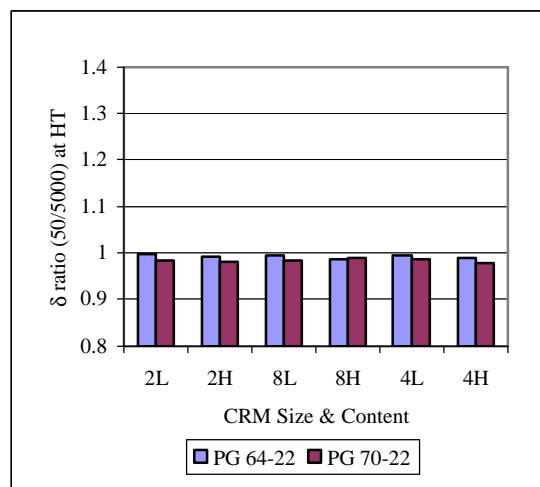
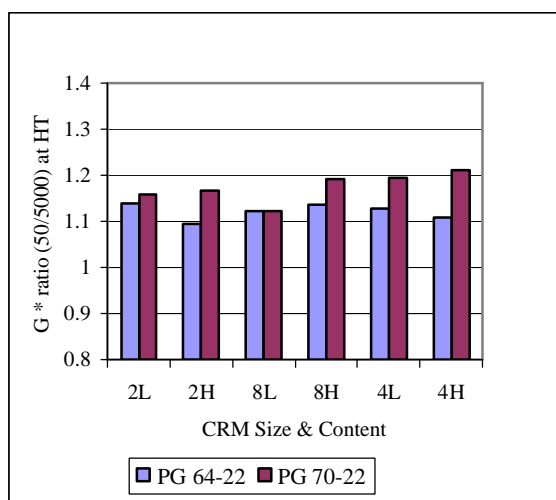
to show the effect of mechanical working at high and intermediate temperatures, respectively. The effect is quantified by calculating the ratio of G^* or δ values measured after 50 cycles to the values measured at 5000 cycles. These cycles were selected arbitrarily to avoid the initial experimental noise at low cycles and to avoid making the test larger than 50 minutes. The results indicate the following trends:

- The phase angles (δ) is not sensitive to mechanical working. In fact the δ ratios for all samples vary between 0.96 and 1.02, which is within the experimental error.
- At high temperature, most of the binders with high rubber concentration show more sensitivity than binder with low rubber concentration. This is particularly true for the Boscan PG 70-22 binder.
- At intermediate temperatures, the trend is not consistent and varies depending on binder and rubber.
- At intermediate temperatures, the sensitivity to mechanical working is higher at large strains compared to low strains.
- The maximum ratios are observed at intermediate temperatures at high strains. The ratios vary from a minimum of 1.35 to a maximum of 2.00. The ratios for the smaller crumb rubber are higher than the larger crumb rubber sizes. The effect of the crumb rubber size is consistent for both binders.

The mechanical working effects for the two binders (AC 10 and AC 20) from FHWA are shown in Figure 3.3.3. The test was performed at two different temperatures, the high and intermediate temperatures. The AC 20 was tested at 76°C and AC 10 was tested at 70 °C for the high temperatures, and regardless of the type of binder, 22 °C was selected for intermediate temperature testing. At the high temperatures, the changes in G^* due to strain



G* Ratio (10% Strain) at HT

 δ Ratio (10% Strain) at HT

G* Ratio (42% Strain) at HT

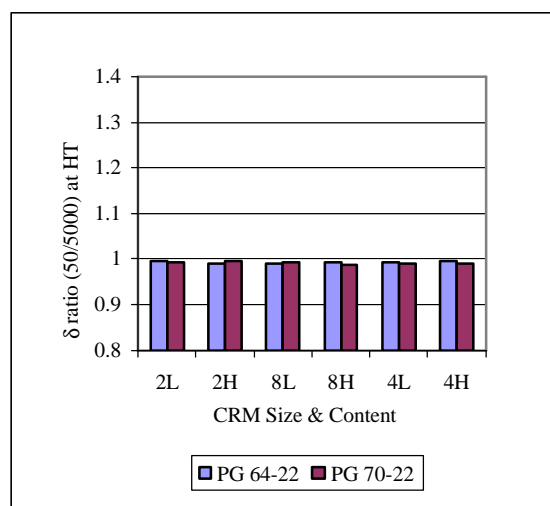
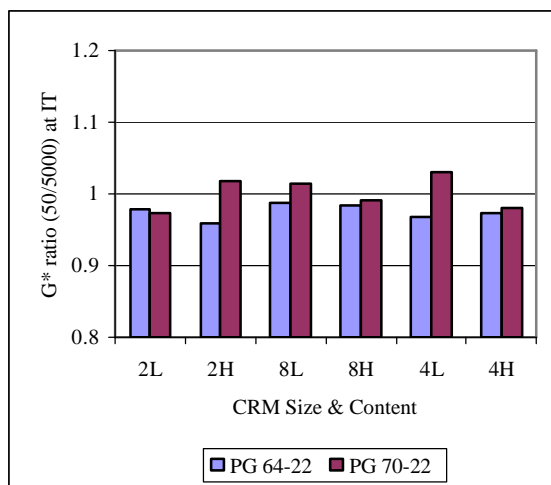
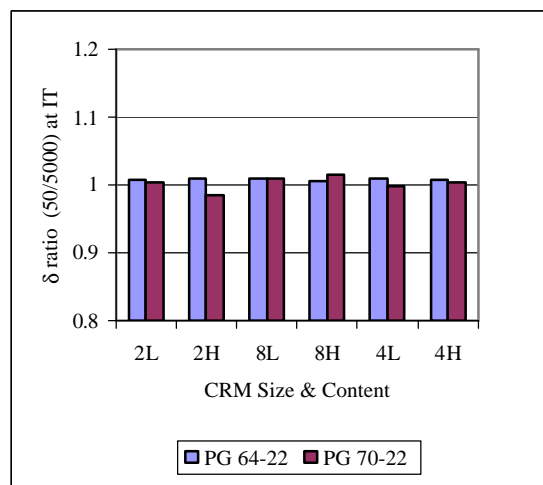
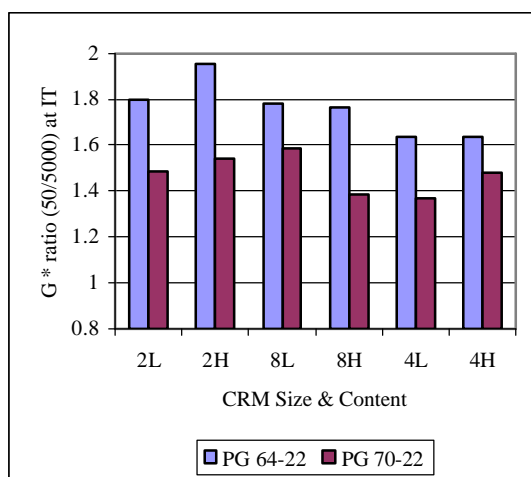
 δ Ratio (42% Strain) at HT

Figure 3.3.1 Effect of Repeated Loading at 10% and 42% Strain on G* and δ Ratio at HT



G* Ratio (1% Strain) at IT

 δ Ratio (1% Strain) at IT

G* Ratio (10% Strain) at IT

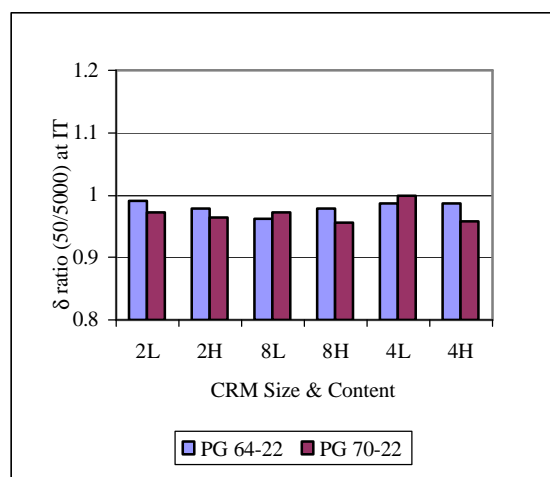
 δ Ratio (10% Strain) at IT

Figure 3.3.2 Effect of Repeated Loading at 1% and 10% Strain on G* and δ Ratio at IT

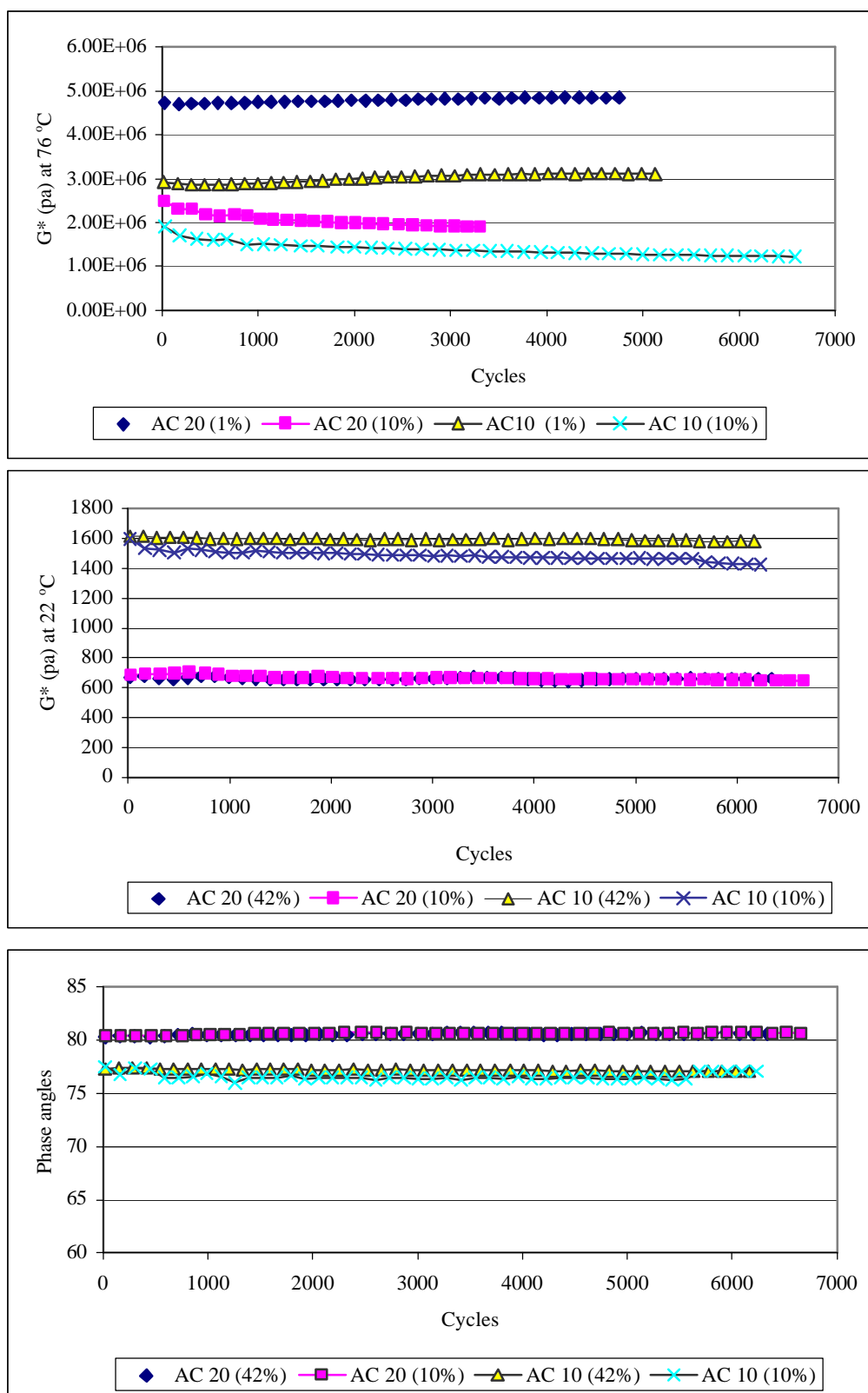


Figure 3.3.3 Time Sweeps with Different Strain Levels for AC 10 and AC20

level differences is prominent, while at the intermediate temperature, there does not appear to be any effect. At the high temperatures, when the high strain (10%) is used, the value of G^* significantly decreased compared to using the low strain (1%). At the intermediate temperature, the G^* value decreased significantly for the AC 20 compared to the AC 10. The strain level had no impact on the G^* values for either the AC 20 or the AC 10 binders. There appears to be no effect on δ for levels of temperature and strain. The performance of these reacted binders does not appear to be very different than the other binders.

3.3.1 Statistical Analysis for Mechanical Working Dependency

To normalize the effects of mechanical working relative to the base asphalts used, the parameters, G^*_n ratio ($G^*_{\text{rubber (50/5000)}}/G^*_{\text{no-rubber(50/5000)}}$) and δ_n ratio ($\delta_{\text{rubber (50/5000)}}/\delta_{\text{no-rubber(50/5000)}}$) are used in the statistical analysis for mechanical working dependency. First, we prepare the box plots for the main factors that we are interested in. Figure 3.3.4 shows the box plots for the responsible variable G^* ratio. The summary for the box plots which includes only the marginal effects of various variables are as follows:

- All normalized ratios are significantly higher than 1.0, which indicates that CRM binders are more sensitive to mechanical working than base asphalts.
- The mean G^* value of the two different binders is almost the same, but the variation is large for the PG70-22 binder.
- The effect of size of CRM does not seem to be important.
- The variation at 12% CRM is larger than at 8% of CRM, however the effect of concentration does not appear to be of significance.

- The effect of strain on the mechanical working is significant compared to the other variables. When the high strain level is selected, the G^* ratio has a higher value than at the low strain.

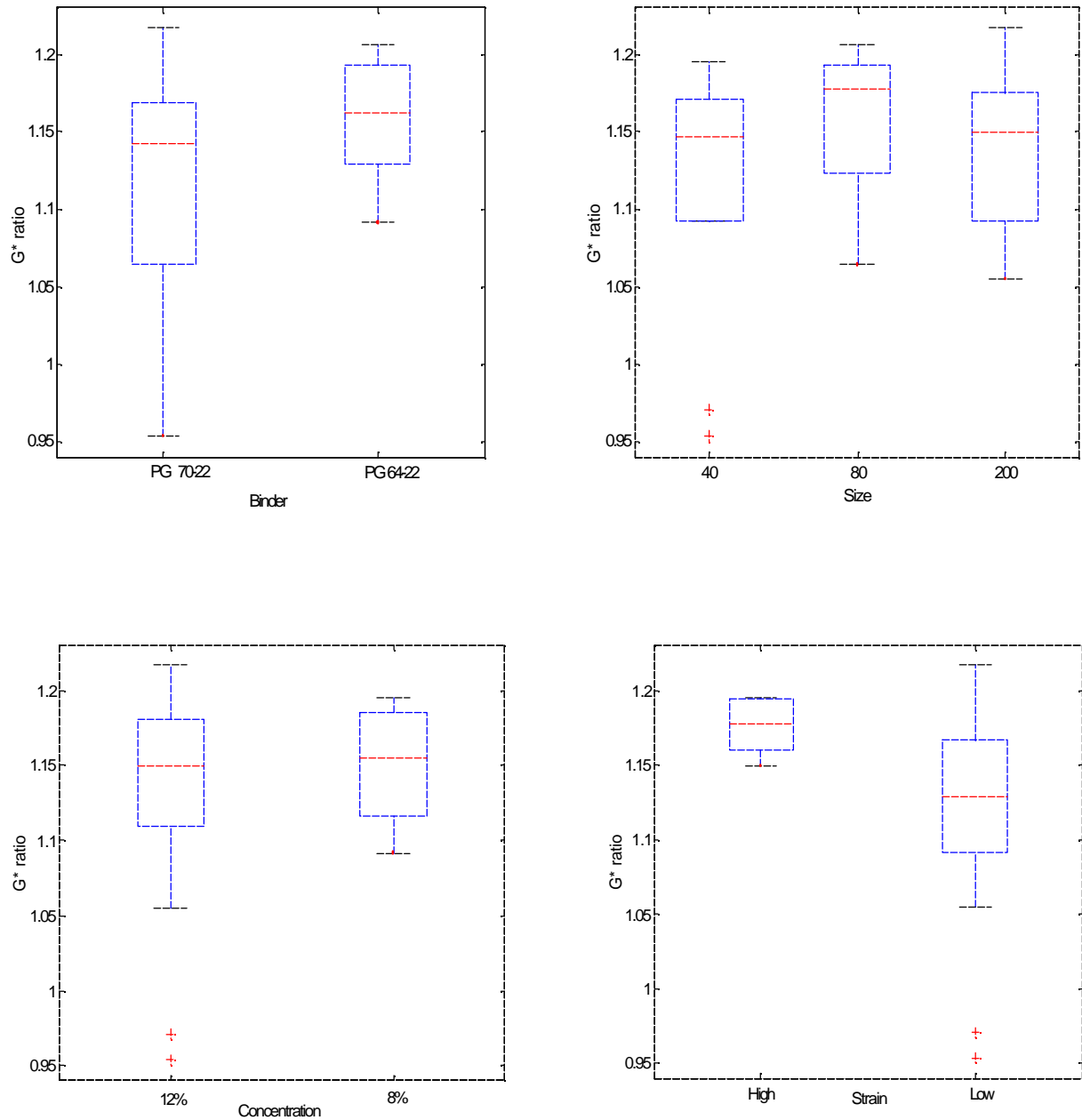


Figure 3.3.4 The box plots for G^*_n ratio ($G^*_{\text{rubber 50/5000}}/G^*_{\text{unmodified 50/5000}}$) vs binder, size, concentration, and strain

In addition to the box plots, an analysis of variance was performed to investigate the effects of the controlled variables. The full model was assumed including all the independent variables and their interaction. We ran SAS several times to decide the fitting model. The result is summarized in Table 3.3.1. As shown in this table, the main effects of all four variables were found to be statistically significant. The interaction of binder with strain and the interaction of concentration and strain were also found significant. As measured by the F-ratio, it is observed that the main effect of strain is significantly higher than the other main effects (binder, size, and concentration). Using a reduced model with only these variables gives an R^2 of 0.870, which is lower than the R^2 value of 0.959 calculated for the full model with interaction effects.

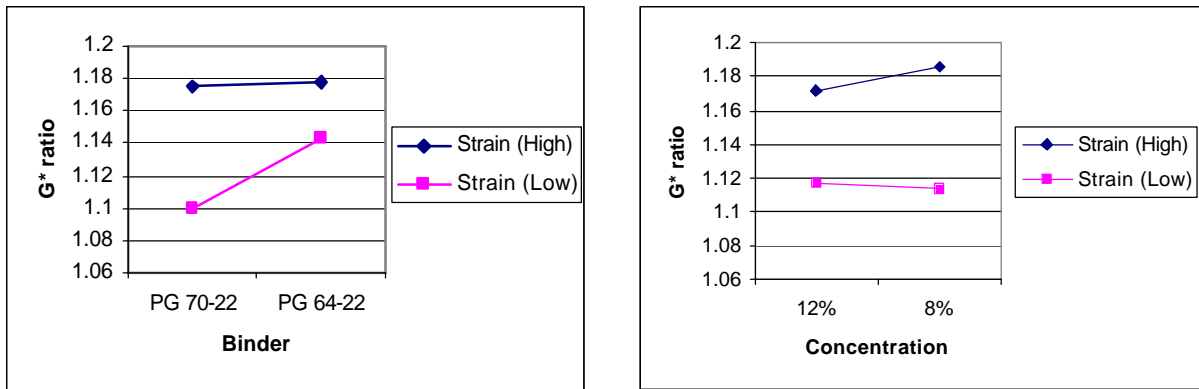
As shown in Table 3.3.1, linear regression was used to fit different models to model the effects of the variables. The model with all four variables gives R^2 values and a standard error of estimate that are similar to the model without the size. It illustrates that the size is not an important factor. Interaction terms do not seem to be as important as the standard error of estimates and the R^2 indicates a high level of goodness of fit.

Two-way interactions are shown in figure 3.3.5. This figure shows the interaction effect between binder and strain. It shows no interaction between two variables in Figure 3.3.5 (a). When the level of strain is high, it does not have an effect on the value of the G^* ratio, while at the low level of strain, the G^* ratio has a different value for the different types of binders. Figure 3.3.5 (b) illustrates the interaction between concentration and strain. It does not appear to have an interaction effect. As the concentration decreases, the G^* ratio increases when the level of strain is high. At low strain, the concentration does not appear to have an influence on the G^* ratio.

Table 3.3.1 Statistical Models for Estimation of the normalized G^*_n ratio for Mechanical Working Dependency

Analysis of Variance (G^* ratio)					
Source of Variance	Sum of Square	d.f.	Mean Square	F-ratio	Sig.level
A : Binder	0.07039528	1	0.07039528	6.62	0.0278
B : Size	0.08051902	2	0.04025951	3.78	0.0598
C : Concentration	0.07567870	1	0.07567870	7.11	0.0236
D : Strain	1.01544758	1	1.01544758	95.43	<.0001
Interaction					
AB	0.02220140	2	0.01110070	1.04	0.3877
AC	0.00000000	0	-	-	-
AD	0.07727042	1	0.07727042	7.26	0.0225
BC	0.03568537	2	0.01784269	1.68	0.2355
BD	0.06700607	2	0.03350304	3.15	0.0870
CD	0.07791713	1	0.07791713	7.32	0.0221
Residual	0.10640959	10	0.01064096		
Total (Corrected)	2.59202733	23	$R^2 = 0.958947$		
Reduced Model					
Main Effects					
A : Binder	0.07961282	1	0.07961282	4.25	0.0539
B : Size	0.08466759	2	0.04233379	2.26	0.1329
C : Concentration	0.06182961	1	0.06182961	3.30	0.0858
D : Strain	1.99054060	1	1.99054060	106.37	0.0000
Residual	0.33682816	18			
Total (Corrected)	2.59202733	23	$R^2 = 0.870052$		

Model for estimating (G^*_n ratio)	Std. Error of Y est	Std. Error of Coefficient	R^2
For all rubbers : $G^*_n\text{ratio} = 2.0604 + 0.13610(B) + 0.00060(S) - 0.14791(C) - 0.5791(ST)$	0.1422	0.13602 0.07246 0.000442 0.07926 0.05869	0.8517
For all rubbers : $G^*_n\text{ratio} = 2.12324 + 0.14372(B) - 0.14958(C) - 0.58751(ST)$	0.145	0.13046 0.07373 0.08088 0.05956	0.8374
For all rubbers : $G^*_n\text{ratio} = 2.08745 + 0.56373(B) - 0.62458(C) - 0.55545(ST) - 0.28190(B*ST) + 0.31225(C*ST)$	0.1341	0.30143 0.21350 0.24182 0.19205 0.13635 0.14997	0.8751
B : Binder Type (1,2=PG 70-22, PG64-22) S : Size of CRM (40,80,200) C : Concentration of CRM (1,2=12%,8%) ST : Strain (1,2=High,Low)			



(a) Binder and Strain

(b) Concentration and Strain

Figure 3.3.5 Interaction effects when G^* ratio (50/5000) is selected as a response variable

Next, the normalized δ ratio ($\delta_{\text{rubber (50/5000)}}/\delta_{\text{no-rubber(50/5000)}}$) was selected as a responsible variable. The box plots are shown in Figure 3.3.6. The findings can be summarized as follows.

- The mean value of the two different binders is of significance. When the binder of PG 64-22 is taken, the value of the δ ratio is higher than the value of the PG 70-22.
- There is no prominent significance of different sizes.
- The mean value of the two different concentrations is of significance. The variation at 12% CRM is larger than at 8%.
- The effect of strain is very significant. In the case where the high strain level is adopted, the value of the δ ratio is a higher value than that at low strain.

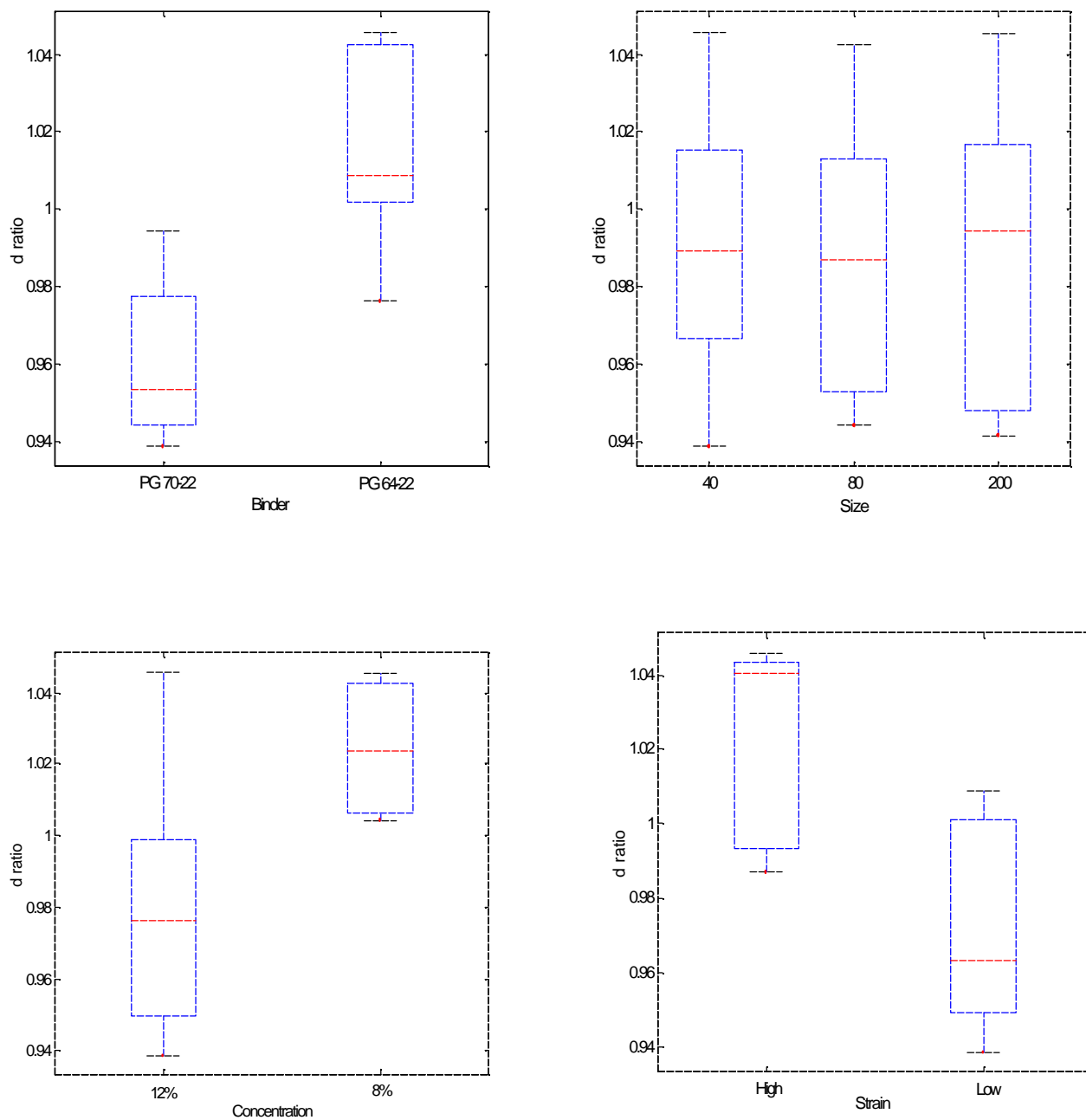


Figure 3.3.6 The box plots for d_n ratio ($d_{\text{rubber 50/5000}}/d_{\text{unmodified 50/5000}}$) vs binder, size, concentration, and strain

Table 3.3.2 illustrates the fitting model using SAS analysis when the δ ratio is the response variable. Analysis of variance and linear regression analyses were carried out to study the effects of the different variables. Similar to the G^* ratio, the main effects of the two variables (binder, strain) are found to be significant. The effect of strain is found to be more important than the binder. The interaction of size with strain was found significant. The full model with interaction effects gives an R^2 of 0.898, while the R^2 value of 0.800 was calculated for the main effects. Table 3.3.2 lists the statistical analyses for the final selected models. The first includes all main factors studied: binder, size, and strain. The model fit is relatively good with an R^2 value of 0.825 and a standard error of estimate of 0.151. The factor of size did not show a significant effect. When the size was dropped as shown in the second model in Table 3.3.2, the R^2 values decreased slightly and the standard error of estimate decreased by a small margin. The last model included several combinations of interactions. As shown the interactions that were found important are binder and strain. This model shows a significantly higher R^2 of 0.8751 and a standard error of estimate of 0.1341.

Table 3.3.2 Statistical Models for Estimation of the normalized d_n ratio for the Mechanical Working Dependency

Analysis of Variance (δ ratio)					
Source of Variance	Sum of Square	d.f.	Mean Square	F-ratio	Sig.level
A : Binder	0.00188864	1	0.00188864	15.19	0.0016
B : Size	0.00060595	2	0.00030297	2.44	0.1236
C : Strain	0.00923707	1	0.00923707	74.30	0.0000
Interaction					
AB	0.00017778	2	0.00008889	0.71	0.5062
AC	0.00107150	1	0.00107150	8.62	0.0108
BC	0.00039768	2	0.00019884	1.60	0.2368
Residual	0.00174060	14	0.00012433		
Total (Corrected)	0.01704533	23	$R^2 = 0.898$		
Reduced Model					
Main Effects					
A : Binder	0.00205317	1	0.00205317	11.35	0.0032
B : Size	0.00092968	2	0.00046484	2.57	0.1029
C : Strain	0.00957418	1	0.00957418	52.93	0.0000
Residual	0.00343700		0.00018089		
Total (Corrected)			$R^2 = 0.800$		

Model for estimating (δ ratio)	Std. Error of Y est	Std. Error of Coefficient	R^2
For all rubbers : G*ratio = 1.99867 +0.05679(B)+ 0.00061(S) -0.58460(ST)	0.1510	0.13988 0.06223 0.00047 0.06215	0.8245
For all rubbers : G*ratio = 2.07478+0.00064(S)- 0.57938(ST)	0.1502	0.11185 0.000465 0.06164	0.8172
For all rubbers : G*ratio = 2.08745+0.56373(B)- 0.62458(C)-0.55545(ST)- 0.28190(B*ST)+ 0.31225(C*ST)	0.1341	0.30143 0.21350 0.24182 0.19205 0.13635 0.07800	0.8751
B : Binder Type (1,2=PG 70-22, PG64-22) S : Size of CRM (40,80,200) C : Concentration of CRM (1,2=12%,8%) ST : Strain (1,2=High,Low)			

3.4 Strain Dependency Evaluation

A strain dependency evaluation test was conducted to examine the effects of strain and frequency on the rheological properties of the binders. Two levels of temperature, high and intermediate, were used and the frequency was fixed at 1.6Hz. The temperatures for each binder type were determined to be the same as the ones used in the experiments for the mechanical working dependency evaluation. The types of plate and aging conditions were the same as they were in the test for mechanical working dependency evaluation.

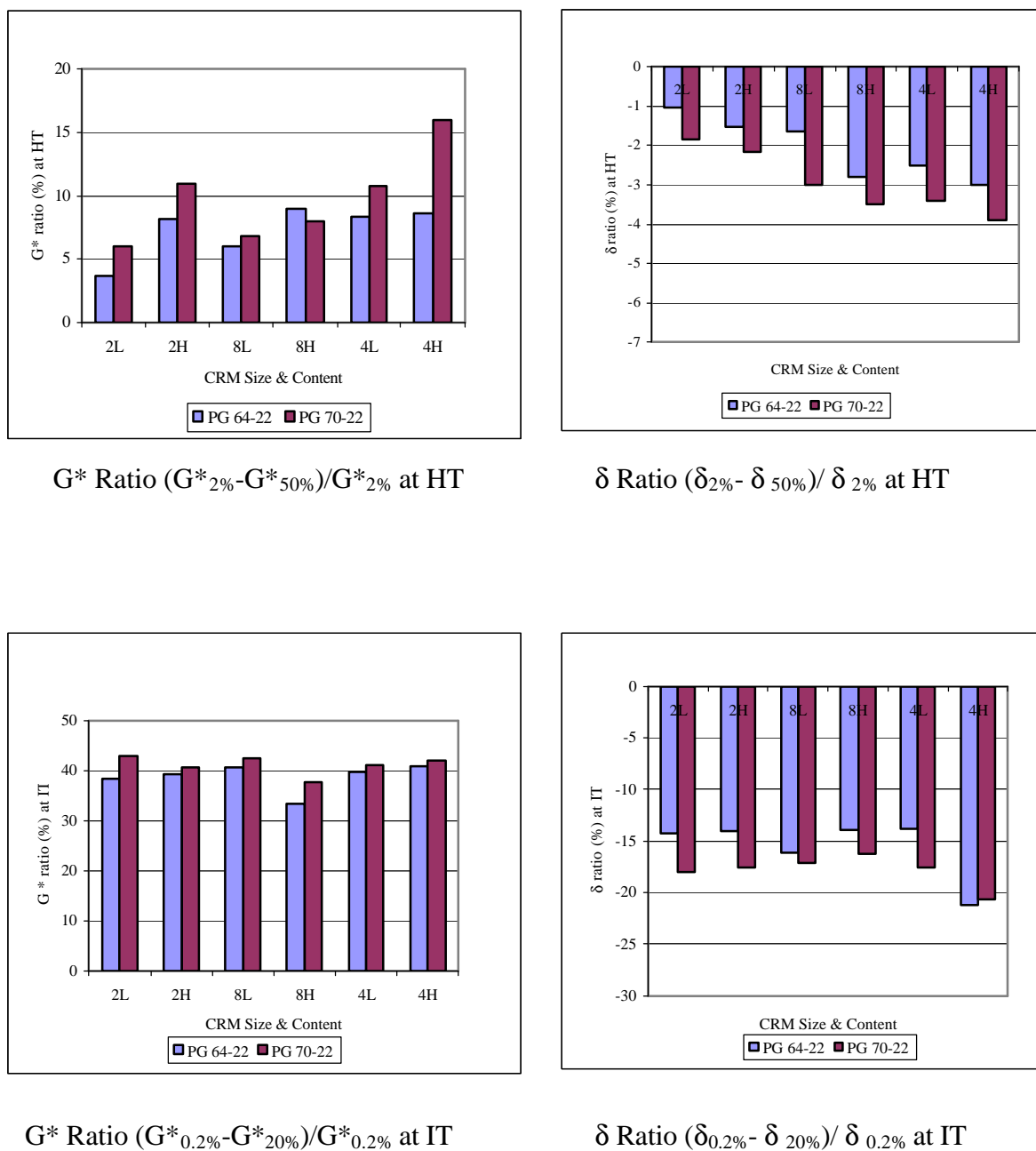
At the high temperatures, 2% and 50% strain levels were compared, and at the intermediate temperatures, 0.2% and 20% strain levels were compared. Since the DSR is stress controlled and not strain controlled, the exact values at the above strain levels were not available.

Therefore the interpolation method was used to obtain the exact values. As before, G^* and phase angle (δ) were measured with the DSR.

The results were summarized by calculating the percentage change relative to the small strain value. The results are shown in Figure 3.4.1. A summary of the observations is as follows:

- The binders demonstrate greater strain dependency when tested at intermediate temperature than at high temperature. The G^* values can reduce by 42% of the small strain value by increasing strain to 20%.
- At both temperature levels, as the crumb rubber concentration increases, the change in G^* increases. This is particularly true at high temperatures.
- The particle size of CRM also appears to have an effect on changes, particularly at high temperature. There is a consistent trend showing higher size rubber resulting in more sensitivity to strain.

Figure 3.4.1

**Figure 3.4.1 G^* and δ Ratios (%) Measured from Strain Sweeps at HT and IT**

- The effects of crumb rubber content and size are different depending on the base binder. PG 70-22 based binders show more sensitivity to the crumb rubber concentration and size than the PG 64-22 based binders.
- The percent change in δ values increases as the concentration of crumb rubber and the particle size increases.
- It appears that the percentage of change is very dependent on temperature. Only few binders show dependency on strain at the HT, with the average values being within a 10% range. The higher strain dependency is observed in binders modified with 12 % CRM.

3.4.1 Effect of Strain Dependency and Geometry Dependency on Rheological

Properties

The strain sweeps were conducted with the parallel plate and cone-plate to develop the effect of geometry at high temperature. In this section, the combined effect of strain and geometry on rheological properties will be discussed.

Figure 3.4.2 shows the comparison of data collected using the two different geometries for GF 40 crumb rubber binders at two different concentration levels, 8% and 12%. At the high temperatures, the binders appear not to be sensitive to strain. In addition, it illustrates that the strain dependency is not sensitive to geometry because the values of G^* for both geometries show that the difference between response for a strain range of 2% and 50% is within 10%. Therefore geometry inflicts no significant effect on rheological properties at the high temperature. The data also shows that neither the size

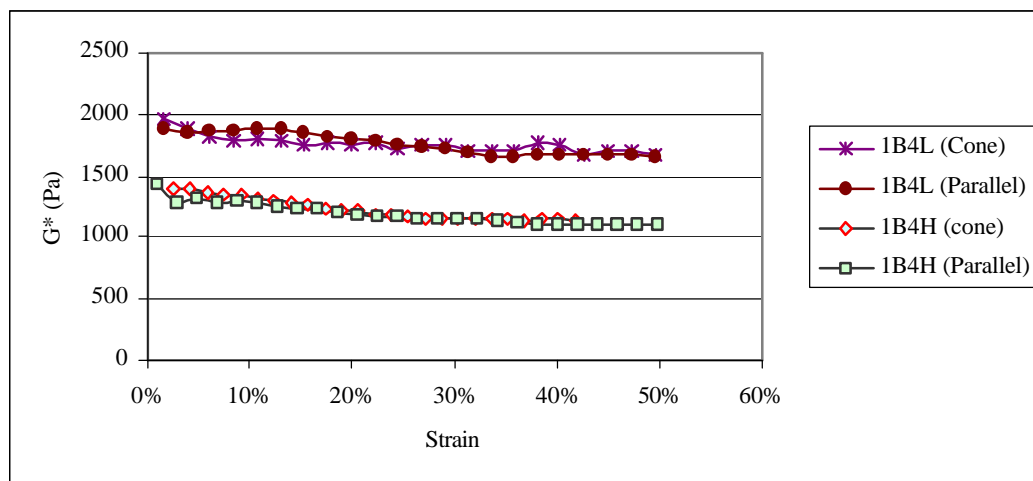


Figure 3.4.2 Effect of the plates for PG 70-22 with different concentration of CRM

nor the concentration affect the strain. There is no clear reduction in G^* as the strain increases regardless of the level of concentration. Therefore the concentration of CRM does not play an important role in the effect of geometry at high temperatures.

The effect of CRM concentration while using different plates (cone and parallel) can also be seen in Figure 3.4.2. According to the studies related to the effect of geometry, the testing temperature plays an important role in the effect of geometry. Because the tests conducted for this study were only measured at high temperatures, we should also consider the effect of geometry at the intermediate temperature. All the modified binders illustrate rheological behavior that is highly dependent on the strain amplitude at all the temperatures. The previous researches showed that solid additives result in higher strain dependency and very important geometry dependency. The results shown lead to the following findings:

- At high temperatures, the geometry has no significant effect on the value of the G^* and δ .
- The strain dependency is not sensitive to geometry at the high temperature.

- The concentration of CRM does not play an important role in the effect of geometry at the high temperature. Regardless of the concentration of crumb rubber, the value of G^* does not change significantly with the effect of geometry.
- The strain dependency is larger at intermediate temperatures than at high temperatures.

3.4.2 Statistical Analysis for Strain Dependency

For the statistical analysis, the parameters for strain dependency used in the comparative study were used to calculate the normalized G^* ratio and the normalized δ ratio. The normalized G^* ratio represents the value of rubber modified divided by the ratio for the unmodified ($G^*_{\text{rubber ratio}}/G^*_{\text{no-rubber ratio}}$). At the intermediate temperature, 0.2% and 20% strain levels were compared using the ratio $((G^*_{0.2\%}-G^*_{20\%}) / G^*_{0.2\%})$ and the statistical analysis, the value of the normalized G^*_n ratio represents $G^*_{\text{rubber ratio}}/G^*_{\text{no-rubber ratio}}$. The δ ratio used represents $\delta_{\text{rubber ratio}}/\delta_{\text{no-rubber ratio}}$. The box plots for G^*_n ratio are in Figure 3.4.3 including the marginal effects of plate, binder, size, concentration, replicates and temperature. The summary for the box plots is as follows:

- The effect of plate could not be regarded significant. The range of the G^* ratio for the parallel plate is larger than for the cone plate however there is no significant difference between the mean values of measurements using two different plates.
- The value of the G^* ratio does not appear to be dependent on binder type and on the sizes of rubber.
- The effect of concentrations of CRM does not look to be significant, though at 8% CRM there is a larger variation than that of 12% CRM.
- The difference in the mean value of the three replications is not important.

- The effect of temperature shows a very significant effect on the value of the G^* ratio. At the intermediate temperature, G^* ratio shows a higher value than at high temperature, therefore the strain dependency is highly dependent on the temperature of testing.

An analysis of variance using the G^*_n ratio as the response variable is summarized in Table 3.4.1. In addition, the table includes the linear regression results used to evaluate different models. The full model was used, which includes all the independent variables and their interaction effects. The effect of temperature was found to be more significant than the other three variables (binder, size, and concentration). The R^2 value of 0.943 for the full model with interaction effects is not significantly higher than the reduced model which gives an R^2 value of 0.911. It could be assumed that the interaction effects are not so important in this analysis. The estimated model including only two main effects (binder and temperature) indicates a high level of goodness of fit with the R^2 value of 0.932. Also, with adding the interaction effect (concentration and temperature), the R^2 value and the standard error of estimate remain similar to the other models.

The statistical analysis indicates that the binder type and the temperature are the most important factor. It appears that neither rubber size nor concentration are important regarding the normalized G^* ratio. It is however clear that there is an important interaction between binder and rubbers. This is because although ratios are normalized by dividing by the G^* ratio of no-rubber binder, there is still a need to include binder type in the model. The two-way interaction between concentration and temperature is in Figure 3.4.4. According to this model, the value of G^* ratio decreases as the concentration decreases at the high temperature, while at the intermediate temperature, the G^* ratio increases as the

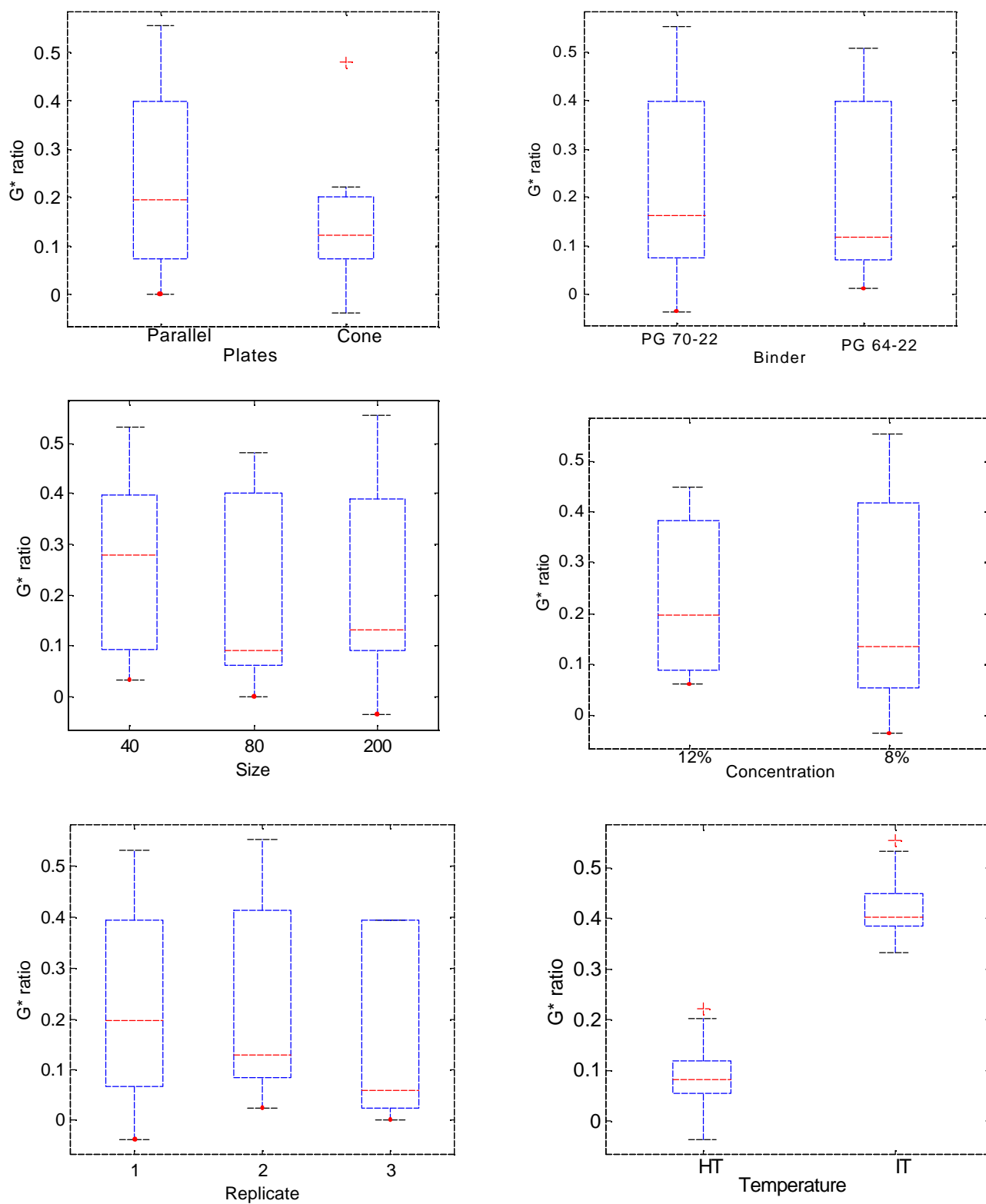


Figure 3.4.3 The box plots for G* ratio ($G^*_{\text{rubber ratio}}/G^*_{\text{unmodified ratio}}$) vs plate, binder, size, concentration, replicate, and temperature

concentration decreases. This plot does not show that there is an important interaction effect between the temperature and the concentration.

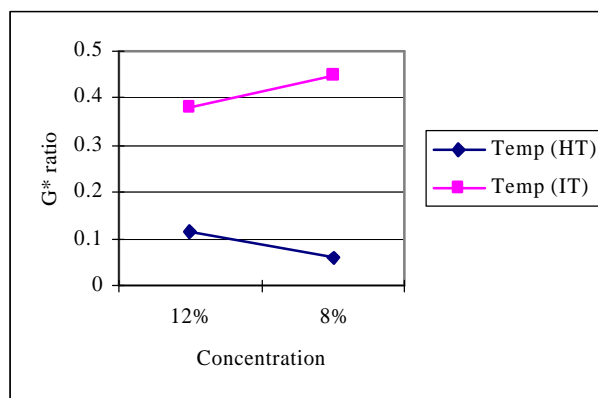
Next, the statistical analysis for the value of δ ratio which represents $\delta_{\text{rubber ratio}}/\delta_{\text{no-rubber ratio}}$ was performed. The box plots for δ ratio are in Figure 3.4.5 for all factors considered (plate, binder, size, concentration, replicates and temperature). The summary for the box plots is as follows:

- The average values of the parallel plate and cone plate geometry appear to be similar. The range, however, is not the same. It should be noted that there was not enough data collected from tests using the cone plate geometry in order to compare with the data from tests using the parallel plate geometry. Therefore, it needs more data from the cone plate to make a reliable conclusion of the effect of plates.
- The effect of binder type does not appear to be important when we consider the marginal effect shown by the results.
- The values of the δ ratio on different sizes of crumb rubber appear to be similar but the mean value of δ ratio with sieve size 40 is lower than at 80 and 200.
- The effect of concentrations of CRM does not look to be significant, though at 8% CRM there is a larger variation than that of 12% CRM.
- The difference in the mean value of the three replications is not different. This indicates that the results are fairly reproducible.
- Like the analysis of the G^* ratio, the effect of temperature shows a very prominent effect on the value of the δ ratio.

Table 3.4.1 Statistical Models for Estimation of the normalized G^*_n ratio for Strain Dependency

Analysis of Variance (G^*_n ratio)					
Source of Variance	Sum of Square	d.f.	Mean Square	F-ratio	Sig.level
A : Binder	0.00778949	1	0.00778949	3.24	0.0787
B : Size	0.01335114	2	0.00667557	2.78	0.0732
C : Concentration	0.00038264	1	0.00038264	0.16	0.6917
D : Temperature	1.41322641	1	1.41322641	588.65	.0000
Interaction					
AB	0.00063275	2	0.00031638	0.13	0.8769
AC	0.00003688	1	0.00003688	0.02	0.9019
AD	0.00018858	1	0.00018858	0.08	0.7806
BC	0.00215794	2	0.00107897	0.45	0.6410
BD	0.00460829	2	0.00230415	0.96	0.3910
CD	0.04949537	1	0.04949537	20.62	0.0000
Residual	0.10323487	43	0.00240081		
Total (Corrected)	1.80364127	57	$R^2 = 0.943$		
Reduced Model					
Main Effects					
A : Binder	0.00672180	1	0.00672180	2.17	0.1467
B : Size	0.01266192	2	0.00633096	2.04	0.1397
C : Concentration	0.00023290	1	0.00023290	0.08	0.7850
D : Temperature	1.59924871	1	1.59924871	516.48	0.0000
Residual	0.16101344	52	0.00309641		
Total (Corrected)	1.80364	57	$R^2 = 0.911$		

Model for estimating (G^*_n ratio)	Std. Error of Y est	Std. Error of Coefficient	R^2 adjusted
For all rubbers : $G^*_n \text{ ratio} = -0.23629 - 0.02542(B) + 0.34223(T)$	0.248596	0.03776 0.01866 0.01821	0.9317
For all rubbers : $G^*_n \text{ ratio} = -0.26791 - 0.02395(B) + 0.35186(T) + 0.06646(CT)$	0.23135	0.04602 0.01856 0.01981 0.05615	0.9353
B : Binder Type (1,2=PG 70-22, PG64-22) S : Size of CRM (40,80,200) C : Concentration of CRM (1,2=12%,8%) T : Temperature (HT+3, HT, HT-3) F : Frequency (0.15,1.5,15Hz) A : Aging (1,2,3= unaged,RTFO,PAV)			



Concentration and Temperature

Figure 3.4.4 Interaction effects when the normalized G^*_n ratio is selected as a response variable.

Table 3.4.2 shows the statistical analysis for the δ ratio. The full model was used that includes all the independent variables and their interaction. The result is similar to the analysis for the G^* ratio. The significant main effects for this data are the two variables, which are binder and temperature. The effect of temperature is found to be most significant. The simplest model in this table includes only two main effects (binder and temperature) and it gives an R^2 of 0.917, a standard error of estimate of 0.1265. Next, we added the factor of concentration but the R^2 value and the standard error of estimate remained similar to the first model. The statistical analysis indicates that the concentration is not an important factor. The third model is carried out to take into account the concentration-temperature interaction effect; no interaction terms appear to be important since this model has a R^2 value of 0.933, which is almost the same as the reduced model with no interaction, which gives an R^2 value of 0.927.

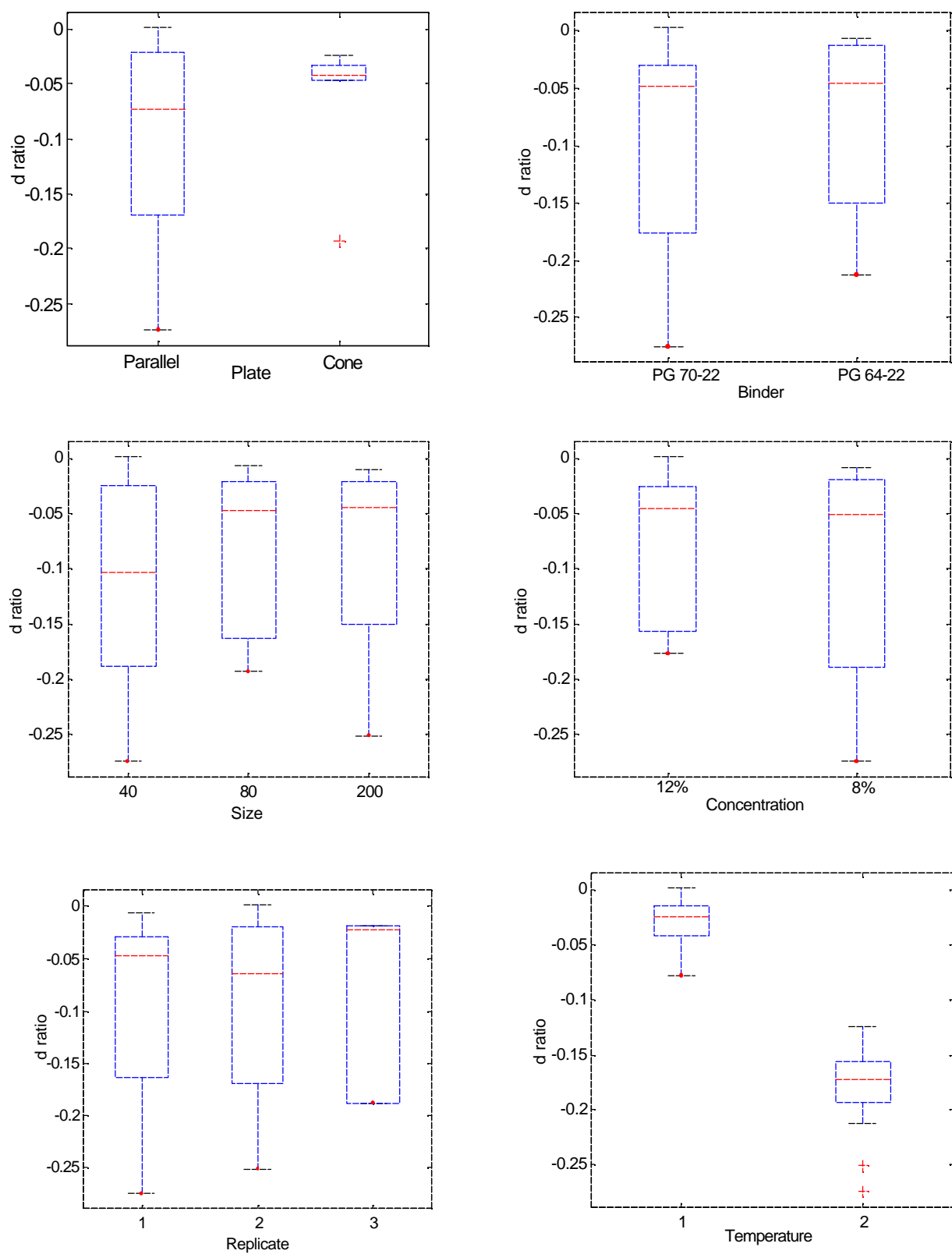


Figure 3.4.5 The box plots for d ratio ($d_{\text{rubber ratio}}/d_{\text{unmodified ratio}}$) vs plate, binder, size, concentration, replicate, and temperature

Table 3.4.2 Statistical Models for Estimation of the normalized d_n ratio for Strain Dependency

Analysis of Variance (δ ratio)					
Source of Variance	Sum of Square	d.f.	Mean Square	F-ratio	Sig.level
A : Binder	0.00627483	1	0.00627483	15.82	0.0003
B : Size	0.00125579	2	0.00062790	1.58	0.2171
C : Concentration	0.00283730	1	0.00283730	7.15	0.0105
D : Temperature	0.27898443	1	0.27898443	703.43	0.0001
Interaction					
AB	0.00122097	2	0.00061049	1.54	0.2261
AC	0.00028042	1	0.00028042	0.71	0.4051
AD	0.00028267	1	0.00028267	0.71	0.4032
BC	0.00061978	2	0.00030989	0.78	0.4642
BD	0.00186879	2	0.00093440	2.36	0.1069
CD	0.00583935	1	0.00583935	14.72	0.0004
Residual	0.01705417	43			
Total (Corrected)	0.36399433	57	$R^2 = 0.953$		
Reduced Model					
Main Effects					
A : Binder	0.00611073	1	0.00611073	11.70	0.0012
B : Size	0.00121896	2	0.00060948	1.17	0.3194
C : Concentration	0.00225802	1	0.00225802	4.32	0.0426
D : Temperature	0.31935122	1	0.31935122	611.38	0.0001
Residual	0.02716190	52			
Total (Corrected)	0.36399	57	$R^2 = 0.925$		

Model for estimating (δ ratio)	Std. Error of Y est	Std. Error of Coefficient	R^2
For all rubbers : δ ratio = 0.09782+0.02414(B)-0.15562(T)	0.1265	0.01923 0.00950 0.00927	0.9171
For all rubbers : δ ratio = 0.12371+0.02306(B)-0.01618(C)-0.15475(T)	0.1191	0.02342 0.00914 0.00901 0.00891	0.9265
δ ratio = 0.13999+0.02229(B)-0.01412(C)-0.16082(T)-0.04114(CT)	0.1138	0.02527 0.00893 0.00890 0.00958 0.02730	0.9329

3.5 Effects of Testing Frequency at High, Intermediate & Low Temperature and Loading Time.

The purpose of the experiment was to study the effects of various factors such as crumb rubber particle size, concentration, aging of the road and binder types on the variation of G^* , phase angle (δ) at different conditions of temperature and loading rates (frequency). Frequency sweeps were performed using the DSR with frequencies from 0.15 Hz to 15 Hz. For this analysis, three different frequencies (0.15 Hz, 1.5 Hz and 15 Hz) are analyzed. The 0.15 Hz represents stop and go traffic speed, 1.5 Hz represents slow speed and 15 Hz is assumed to represent normal traffic.

Binder types, concentration levels and sizes of crumb rubber used in this experiment were the same as in the previous experiments. The binders were tested using the DSR at three levels of high temperature (HT-6, HT and HT+6) and three intermediate temperatures (IT-3, IT and IT+3). For binders with the PG 70-22 grade base asphalt, testing at 70°C, 76°C and 82°C temperature were used in the testing for 8% of crumb rubber concentration, and 76°C, 82 °C and 88°C for 12% of concentration. For binders with the PG 64-22 graded base asphalt, they were tested at 64°C, 70°C and 76°C regardless of crumb rubber concentration. At the intermediate temperature levels, 19°C, 22°C and 25°C were applied for both binder types. Tests for the unaged and RTFO-aged binders were performed at high temperatures, and PAV aged binders were tested at intermediate temperatures. Results from three levels of frequency, 0.15 Hz, 1.5 Hz and 15 Hz were compared. The strain amplitude level was fixed at 10% for high temperature tests and at 1% for intermediate temperature tests.

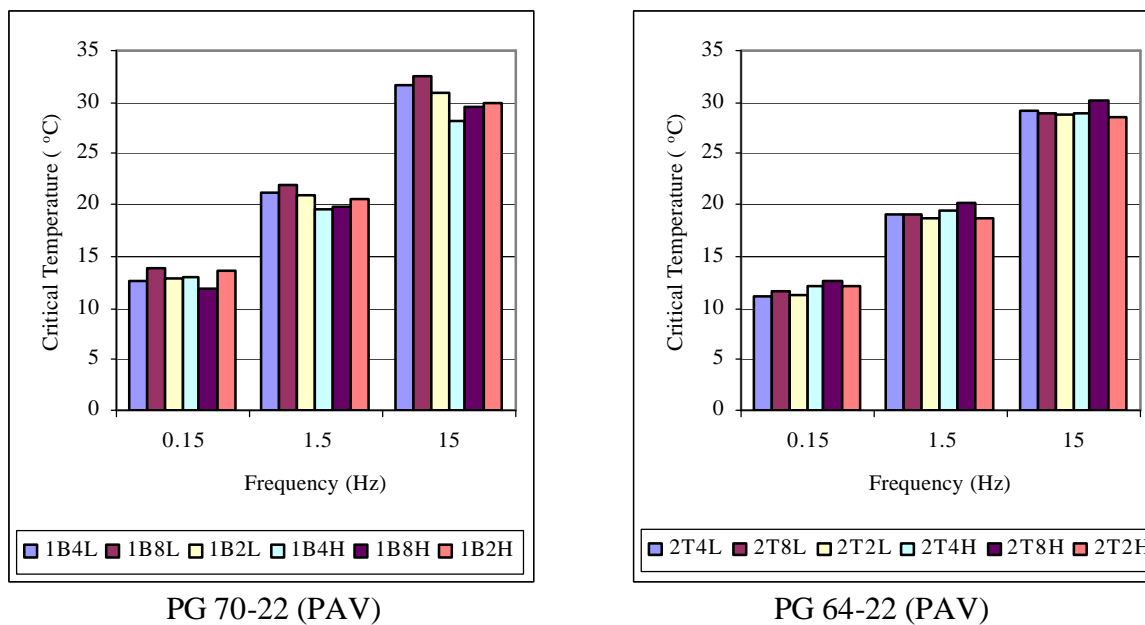
Using this data, it was also possible to determine the critical temperature, which is the temperature at which the specification requirement is met, eg. $G^*/\sin \delta = 1.00$ kPa for unaged binder. Figure 3.5.1 shows the variation of critical temperature with frequency.

The bending beam rheometer test was performed to study the effects of crumb rubber size and concentration, and base asphalt source on the creep stiffness and creep rate of rubber modified asphalt binders at low temperatures. The critical temperature in this case is determined as the temperature at which the creep stiffness achieves a value of 300 MPa, and the temperature at which the creep rate achieves a value of 0.300. Figures 3.5.2 and 3.5.3 show the results of the critical temperatures for creep stiffness, $s(t)$, and creep rate, m -value, respectively.

The following observations were made based on the results shown:

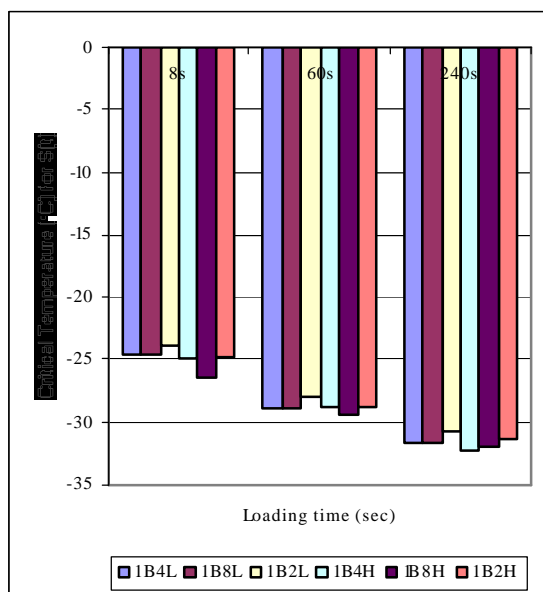
- The G^* value is dependent on the frequency at which the test is run, whether at high temperature or at intermediate temperature.
- By increasing the testing frequency from 0.15 Hz to 1.5 Hz (one order of magnitude) at high temperature, the change in critical temperature is approximately 16 to 18 °C. This means that when the speed of traffic is reduced by one order of magnitude, the high pavement temperature grade would have to be shifted by approximately 3 grades. This is a very significant amount of temperature shift.
- There is also a difference in critical temperature when the testing speed is changed at intermediate temperatures, although this variation is not as large as that at high temperature. It is still sufficient to cause a significant shift in the specification grade of the binder.

- There is no significant difference in the change in critical temperature with respect to change in crumb rubber particle size or concentration.
- The results indicate a dependence of the creep stiffness and creep rate on the loading time. The stiffness decreases with increasing loading time, while the creep rate increases with increasing loading time. The change is also significant, having a range from -2.4 to -5.6 °C.
- There is no significant effect of crumb rubber size or concentration on the change in the critical temperature of $S(t)$ due to an increase in loading time.
- There appears to be a significant effect of crumb rubber concentration and size on the change in the critical temperature due to an increase in loading time.

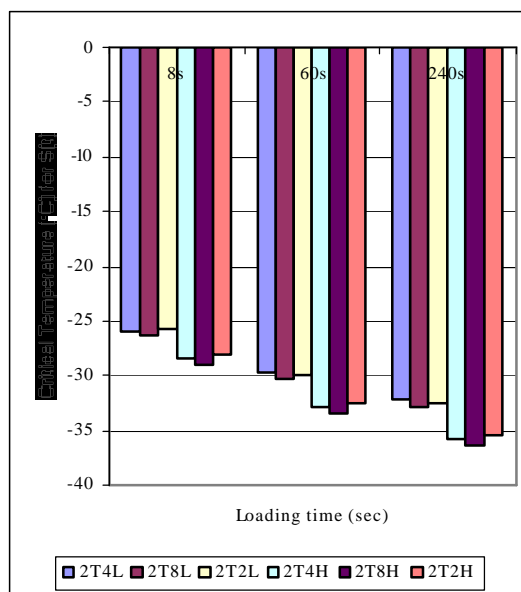
Figure 3.5.1

Critical Temperature: Temperature at which $G^* \sin \delta = 5000$ kPa

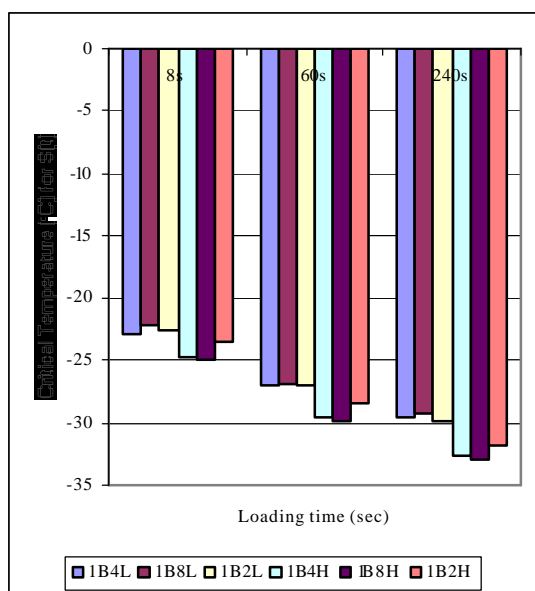
Figure 3.5.1 Effect of Crumb Rubber Particle Size and Concentration on Variation of Critical Temperature with Testing Frequency



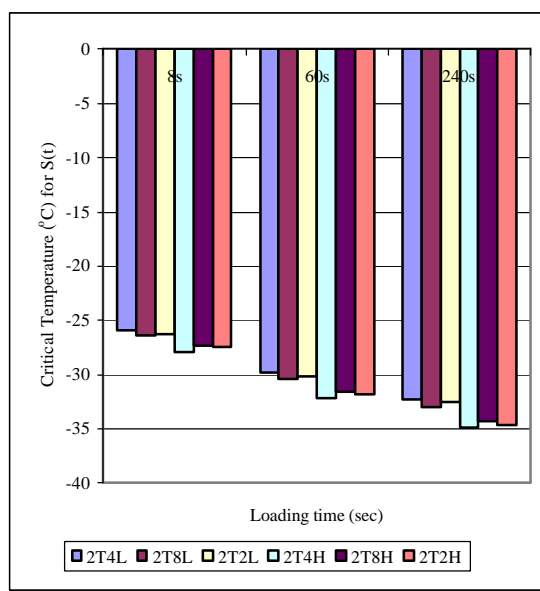
PG 70-22 (RTFO)



PG 64-22 (RTFO)

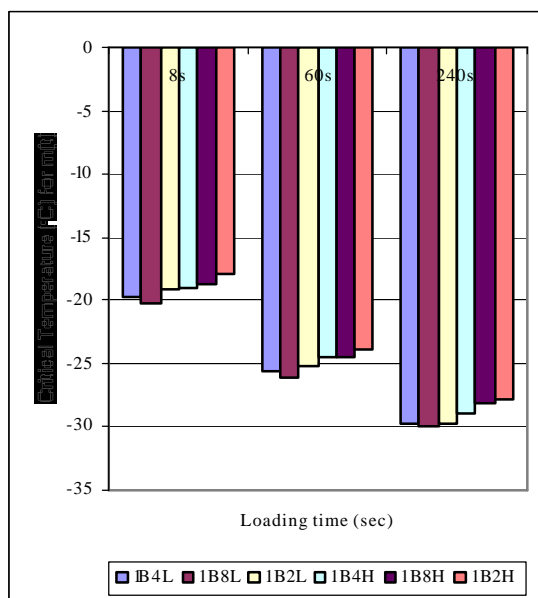


PG 70-22 (PAV)

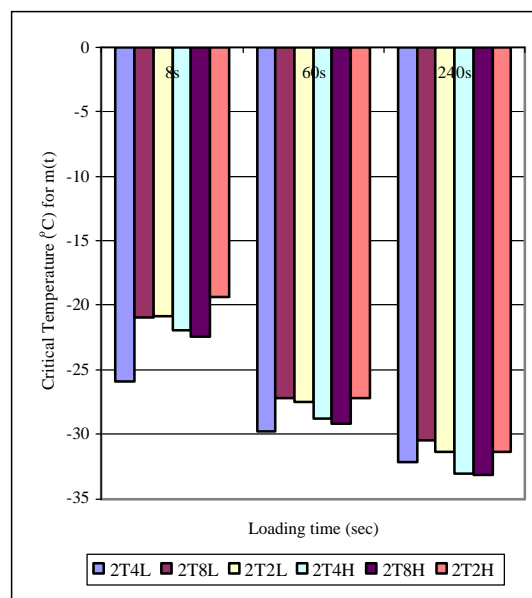


PG 64-22 (PAV)

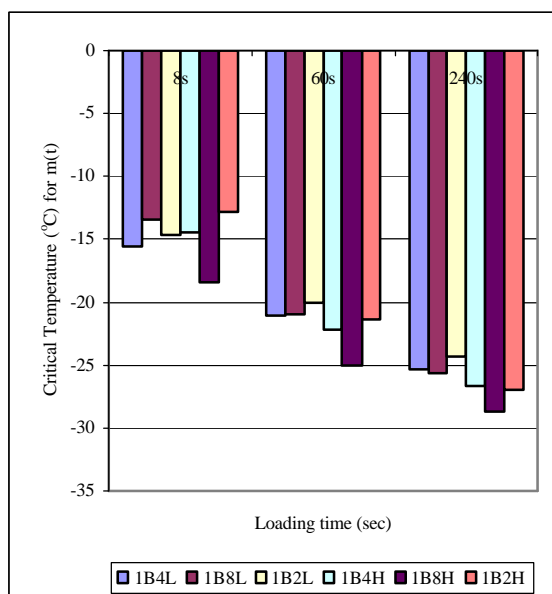
Figure 3.5.2 Effect of Crumb Rubber Particle Size and Concentration on Variation of Critical Temperature for S(t) with Loading Time (Sec)



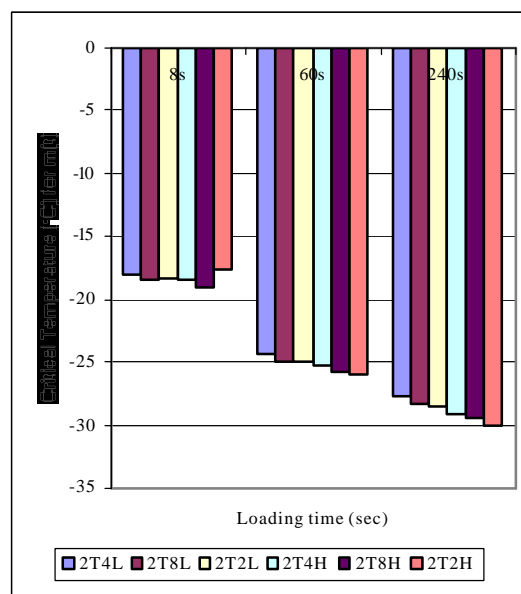
PG 70-22 (RTFO)



PG 64-22 (RTFO)



PG 70-22 (PAV)



PG 64-22 (RTFO)

Figure 3.5.3 Effect of Crumb Rubber Particle Size and Concentration on Variation of Critical Temperature for m-value with Loading Time (Sec)

3.5.1 Statistical Analysis for Frequency Sweeps

There were two response variables, G^* ratio and phase angle (δ) ratio. The parameters, G^* ratio ($G^*_{\text{rubber}}/G^*_{\text{no-rubber}}$), δ ratio ($\delta_{\text{rubber}}/\delta_{\text{no-rubber}}$) are used in the analysis for frequency sweeps. First, we conduct the box plots for the main factors that we are interested in. Figure 3.5.4 shows the box plots for the responsible variable G^* ratio. The summary of the analysis for the box plots which includes only the main effects of controlled variables is as follows:

- As shown in Figure 3.5.4 (a), the marginal effect of temperature on the G^* ratio is not obvious.
- The effect of frequency appear to be more important. As the frequency increases from 0.15 Hz to 15Hz, the G^* ratio decreases.
- In terms of the binder type , the mean value of the two different binders does not vary considerably, but the PG 70-22 has a significantly higher range of G^* ratio than PG 64-22.
- The effect of sizes does not appear to be significant. Therefore it could be considered negligible.
- Figure 3.5.4 shows the marginal effect of the concentration of crumb rubber. The value of (G^*) increases as the concentration increases from 8% of CRM to 12%. This is expected due to the effect of rubber.
- The effect of aging appears to be negligible as shown in Figure 3.5.4(f). The effects of unaged and RTFO aged binders do not appear to be very significantly different.

Table 3.5.1 shows the final model when $\log(G^* \text{ ratio})$ is the response variable. In order to study the relative significance of the different factors and their possible interactions, a statistical analysis for the $\log(G^* \text{ ratio})$ from the frequency sweep was carried out. The results of the analysis for the $\log(G^*)$ are shown in the Table 3.5.1.

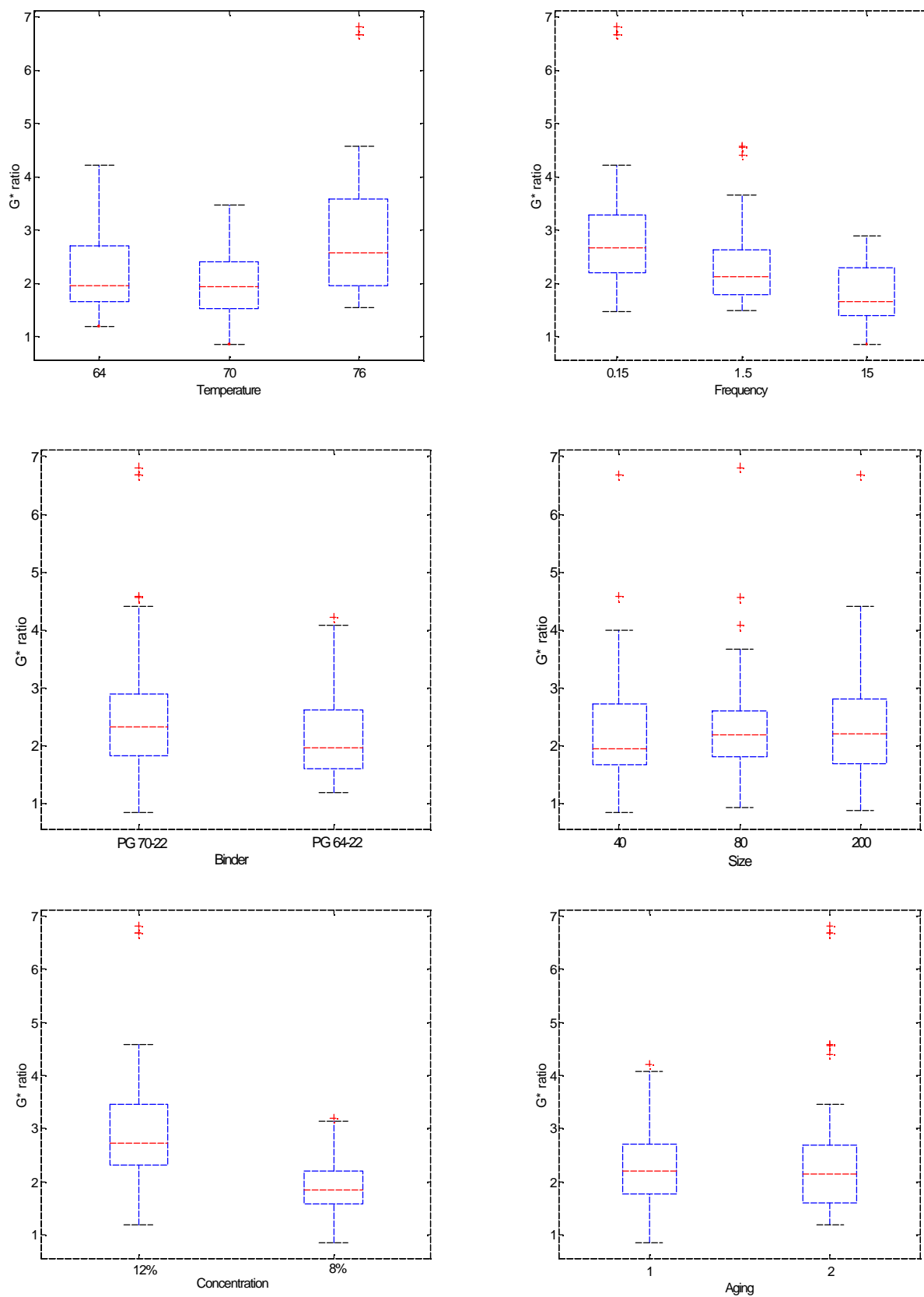


Figure 3.5.4. The box plots for the G^* ratio ($G^*_{\text{rubber}}/G^*_{\text{unmodified}}$) vs temperature, frequency, binder, size, concentration and aging

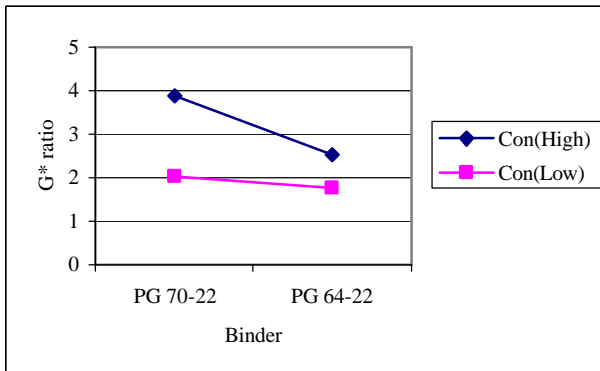
The analysis of variance indicates that temperature, frequency, binder, and concentration show significant effects. The concentration appears to have a much more important effect than the other factors (temperature, frequency, and binder) based on the F-ratios. The analysis also shows that there are important interaction effects. The R^2 value for the model with only the main effects is 0.712, which is lower than the R^2 value of 0.848 for the full model with all two-way interactions. The full model was assumed, including all the independent variables and their interaction. The assumption of linear regression was used to model the effects of the important factors. As shown in this table, the main effects of all four variables were found to be statistically significant. All of the interaction terms were found significant in the full model. Using a reduced model with only these variables gives an R^2 of 0.712, while the R^2 value for the full model with interaction effects was calculated as 0.848.

As shown in Table 3.5.1, linear regression was used to fit different models to model the effects of the variables. The model with all four variables gives an R^2 value and a standard error of estimate that are similar to the model without the interaction terms. Interaction terms do not seem to be important as the standard error of estimates and the R^2 indicates a high level of goodness of fit.

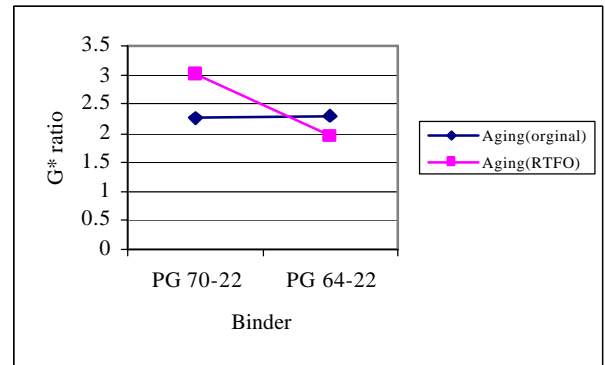
Table 3.5.1 Statistical Models for Estimation of the G* ratio for Frequency sweep

Analysis of Variance (log G* ratio)					
Source of Variance	Sum of Square	d.f.	Mean Square	F-ratio	Sig.level
A : Frequency	1.07915154	2	0.51398471	115.71	.0000
B : Binder	0.39241477	1	0.32503796	84.15	.0000
C : Concentration	1.25394963	1	1.15275303	268.89	.0000
D : Aging	0.00722696	1	0.00134541	1.55	0.2158
Interaction					
AB	0.03339502	2	0.01669751	3.58	0.0311
AC	0.02927171	2	0.01463586	3.14	0.0472
AD	0.10280752	2	0.05140376	11.02	.0000
BC	0.11501581	1	0.11501581	24.66	.0000
BD	0.23511216	1	0.23511216	50.42	.0000
CD	0.01970489	1	0.01970489	4.23	0.0422
Residual	0.51763380	111	0.00466337		
Total (Corrected)	3.41502	125	R ² = 0.848		
Reduced Model					
Main Effects					
A : Temperature	0.09196934	2	0.04598467	5.56	0.0049
B : Frequency	1.02796943	2	0.51398471	62.10	0.0000
C : Binder	0.03551167	1	0.03551167	4.29	0.0405
D : Concentration	0.86396506	1	0.86396506	104.38	0.0000
Residual	37.99801	116	0.32757		
Total (Corrected)	3.41502	125	R ² = 0.712		

Model for estimating (δ ratio)	Std. Error of Y est	Std. Error of Coefficient	R ² adjusted
For all rubbers : G*ratio = -0.84496+0.02193T- 0.01275F+0.39159C-0.00815TC	0.1	0.43797 0.00624 0.00134 0.27691 0.00395	0.6423
G*ratio = 0.90978-0.0179(F)- 0.1041(B)-0.2142(C)+0.0033(FC)	0.0983	0.00435 0.01795 0.02317 0.00264	0.6576
G*ratio = 0.66512+0.00260(T)- 0.01275(F)-0.08539(B)-0.19291(C)	0.0986	0.25876 0.00306 0.00131 0.02847 0.01838	0.6553
B : Binder Type (1,2=PG 70-22, PG64-22) S : Size of CRM (40,80,200) C : Concentration of CRM (1,2=12%,8%) T : Temperature (HT+3, HT, HT-3) F : Frequency (0.15,1.5,15Hz) A : Aging (1,2,3= unaged,RTFO,PAV)			



(a) Binder and Concentration



(b) Binder and Aging

Figure 3.5.5 Interaction effects when the G^* ratio is selected as a response variable.

Figure 3.5.5 illustrates the two way interaction terms on values of the G^* ratio. For both binder types, the G^* ratio values vary as the concentration of CRM changes in figure 3.5.5(a). When the concentration is low, the values of the G^* ratio between two different binders are almost same. For the PG 70-22, the G^* ratio has a higher value than when PG 64-22 asphalt is used. Figure 3.5.5(b) shows the interaction terms between binder and aging. There is an interaction effect between binder and aging. The value of the G^* ratio is not affected by the type of binder when the condition of binder is unaged. When the condition of binders is aged (RTFO), $\log(G^* \text{ ratio})$ has a different value with the type of binders. PG 70-22 has a higher value of the G^* ratio than PG 64-22 when the aged binders are taken.

We analyze the data at the high temperature with phase angle (δ) ratio being the response variable. The box plots for the δ ratio are shown in figure 3.5.6. The findings are as follows:

- The effect of temperature on phase angle ratio is considered to be negligible since it is not significant.
- The effect of frequency on the ratio indicates a gradual decrease in δ ratio as the frequency increases. The effect of frequency appears to be prominent.
- Considering the comparison of different binders, the mean values of the two different binders are very similar, however the range of the ratio of phase angle with PG 70-22 is wider than PG 64-22.
- The mean values of different sizes of CRM are almost the same because the effect of size could be considered negligible.
- When the crumb rubber concentration is 12%, the phase angle has a lower value than for 8% concentration. According to this box plot, the effect of concentration should be considered.
- The effect of aging is more significant than other effects (frequency, binder and concentration). There is a significant difference between the different aging types.

A statistical analysis for the frequency sweep was carried out in order to study the relative significance of the different factors and their possible interactions. The results of the analysis for the frequency are shown in Table 3.5.2. The full model was assumed, including all the independent variables and their interaction. As shown in this table, the main effects of all four variables were found to be statistically significant. Using the value of phase angle ratio, the analysis of variance indicates that for this data, aging and concentration show more

significant effects than other factors (temperature, frequency, and binder). The R^2 value for the model with only the main effects is 0.863 and for the full model with all two-way interactions is 0.944. Therefore it indicates that there are some interaction effects. The interaction of temperature and frequency and the interaction of temperature and aging were found to be more significant than the other interaction effects, as shown in Table 3.5.2. Using a reduced model with only these variables gives an R^2 of 0.863, which is lower than the R^2 value of 0.944 calculated for the full model with interaction effects.

Interaction terms do not seem to be as important as the standard error of estimates and the R^2 indicate a high level of goodness of fit. The first includes all main factors studied: temperature, frequency, binder, concentration, and aging. The model fit is relatively good with an R^2 value of 0.811 and a standard error of estimate of 0.032. The factor of temperature did not show a significant effect. When the temperature was dropped, as shown in the second model in Table 3.5.2, the R^2 value decreased slightly to 0.791. The last model included only three main factors (frequency, concentration, and aging), and showed a slightly decreased R^2 value of 0.790 and a standard error of estimate of 0.0336. Thus, the binder was also an insignificant factor. The simplicity of the models is also seen in the absence of interaction effects between the main factors.

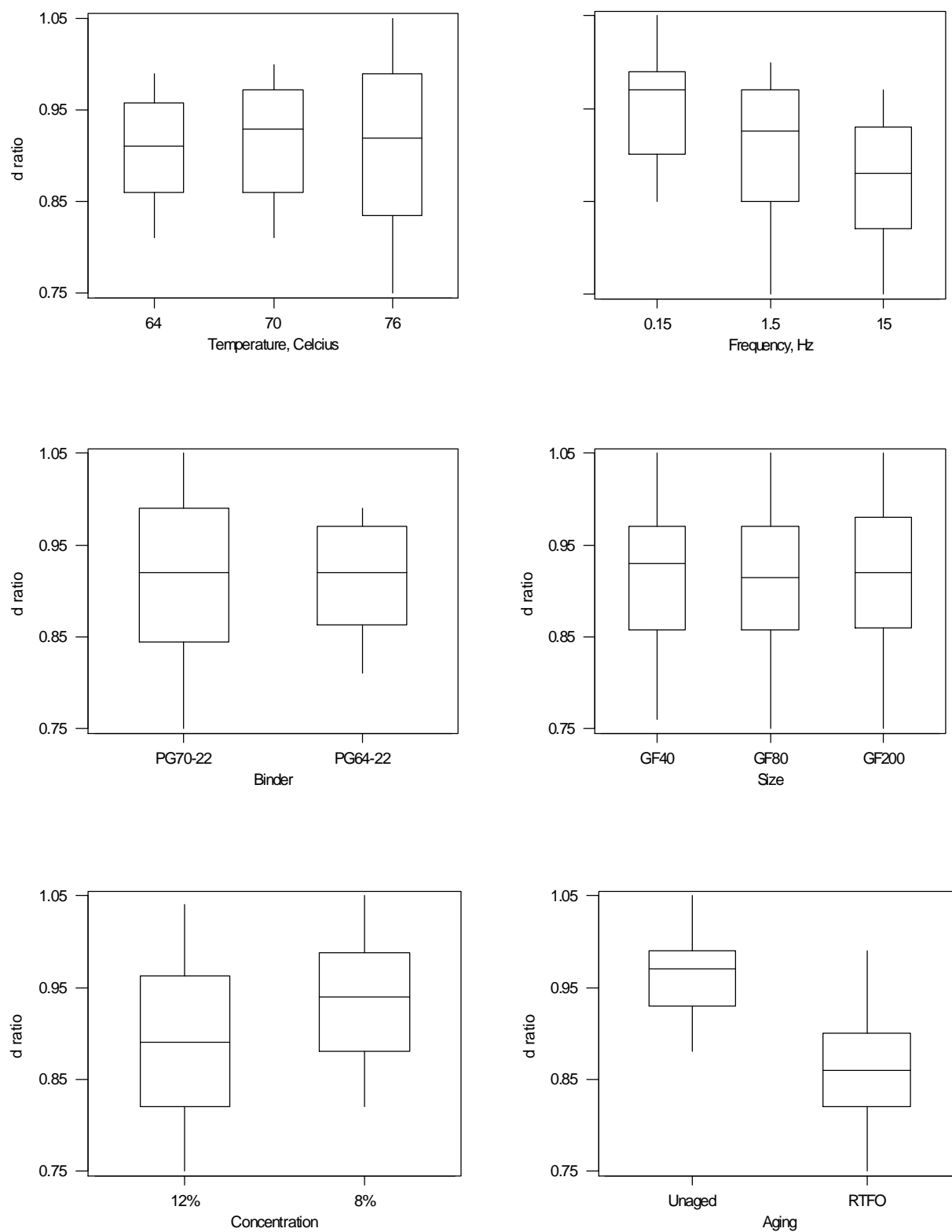


Figure 3.5.6. The box plots for dratio ($d_{\text{rubber}}/d_{\text{unmodified}}$) vs temperature, frequency, binder, size, concentration and aging

Table 3.5.2 Statistical Models for Estimation of the δ ratio for Frequency sweep

Analysis of Variance (δ ratio)					
Source of Variance	Sum of Square	d.f.	Mean Square	F-ratio	Sig.level
A : Temperature	0.00268944	2	0.00134472	3.90	0.0232
B : Frequency	0.14671243	2	0.07335621	212.72	0.0000
C : Concentration	0.06338409	1	0.06338409	183.80	0.0000
D : Aging	0.35232412	1	0.35232412	1021.68	0.0000
Interaction					
AB	0.03233352	4	0.00808338	23.44	0.0000
AC	0.00737500	2	0.00368750	10.69	0.0000
AD	0.01226259	2	0.00613130	17.78	0.0000
BC	0.00026963	2	0.00013481	0.39	0.6774
BD	0.00363333	2	0.00181667	5.27	0.0066
CD	0.00811259	1	0.00811259	23.53	0.0000
Residual	0.03655389	106	0.00034485		
Total (Corrected)	0.65387	125	$R^2 = 0.944$		
Reduced Model					
Main Effects					
A : Temperature	0.01352	2	0.00676	8.85	0.0003
B : Frequency	0.13955	2	0.06977	91.39	0.0000
C : Binder	0.01251	1	0.01251	16.39	0.0000
D : Concentration	0.07060	1	0.07060	92.47	0.0000
E : Aging	0.34760	1	0.34760	455.28	0.0000
Residual	0.09009	118	0.00076		
Total (Corrected)	0.65314	125	$R^2 = 0.863$		

Model for estimating (δ ratio)	Std. Error of Y est	Std. Error of Coefficient	R^2
For all rubbers : δ ratio = 0.72046+0.00354(T)- 0.00432(F)+0.03139(B)+0.04986(C)- 0.10524(A)	0.032	0.08464 0.00100 0.00043 0.00927 0.00598 0.00572	0.8109
δ ratio = 1.01513-0.00432(F)+ 0.00589(B)+0.04561(C)-0.10524(A)	0.0336	0.01768 0.00045 0.00614 0.00614 0.00599	0.7910
δ ratio = 1.02593-0.00432(F)+ +0.04463(C)-0.10524(A)	0.0336	0.01364 0.00045 0.00605 0.00599	0.7895
B : Binder Type (1,2=PG 70-22, PG64-22) S : Size of CRM (40,80,200) C : Concentration of CRM (1,2=12%,8%) T : Temperature (HT+3, HT, HT-3) F : Frequency (1,2,3 = 0.15,1.5,15Hz) A : Aging (1,2,3= unaged,RTFO,PAV)			

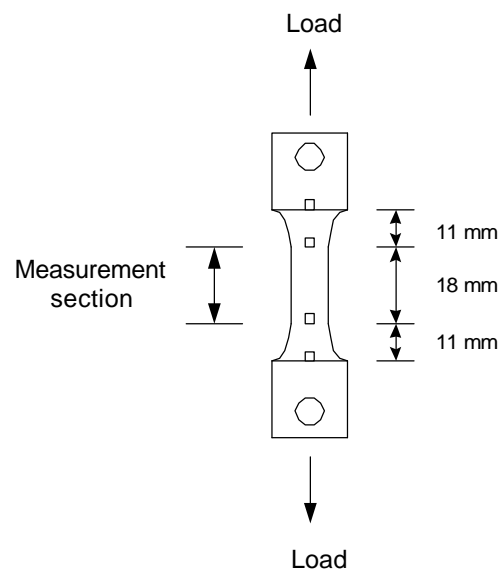
3.5.2 Low Temperature Failure Properties of CRM Binders

The Direct Tension Test (DTT) is the standard specification test that measures the failure strain and failure stress of asphalt binders. This test is performed at relatively low temperatures ranging from 0°C to -36°C, the temperature range within which asphalt exhibits brittle behavior. The asphalt binders have been aged using RTFO and/or PAV.

Consequently, the test measures the performance characteristics of binders as if they had been exposed to hot mixing in a mixing facility and several years of aging.

A small dog-bone shaped specimen as shown in the figure below is loaded in tension at a constant, strain controlled, rate. In this test, failure occurs at the point where the load on the specimen reaches its maximum value, and not necessarily the load when the specimen breaks. Failure stress is the failure load divided by the original cross section of the specimen. The SUPERPAVE binder specification requires a minimum strain at failure of one percent.

Strategic Highway Research Program (SHRP) measures the parameters of creep response and creep rate for the low pavement temperatures using a bending beam rheometer



(BBR) for the PAV-aged asphalts. However, it is not enough to use only the BBR test to present failure properties of the asphalt binders at the low temperatures. We can evaluate the low temperature ability of asphalt binders with the output of DTT, which includes failure stress and failure strain.

Typically, each asphalt binder is tested at three different temperatures and three different strain rates which can represent the effect of cooling rate. However, for this project, the optional condition was adopted, as some of binders failed to satisfy the required levels of strain set in the specification. Results, accompanied by the test condition are shown in Table 3.5.3 below.

Table 3.5.3: Results of Direct Tension Test

Binder		-6C		-12C			-18C	
		0.3%/min	3%/min	0.3%/min	3%/min	10%/min	0.3%/min	3%/min
1B2L	Stress (Mpa)	0.59	1.58	1.44	1.97			
	Strain (%)	4.51	3.19	0.86	0.43			
1B2H	Stress (Mpa)			1.16	2.48		1.79	2.03
	Strain (%)			3.36	1.59		1.16	0.60
1B4L	Stress (Mpa)	0.63	1.52	0.81	1.23			
	Strain (%)	3.54	1.99	0.91	0.53			
1B4H	Stress (Mpa)	0.52	1.58	1.14	1.54			
	Strain (%)	4.61	2.56	1.22	0.43			
2T2H	Stress (Mpa)			0.94	2.19		1.89	3.23
	Strain (%)			14.30	4.34		2.16	1.36
AC 10	Stress (Mpa)			0.98	2.19		1.99	3.05
	Strain (%)			8.14	6.16		3.73	1.56
AC 20	Stress (Mpa)				2.49	2.32	2.08	3.90
	Strain (%)				7.13	4.34	2.61	1.81

Figure 3.5.7(a) indicates that there is a reduction in the value of failure strain as temperatures decreases, for measurements taken at 3%/min strain. The failure strain measured at -12°C with the strain rate of 3%/min is shown in the Figure 3.5.7(b). It illustrates that strain is more sensitive to the types of binder than the CRM size. The failure

stress, shown in Figure 3.5.7(c) varies according to the type of binders, but it is less sensitive to the effect of binder than failure strain. As the concentration of crumb rubber increases, the failure stress increases. The effect of cooling rate on stress can be seen in the Figure 3.5.8 (a). The figure shows that there is a reduction in failure stress as the CRM size increases. This indicates that failure stress increases as the cooling rate decreases. Figure 3.5.8(b) shows the effect of cooling rate on strain, and it indicates that the failure strain decreases significantly with the rate of cooling. As the rate of cooling increases, the failure strain decreases. The summary for the results is as follows:

- Strain is more sensitive to the binder type than stress. The reacted rubber binders show significantly better failure properties than all other binders.
- As the concentration of CRM increases, the failure stress and failure strain also increase.
- There is a reduction in failure stress and failure strain as the size increases at a given temperature.
- Rate of cooling has a significant effect on failure stress and failure strain.
- Stress increases with an increased rate of cooling.
- Strain decreases significantly with an increase in the rate of cooling.

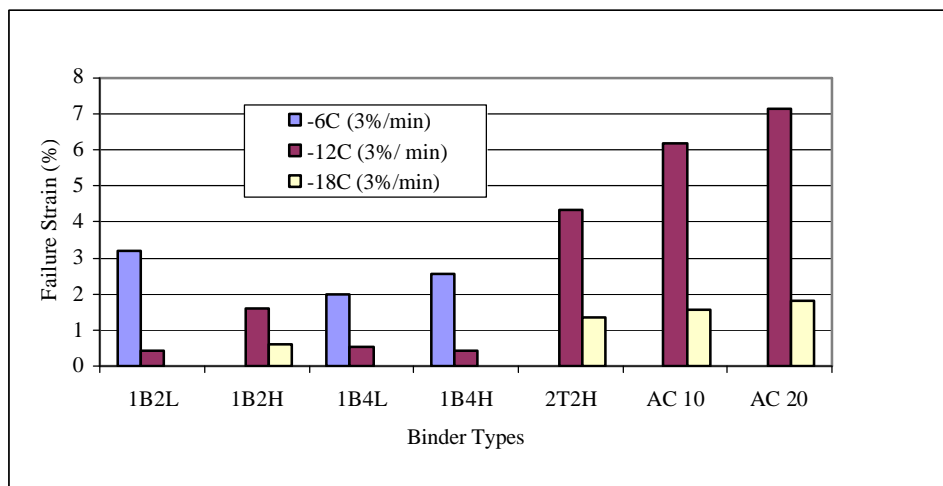


Figure 3.5.7(a) Effect of Temperatures

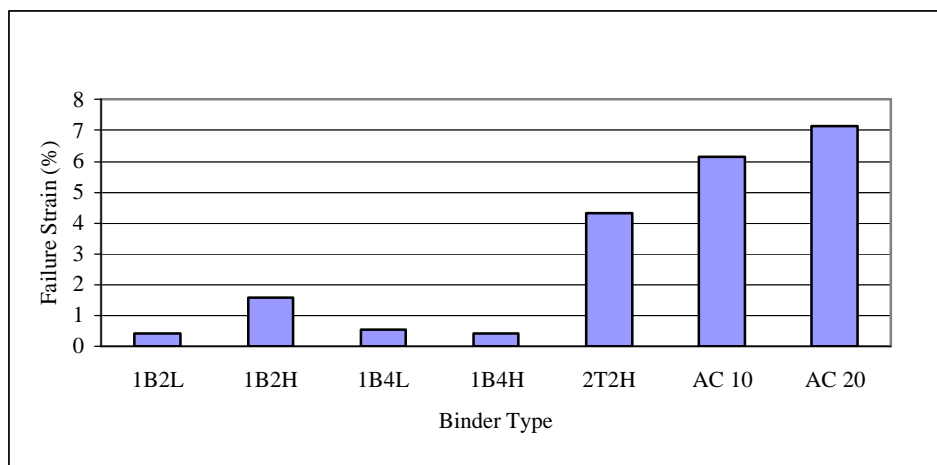


Figure 3.5.7(b) Failure Strain at -12 °C with the Rate of 3%/Min Strain

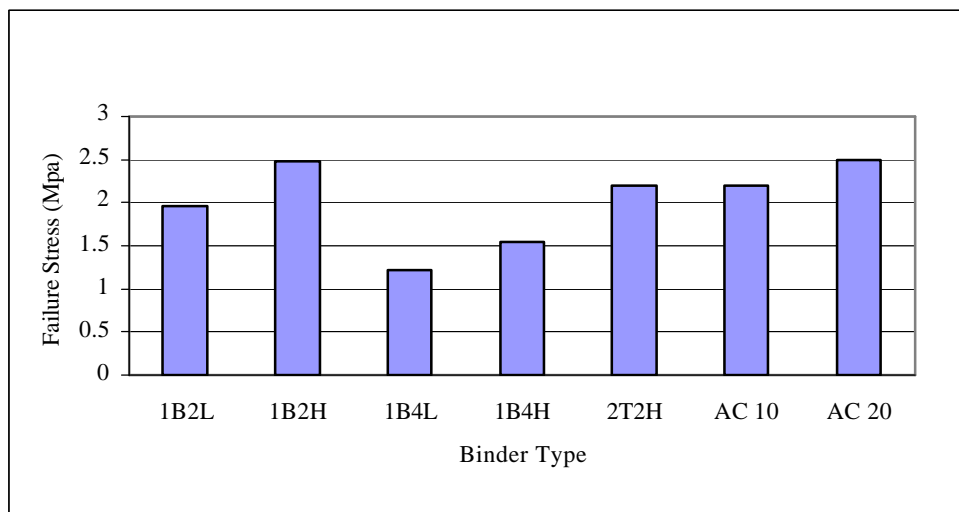


Figure 3.5.7(c) Failure Stress at -12 °C with the Rate of 3%/Min Strain

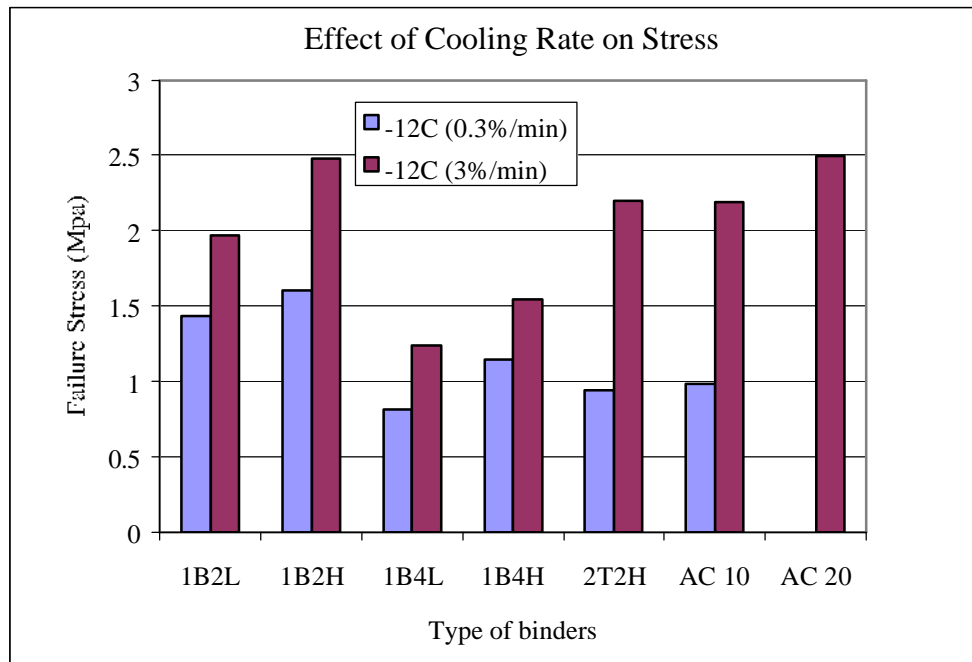


Figure 3.5.8(a) Effect of Cooling Rate on Stress

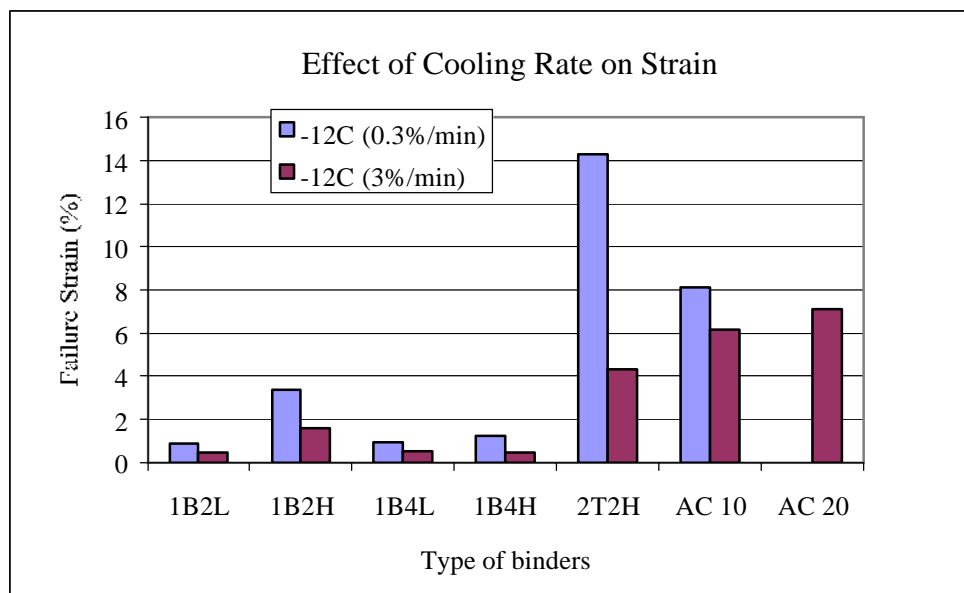


Figure 3.5.8(b) Effect of Cooling Rate on Strain

3.6 Laboratory Asphalt Stability Test (LAST)

The LAST measures the potential for separation and the potential for degradation of additives in asphalt. This procedure was developed as part of the NCHRP 9-10 project [10]. It covers the determination of the thermal stability of modified asphalts during storage at a high temperature by simulating the same conditions of the 20,000 gallon storage tank in the field. The objective of this test is to determine whether a modified binder is stable if left in storage over time. If separation occurs under static conditions using external heat, it would indicate that the binder is not stable in such conditions and that agitation is required to maintain homogeneity.

Testing the binder with agitation during sampling helps determine if the modified asphalt will be stable under such conditions. The parameters for the LAST analysis are the separation ratios (R_s), the degradation ratio (R_d), critical times for separation (T_{cs}), and degradation (T_{cd}). The critical time is the time period required for the separation or the degradation to fully develop such that changes in properties cease to occur. The separation ratios (R_s) are calculated as follows:

$$R_{sG^*} \text{ Ratio} = G^*_{Top} / G^*_{Bot} * 100 (\%) \quad (1)$$

$$R_{s\delta} \text{ Ratio} = \delta_{top} / \delta_{bot} * 100 (\%) \quad (2)$$

where G^*_{Top} and δ_{top} are the G^* and (δ) values of the binder sample from the top 1/3 of the LAST container, respectively. G^*_{Bot} and (δ_{bot}) are the G^* and (δ) values of the binder sample from the bottom 1/3 of the LAST container, respectively.

The degradation Ratios (R_d) are calculated as follows:

$$R_{dG^*} \text{ Ratio} = 0.5 * (G^*_{Top} + G^*_{Bot}) / G^*_{initial} * 100(\%) \quad (3)$$

$$R_{d\delta} \text{ Ratio} = 0.5 * (\delta_{Top} + \delta_{Bot}) / \delta_{initial} * 100(\%) \quad (4)$$

where G^*_{Top} , δ_{top} , G^*_{Bot} , and δ_{bot} are as defined before, and $G^*_{initial}$ and $\delta_{initial}$ are the G^* and δ values measured at the beginning of the test temperature. The test is conducted under a static condition or with agitation using internal or external heating. In this study, only external heating was used to simulate extreme conditions.

3.6.1 Analysis of Separation Results

Table 3.6.1 is an example of the data for the separation ratios and the critical times calculated for the static storage (with and without agitation) condition. According to the proposed procedure, changes of less than 80% or more than 120 % are considered to be significant enough to indicate a high potential for separation. The first important observation in the condition without agitation is that there are significant separation effects on G^* values ranging from a minimum of 37% at low frequency and high temperatures (HT) to a high value of 231 % at low frequency and intermediate temperatures. The effects on phase angle are minimal and mostly within the range of 80 % to 120%.

Table 3.6.1: LAST Test Results - Separation**External without Agitation (Separation)**

Modifier	DSR Test	Rs(G*) (%)			Rs (δ) (%)			Tsd (Hrs)
		0.15 Hz	1.5 Hz	15 Hz	0.15 Hz	1.5 Hz	15 Hz	
PG 70-22	HT	37	52	76	118	118	122	24
8% GF 80	6 °C	231	213	194	97	92	86	24
PG 70-22	HT	65	65	70	99	101	101	48
8% GF 200	6 °C	130	128	127	99	98	94	48
PG 70-22	HT	38	51	74	117	119	120	48
12% GF 80	6 °C	153	150	145	98	95	95	48
PG 70-22	HT	41	55	72	116	114	117	48
12% GF 200	6 °C	123	102	66	86	68	67	48
PG 64-22	HT	70	81	100	108	107	108	24
8% GF 80	6 °C	97	101	104	94	92	93	24
PG 64-22	HT	77	67	77	102	107	109	24
8% GF 200	6 °C	151	150	126	98	97	101	24
PG 64-22	HT	85	96	109	107	105	106	24
12% GF 80	6 °C	93	99	107	104	104	99	24
PG 64-22	HT	83	92	98	107	105	104	24
12% GF 200	6 °C	90	96	101	104	106	101	24
External with Agitation (Separation)								
PG 70-22	HT	101	102	100	100	100	101	24
8% GF 80	6 °C	99	95	98	100	101	106	24
PG 70-22	HT	110	108	108	98	104	101	48
8% GF 200	6 °C	114	112	110	101	101	104	48
PG 70-22	HT	99	98	101	101	101	101	48
12% GF 80	6 °C	106	106	108	103	101	100	48
PG 70-22	HT	104	103	100	99	99	99	48
12% GF 200	6 °C	95	96	99	102	104	102	48
PG 64-22	HT	114	99	103	99	99	101	24
8% GF 80	6 °C	98	100	101	102	102	100	24
PG 64-22	HT	108	102	99	99	98	99	24
8% GF 200	6 °C	98	98	99	98	101	106	24
PG 64-22	HT	110	108	106	99	99	99	24
12% GF 80	6 °C	81	88	91	104	103	104	24
PG 64-22	HT	109	108	106	100	100	100	24
12% GF 200	6 °C	94	97	96	102	100	100	24

To understand the effects of rubber variables and to compare these effects to the other effects, the box plot in Figure 3.6.1 is prepared to show the values of the separation ratio (R_s) in terms of G^* and the use of external heat without agitation at HT. The findings are as follows:

- Both binders show separation ratios below 100 %, indicating that rubber particles are settling during storage. The ratios for the PG 70-22 binder are much lower than the ones for the PG 64-22 binder, which indicates more separation for the PG 70-22 binder. These two binders are very different in their chemical composition, which is an expected result. The differences are significant and indicate that the binder composition is an important factor in storage stability.
- All rubber sizes and concentration show important separation effects as the average values are below 80 %.
- Crumb rubber factors (i.e., size and concentration), however, do not appear to be significant. The box plots show that the averages are similar for the three sizes and the two concentrations used. There are variations in the range of values, which imply that some interactions can be important.
- There is an important effect of frequency. High frequency values show less separation compared to low frequency values. It appears that the shape of the frequency sweep curve is changing such that the G^* values at a lower frequency are more likely to be affected by separation compared to the values at a high frequency.

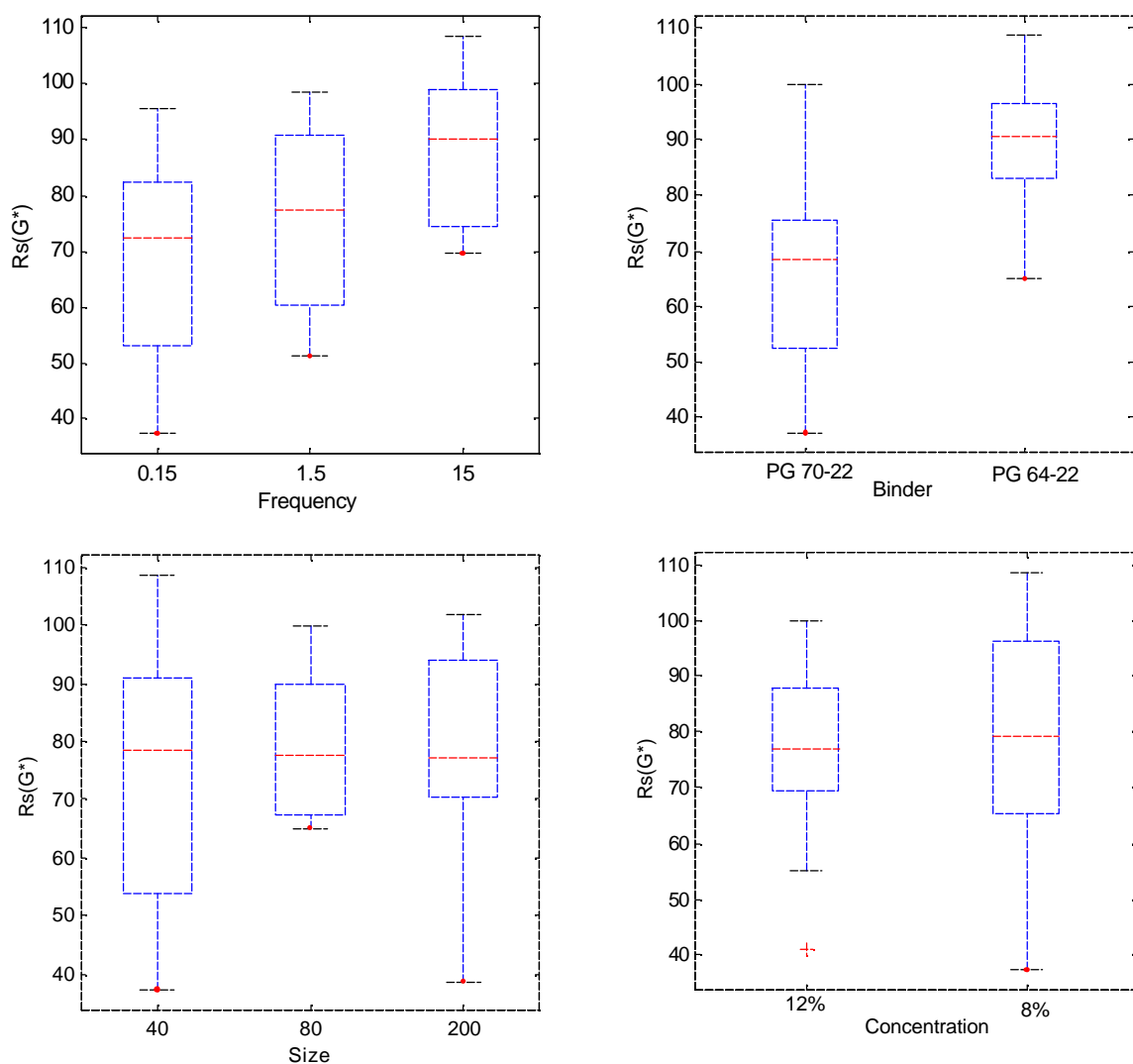


Figure 3.6.1: The Box Plots for the External without Agitation (separation ratio) at HT vs Frequency, Binder, Size, and Concentration

Table 3.6.1 also shows the separation ratios with agitation. Changes in the G^* values are all within the range of 80% to 120%, indicating a low potential for separation for all combinations of binders, rubber sizes, and concentration. This is a very important improvement, which suggests that maintaining adequate agitation could solve all potential separation problems.

3.6.2 Analysis of the Degradation Ratio

As mentioned earlier, using the data collected, an evaluation of the possible degradation or continued reaction could be determined from the LAST data. Table 3.6.2 is prepared to show the values of R_d in terms of G^* and phase angle for all the combinations of binders and rubbers under no agitation conditions. The results shown indicate that there are significant effects ranging from an R_d value of 195 % to 54 % in terms of the G^* . Most of these changes are the result of separation that was discussed previously. Similar to the separation results shown in Table 3.6.1, the effect on phase angle is minimal.

Table 3.6.2: LAST Test Results - Degradation
External without Agitation (Degradation)

Modifier	DSR Test	$R_d (G^*) (\%)$			$R_d (\delta) (\%)$		
		0.15 Hz	1.5 Hz	15 Hz	0.15 Hz	1.5 Hz	15 Hz
PG 70-22 8% GF 40	HT	162	130	109	94	93	94
	6 °C	89	94	102	102	106	110
PG 70-22 8% GF 80	HT	76	83	96	100	102	103
	6 °C	87	83	85	96	96	100
PG 70-22 8% GF 200	HT	131	104	87	92	91	92
	6 °C	78	76	74	97	98	102
PG 70-22 12% GF 40	HT	116	112	97	95	93	93
	6 °C	77	68	54	88	80	80
PG 70-22 12% GF 80	HT	136	114	101	104	103	103
	6 °C	74	79	86	99	99	99
PG 70-22 12% GF 200	HT	191	132	102	87	85	86
	6 °C	94	89	72	94	95	101
PG 64-22 8% GF 40	HT	145	125	95	90	90	88
	6 °C	122	117	118	97	96	97
PG 64-22 8% GF 80	HT	171	130	101	88	89	91
	6 °C	120	114	112	97	96	99
PG 64-22 8% GF 200	HT	115	111	105	99	98	98
	6 °C	110	109	115	98	98	98
PG 64-22 12% GF 40	HT	114	103	95	96	96	97
	6 °C	102	101	102	99	100	101
PG 64-22 12% GF 80	HT	152	121	98	91	90	90
	6 °C	103	91	88	96	98	102
PG 64-22 12% GF 200	HT	139	119	103	88	91	94
	6 °C	195	154	138	82	82	67

Table 3.6.2: LAST Test Results– Degradation (Cont'd)**External with Agitation (Degradation)**

Modifier	DSR Test	R _d (G*) (%)			R _d (δ) (%)		
		0.15 Hz	1.5 Hz	15 Hz	0.15 Hz	1.5 Hz	15 Hz
PG 70-22	HT	134	123	108	97	95	94
8% GF 40	6 °C	112	107	106	101	100	102
PG 70-22	HT	106	102	98	98	98	99
8% GF 80	6 °C	120	114	112	95	94	92
PG 70-22	HT	113	115	103	98	98	96
8% GF 200	6 °C	103	101	102	98	97	99
PG 70-22	HT	118	107	98	96	95	95
12% GF 40	6 °C	92	96	96	102	102	103
PG 70-22	HT	132	124	108	96	94	92
12% GF 80	6 °C	96	94	95	98	99	102
PG 70-22	HT	132	123	106	93	92	92
12% GF 200	6 °C	104	99	94	96	95	96
PG 64-22	HT	122	112	105	97	97	97
8% GF 40	6 °C	109	106	107	101	100	104
PG 64-22	HT	115	108	101	97	97	96
8% GF 80	6 °C	85	93	112	107	107	108
PG 64-22	HT	129	117	102	97	95	94
8% GF 200	6 °C	98	99	99	98	101	106
PG 64-22	HT	129	119	100	94	93	92
12% GF 40	6 °C	95	95	95	101	102	105
PG 64-22	HT	125	100	87	92	92	93
12% GF 80	6 °C	92	94	102	101	102	106
PG 64-22	HT	133	106	96	100	99	91
12% GF 200	6 °C	83	86	94	103	104	105

To study the effect of agitation on degradation ratios, Table 3.6.2 is prepared to show the values for G* and phase angle under the agitation condition. It appears that, although agitation can solve the potential for separation, degradation continues during storage. Several binders, particularly those tested at a low frequency, show ratios in excess of 120 %. The highest ratios are shown at high temperature and low frequency. The effects at intermediate temperatures are less than those at high temperatures. A summary of findings from the separation and degradation measured using the LAST is as follows:

- Base asphalt source appears to play an important role in the separation and degradation under static storage conditions. The effect is different at high temperatures than at intermediate temperatures.
- Agitation can significantly reduce the separation effects for almost all combinations of temperature, rubber size, and frequency.
- Neither rubber size nor concentration shows specific trends in the separation and degradation analysis. It appears that all CRM binders will separate if no agitation is involved. There are minor differences in the degradation results, indicating that finer rubber could show more degradation.
- Frequency is important for both separation and degradation. This indicates possible continued reaction during storage that results in changing the rheological type of the binder. The effect of frequency is also important in the case of degradation during storage with agitation, which confirms the theory of possible continued reaction.

CHAPTER 4 : SUMMARY OF FINDINGS OF PART I

4.1 Summary of Findings

This research was focused on the evaluation of using crumb rubber (CRM) to modify asphalt binders. The evaluation was conducted by measuring the change in performance-related properties of the selected asphalt binders as a result of mixing various levels of CRM content and particle with asphalts. Testing was conducted at different temperatures, testing frequencies, and strain conditions using methods recently developed as part of the NCHRP 9-10 project (Superpave Protocols for Asphalt Binders). Statistical analysis was used to develop models that predict the nature of effects on the performance-related properties of asphalts and that can quantify the role of different variables. The following sections summarize the findings of this study.

4.1.1 Viscosity Results

- Concentration of CRM is found to have a statistically significant effect on the increase in viscosity. The increase in some cases result in exceeding the allowable limits used currently in the Superpave specifications.
- The results indicate that the size of the crumb rubber has a significant effect on viscosity. The trend shows that viscosity values of binders with smaller particle size are higher than binders with larger particle size. The effect is more pronounced at higher crumb rubber concentrations. The effect of the size, however, is less than the effect of the concentration.
- The effect of concentration and size are very important. For example changing from 8% rubber to 12 % for the 200 mesh size result in increasing the critical viscosity temperature

by 18 °C for the Boscan asphalt and by 22 °C for the Texas blend asphalt. Changing the size from 40 mesh to 200 mesh at the same concentration of 12 % result in changing the critical temperature by 6°C in case of the Boscan asphalt and by as much as 10 °C in case of the Texas blend asphalt.

- All CRM binders display a significant dependency on the shear rate. There is, however, no consistent trend related to the size or concentration. It appears that the strain dependency is binder specific because the Texas blend binders show higher dependency at high concentrations than the Boscan while the opposite is true at low concentration. The reacted rubber binders also show high shear rate dependency.
- It is observed that there are many interactive effects on viscosity. The statistical analysis shows that 8 of the 2-way interactions and 3-way interactions are clearly statistically significant.

4.1.2 The Particulate Additive Test Results

A new test called the Particulate Additive Test (PAT) is introduced to separate additives from asphalts and measure their effective volume. The results collected indicate that the rubber size has a significant effect on the volume of residue collected. The variation between the volume extracted and the expected value is due to possible variability during the sampling of the modified binder and the possible interactions with the asphaltenes in the asphalt. It is reasonable to assume, based on the results that the rubber particles undergo a certain amount of swelling.

4.1.3 Mechanical Working Dependency Results

- CRM binders have high mechanical working dependencies. It is found that the addition of rubber in all cases increased the dependency of binders on mechanical working.
- Using the relative change in G^* between 50 cycles and 5000 cycles (G^* ratio) as an indicator, it is found that the effect of CRM on the G^* ratio is found to depend on asphalt binder type, concentration of CRM, and strain.
- The main effect of strain is found to be the most important factor followed by rubber content and the asphalt binder type. When the high strain level is selected, the G^* ratio has a higher value than at the low strain. The interaction of the binder with strain and the interaction of concentration and strain were found to be significant.
- The effect of CRM on the δ ratio measured from the mechanical working test results was found to be dependent on the asphalt binder type and strain. The effect of strain is found to be more important than the binder. A linear regression model with interaction terms was found to give a good estimate of the change in the δ ratio. The interaction between size and strain was found to be significant.

4.1.4 Strain Dependency Results

- Using the ratio of G^* and δ values at high strains to low strain the strain dependency of the binder at high and intermediate temperatures were calculated. Based on the results, all CRM binders are found highly dependent on strain.
- A few factors are found to affect the G^* ratio for the strain dependency. The temperature is found to be the most important factor followed by the asphalt binder type and rubber

size. At the intermediate temperature, the G^* ratio is more strain dependent than at high temperature.

- The rate of change in the G^* ratio for the strain dependency can be positive or negative depending on the asphalt properties, plate and size, which indicates that the interaction effects between the factors are important.
- The effect of variables on the δ ratio for the strain dependency is similar with that of the G^* ratio. The significant main effects are the asphalt binder type and the temperature. The effect of temperature was found to be the most significant. The effect of rubber size is found to be negligible. It could be assumed that the interaction effects are not so important in this analysis.
- The statistical analysis indicates that the testing geometry is not an important factor because the overall average of the two geometries used are very close. The variation in the range is significantly higher for the parallel plate. This could be explained by the variation in applied strain in this geometry.

4.1.5 Frequency Testing at High and Intermediate Temperatures

- Using the ratio of G^* and δ of the CRM binders relative to the base binder (no rubber) the effect of CRM on binder properties were evaluated. The effect on the G^* ratio for frequency at high and intermediate temperature was found to be highly dependent on temperature, frequency, binder type, and concentration. The concentration of CRM appears to have the most significant effect.

- There are interaction effects between the binder and aging for the test of frequency sweep since the change of the G^* ratio can be positive or negative depending on the binder type and aging.
- The effect of CRM on the δ ratio for frequency was found to be highly dependent on temperature, frequency, binder, concentration, and aging. Aging shows to be the most important effects followed by concentration and frequency. It indicates that there are some interaction effects since there is a large difference in the value of R^2 between a full model with interaction effects and a reduced model.
- The critical temperatures calculated from the results of frequency sweeps are found sensitive to frequency, binder, concentration, and aging. The effect of frequency is higher at high testing temperatures compared to the intermediate testing temperatures.
- The frequency sweeps were used to calculate the time-temperature shift factors. There is no specific trend in the values of the shift factors that could be associated with the types of binder, CRM particle sizes, concentrations of CRM, and aging conditions.

4.1.6 Creep and Direct Tension Testing at Low Temperatures.

- The effect of CRM on creep response at low temperatures was measured using the Bending Beam Rheometer. The creep response of CRM binders was found to be sensitive to temperature, the time of loading, binder, size and concentration of rubber. The effects of temperature and time of loading are considerably more significant than other factors. Although the effect of size was found to be statistically significant, it can be considered minimal compared to the other factors. The effect of concentration is significantly higher

than the size for the Texas blend asphalt compared to the Bosacn asphalt. The effects are highly interactive and highly dependent on aging of the binders.

- The critical temperature for the creep stiffness (S) and the creep rate (m) was found to be highly dependent on the loading time and the asphalt binder type. The critical temperatures decrease with increasing the loading time. For certain binders, the concentration of the rubber made a significant difference.
- The critical temperature for the m-value was found to be more dependent than the critical temperature of the stiffness on aging and rubber size. The effect of concentration is found to be negligible in most cases.
- The effect of CRM variables on failure properties, as measured using the Direct Tension Test device (DTT), was also found to be significant. Higher strain at failure and higher stress at failure values are measured with increasing concentration of CRM.
- The failure stress is found to reduce with increasing rubber size. It is found to increase with rubber concentration. The effects in both cases are however less than the effect of the testing rate (change from 0.3 % to 3.0%). Failure stress increases with increasing testing rate.
- The failure strain, similar to failure stress, is found to reduce with size of the rubber and increase with concentration. The effects are smaller than the effects of changing the testing rate.
- The chemically reacted rubber asphalts show superior failure properties in many cases. Strain at failure is particularly high for these binders.

4.1.7 The Storage Stability Test Results

- The Laboratory Asphalt Stability Test (LAST), as developed by the NCHRP 9-10 project, was used to measure the potential for separation and for degradation of additives in asphalt during high temperature storage.
- All rubber sizes and concentrations show important separation effects, as the average values are below 80%. It is found that the different CRM sizes and concentrations, however, have a minimal effect on the separation potential and degradation potential of the binder. The box plots show that the averages for the three sizes and the two concentrations used are similar. There are variations in the range of values, which suggest that some interactions can be important.
- There is an important effect of frequency: higher frequency values show less separation compared to lower frequency values. It appears that the shape of the frequency sweep curve is changing so that the G^* values at lower frequencies are more affected by separation compared to higher frequencies.
- Agitation changes separation results significantly. For most binders, the effects of separation with agitation are negligible and do not exhibit any specific trend.
- Although agitation can solve the potential for separation, degradation (continued reaction) continues during the storage. Several binders, particularly at a low frequency, show ratios in excess of 120 %. The highest ratios are shown at high temperature and low frequency. The effects at intermediate temperatures are smaller than those at high temperatures. This is an indication that continued reaction results in these changes. It is important to notice that there is an influence of the binder type in these changes, which confirms the reaction theory.

4.2 Summary for Construction Applications

- CRM's result in increased viscosity at pumping and mixing temperatures. This effect is not favorable, since it makes the pumping of binders, mixing, and compacting of HMA produced with these modified binders more difficult. The benefit of increased viscosity of the asphalt-rubber binder is that additional binder can be used in the asphalt mix to reduce reflective cracking, stripping, and rutting, while improving the binder's response to temperature change and long-term durability, as well as its ability to adhere to the aggregate particles in the mix and to resist aging.
- Adding CRM for highway applications is favorable for rutting resistance. CRM results in increased values of $G^*/\sin\delta$ depending on testing temperature. The increase in $G^*/\sin\delta$ is significant and is considered very favorable with respect to increasing the contribution of binders to resist rutting.
- CRM is also favorable for resistance to thermal cracking at low temperature. The ductile properties of the modified binder enhance the mixture's ability to resist tensile stresses.
- The addition of CRM to binder results in improving the binder's durability. In addition, these binders are more viscous and typically retain thicker binder films on the aggregate. The thicker film delays the detrimental effect of oxidation.

4.3 Limitation of Current Research and Suggested Future Work

The Superpave binder specification is based on the simplification of assumptions which might not be valid for all asphalt binders, particularly modified asphalt like crumb rubber. This study is performed to determine the effect of particle size and content of CRM binders at different temperatures using the new tests. These tests represent an extension of

the applicability of the Superpave system and also include methods for evaluation of storage stability.

The role of CRM binders in pavement performance, however, cannot be estimated based only on binder testing because geometric and loading conditions of binders in mixtures cannot be simulated in a simple binder test. The mixture testing should be conducted to evaluate the effects of CRM. These findings should not be generalized and may not apply to other combinations of asphalt and crumb rubbers since these results only focused on the rheological properties of CRM binders.

The statistical models that were developed in this research should not be used to predict the effects of CRM on different types of mixtures because they are simplified models based on the assumption of linear regression. The models are introduced as a contribution to the body of knowledge about the behavior of asphalt binders modified with crumb rubber.

CHAPTER 5: MIXTURE TESTING

5.1 Study Objectives

The objectives for this task were to evaluate the Superpave mix design mixing and compaction requirements for crumb rubber modified asphalt binders. There are a number of challenges that need to be addressed when using crumb rubber modified (CRM) binders in asphalt mixtures. In this study the following issues were investigated:

- Volume change due to rebound effects of the CRM mixtures
- Effects of CRM size, CRM concentration, aggregate gradation, and aggregate source on mix densification and frictional resistance curves
- Effects of temperature on compaction of CRM mixtures

The results of this study were used to make comparisons between mixtures containing different levels of CRM concentrations, and different CRM particle sizes. It also considered the effects of aggregate source as well as the aggregate gradations. More specific information on the levels of the control variables is reported in the next section, where the experimental plan is discussed.

The rebound effects of the CRM mixtures are investigated by measuring the swelling potential of the mixtures. This is done by measuring the volume change in the mixtures before and after cooling.

The current standard method for preparing specimens using the Superpave Gyrotory Compactor (SGC), AASHTO TP4-93, specifies the mixing temperature range to be such that the viscosity of the unaged asphalt binder is 170 ± 20 mm²/s, and the compaction temperature range to be where the viscosity of the unaged binder is 280 ± 30 mm²/s. For CRM binders, these viscosity ranges are not achievable unless the binder is heated to a very high

temperature. Overheating of the asphalt binder may result in excessive aging, and sometimes degradation of the modifier. Therefore, the effect of compaction temperature is studied.

5.2 Experimental Testing Plan

The control variables in the mixture tests were aggregate source, aggregate gradation, and crumb rubber modified binder (which includes crumb rubber size and concentration).

These variables are represented in the Table 5.2.1.

Table 5.2.1 Mixture Control Variables

Variable	Levels
Aggregate Source	2 (crushed aggregates and gravel)
Aggregate Gradation	2 (12.5 mm Coarse and 12.5 mm Fine)
Crumb Rubber Size	2 (GF 200 and GF 40)
Crumb Rubber Content	2 (8 % and 12 % by weight of asphalt binder)

Two sources of aggregates were used, similar to Phase III of the NCHRP 9-10 research project. One set of aggregates was from the Asphalt Institute and the other was from NCAT. Both aggregate blends have a nominal size of 12.5 mm. This aggregate size was selected since it was commonly used in wearing course mixtures for high traffic pavements. The smaller nominal aggregate size also makes specimen preparation easier. Two aggregate gradations were selected. For this study, a fine gradation and a coarse gradation were selected, as shown in Figure 5.2.1. One asphalt binder content was selected for each aggregate blend, which represents the optimum asphalt content as determined by this mix design using the unmodified control asphalt. This asphalt content was determined based

on the Superpave volumetric mix design procedures to achieve 4.0 % air voids at the design number of gyrations (100 gyrations) for the unmodified (PG 70-22) asphalt binder. The mix design details are described in Table 5.2.2.

Table 5.2.2 Mix Design

	NCAT Aggregates		AI Aggregates	
Size Fraction	Fine Gradation	Coarse Gradation	Fine Gradation	Coarse Gradation
AC Content (%)	4.8	4.7	4.5	4.8
Gsb	2.623	2.623	2.700	2.700
Nini	8	8	8	8
Ndes	100	100	100	100
Nmax	160	160	160	160

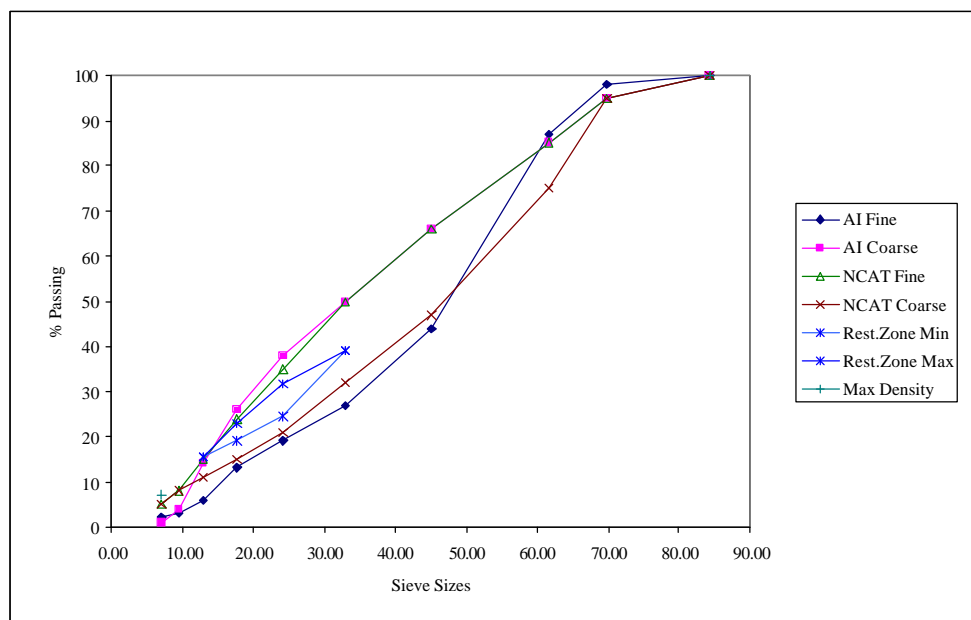


Figure 5.2.1 Aggregate Gradation on 0.45 Power Chart

The complete matrix for the research is shown in Table 5.2.3. All mixtures were compacted to N_{des} , N_{max} , and 600 gyrations. With the exception of mix type 1 and 7, all the aggregates and binders were mixed at 165 °C and compacted at 160 °C. Mix type 1 was the control mix, and it was mixed at 155 °C and compacted at 155 °C. Samples of mix type 7 were mixed at 165 °C and compacted at 80 °C. This was to allow for a consideration of the effect of temperature on the behaviour of the mixture during the compaction procedure.

Table 5.2.3 Mixture Compaction Test Matrix

Mix Type	CRM Binder	NCAT Aggregates (Gravel)		Asphalt Institute Aggregates (Crushed Aggregates)	
		12.5 mm Fine	12.5 mm Coarse	12.5 mm Fine	12.5 mm Coarse
1	PG 70-22 (unmodified)	X	X	X	X
2	1B4H	X	X	X	X
3	1B4L	X	X	X	X
4	1B2H	X	X	X	X
5	1B2L	X	X	X	X
6	FHWA CRM	X	X	X	X
7	1B4H @ 80 °C	X	X	X	X

Notation: 4 – GF 40 CRM Size 2 – GF 200 CRM Size
 L – Low (8%) CRM Content H – High (12%) CRM Content
 FHWA – Patented reacted rubber from FHWA, 6% CRM content

The Superpave Gyratory Compactor (SGC) was used to compact the mix specimens. Along with the SGC, a device for measuring frictional resistance of hot mix asphalt in the SGC, known as the Gyratory Load-cell Plate Assembly (GLPA), was used. This device was developed by the University of Wisconsin-Madison Asphalt Research Group as part of a project funded by FHWA (27). The GLPA and the software that supports its application

enables the measurement of the work required to gyrate the specimen and the resulting vertical load eccentricity in real time. This leads to analysis such that the interaction between rubber and aggregates can be understood and therefore the change in compaction effort for CRM mixtures can be studied. It is believed that frictional shear resistance is related to rut resistance. Data generated from the GLPA could provide information on the effect of CRM modifiers on the compaction of mixtures and the rut resistance of pavements under traffic.

CHAPTER 6: TEST PROCEDURES

6.1 Mixing and Compaction

The asphalt mixtures were prepared and compacted in accordance with Superpave specified procedures.

First the aggregates and asphalt binder is heated in the oven until the mixing temperature is achieved. The aggregates are then weighed in the mixing bucket and the required amount of asphalt binder is computed based on the asphalt content for each aggregate blend. The asphalt is added to the aggregates, and mixed for 4 minutes, until the aggregates are completely coated. The asphalt mixture is then returned to the oven to be conditioned for 2 hours.

During the time the mixture is being conditioned, the mold for the SGC is heated in the oven to compaction temperature. After the mixture has been conditioned for the required amount of time, it is ready for compaction. The mold is removed from the oven, and the mix transferred into the mold. The SGC is set to compact to the desired number of gyrations, 100 (N_{des}), 160 (N_{max}), or 600 gyrations. The load cell is placed at the top of the mix, separated by paper, and the mold set in its slot in the SGC. The computer software is activated, and SGC started.

When the compaction is completed, the load cell is carefully removed from the top of the specimen, and the specimen is then carefully extruded from the mold.

6.2 Rebound Effects of Crumb Rubber Modified Mixtures

After the compacted specimen has been removed from the SGC mold, it is prepared for height and diameter measurement. Measurements are made within 15 minutes of the

completion of the compaction. This allows the specimen to set for a short time such that the aggregates do not come apart upon handling.

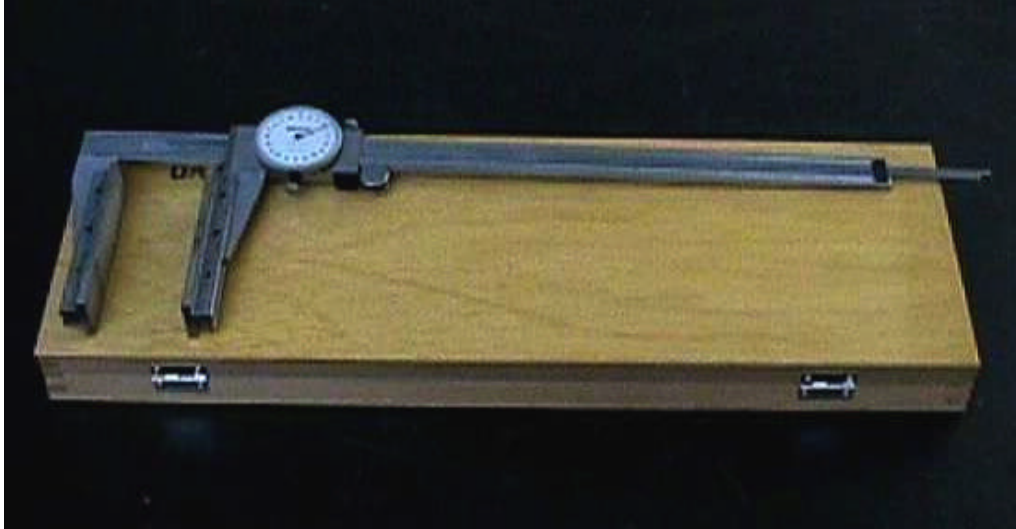


Figure 6.2.1 Modified Calipers for Dimension Measurements



Figure 6.2.2 Jaw of Calipers Attached with Metal Plates

In order to ensure more accurate measurements of the specimen heights and diameters, a set of dial gauge calipers was modified as shown in Figures 6.2.1 and 6.2.2. A metal plate 2.5 mm wide, 8.9 mm long was attached across each jaw of the caliper. This helps to reduce the potential that the jaws may press into the specimen or fall in a void in the specimen and thus result in measurements that may be unusually low.

First, the specimen is labeled. Then the measurement locations are marked with numbers and crosses. The numbers 1, 2, 3, and 4 are written at four equally spaced locations along the top and on the side of the specimen. Under each of the numbers 3 and 4, two crosses are marked, the first at 1 inch from the top of the specimen and the other at 1 inch from the bottom of the specimen. Figure 6.2.3 shows a compacted specimen with the locations for measurements indicated and numbered.



Figure 6.2.3 Locations Where Measurements are Taken are Marked on the Compacted Specimen

After the specimen has been labeled and measurement locations marked, the measurement begins with the diameter, as seen in Figure 6.2.4. This is done with reference to the crosses. The diameter is determined by placing one end of the dial gauge caliper on the cross immediately under the number 3. The caliper is adjusted until it makes contact with the specimen, being careful to keep the caliper faces flat along the specimen surface. This process is repeated at the cross away from the number 3, then the two crosses under the number 4.



Figure 6.2.4 Measurement of Diameter Taken Using the Modified Calipers

The specimen is then turned on its side to begin measurement of the heights. Care was taken to make sure that the platform surface is clean to prevent undesirable fine particles from sticking to the side of the specimen and influencing the subsequent measurements.

Height measurements were taken at points located by the numbers. These heights and diameters are recorded as initial values.

The final values are taken 24 hours after the initial values are taken. The same measuring procedures are followed, with measurements taken at the same points the initial measurements were made.

6.3 Frictional Resistance Measured Using a Gyrotory Load-Cell Plate Assembly (GLPA)

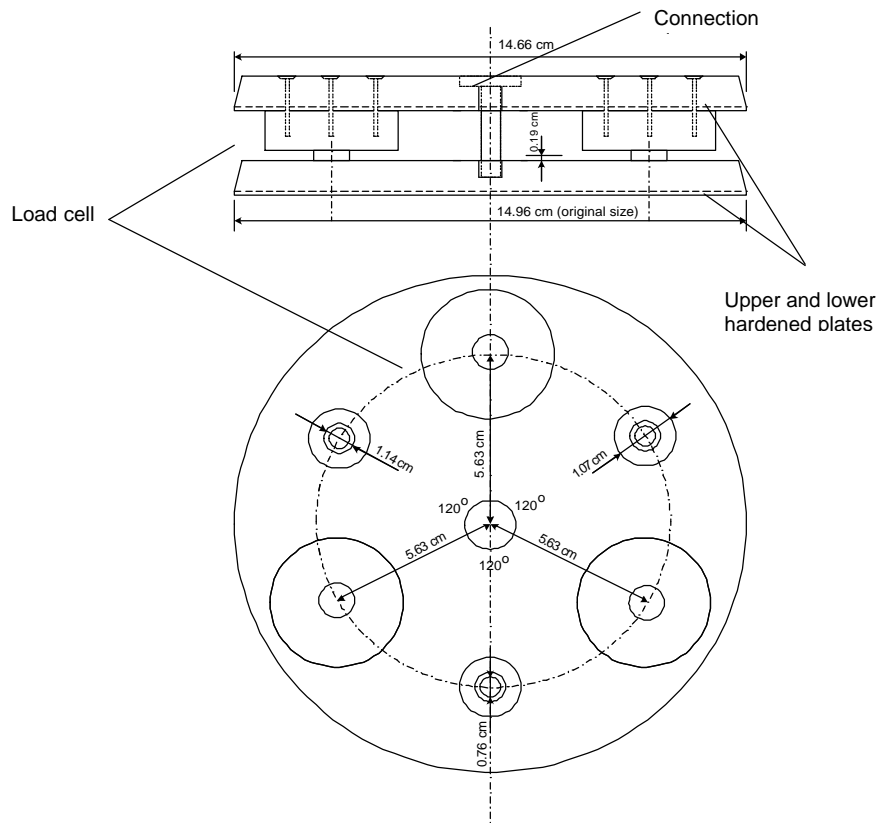


Figure 6.3.1 Sketch of Gyrotory Load Cell Plate Assembly (27)

The frictional resistance of a mix is calculated from data collected using a Gyrotory Load Cell Plate Assembly (GLPA) during compaction. Figure 6.3.1 is a sketch of the GLPA. The plate includes 3 load cells spaced equally on the perimeter of a double-plate assembly, which can be inserted in a typical gyratory mold on the sample of the HMA. During compaction, readings are taken from each load cell, and the data is recorded using a data acquisition system controlled by a graphical programming language LabVIEW®.

The load cells measure the variation in the distribution of forces on top of the sample during each gyration such that the position of the resultant force from the gyratory compactor can be determined in real time. The effective moment required to overcome the frictional resistance of mixtures is calculated using the two dimensional distribution of the eccentricity of the resultant load. It is believed that this effective moment is a direct measure of the resistance of asphalt mixtures to distortion and to densification.

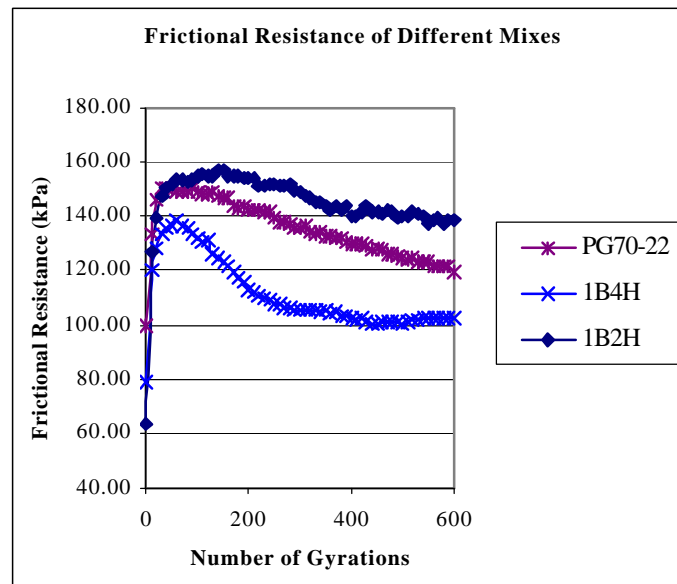


Figure 6.3.2 Varying Frictional Resistance for Different Mix Types

Different mixes will offer differing levels of frictional resistance to distortion and densification initially. This level of frictional resistance can be maintained for high number of gyrations for some mixes. For other mixes, the level of frictional resistance decreases more significantly with increasing number of gyrations. Examples of the variation in frictional resistance are illustrated in Figure 6.3.2.

CHAPTER 7: ANALYSIS OF RESULTS AND DISCUSSIONS

In this section samples of the results collected for each type of measurement are presented and discussed. The main trends are described with regard to the effect of the crumb rubber characteristics and the aggregate characteristics. It is expected that there are interactions between these two variables.

7.1 Results of Volume Change

The percent volume change was calculated using the height and diameter measurements collected, as described earlier. It is assumed that the first measurement, which was done within 15 minutes of compaction, was taken at the compaction temperature. The second measurement, which was taken after 24 hours, represents the sample size at room temperature. The percent volume change is obtained from dividing the difference in the two volumes by the initial volume.

The values presented in this report are from singular specimen measurements. To study the consistency and repeatability of the measurements and calculations, two sets of samples were duplicated and tested. For the first set of duplicate samples, the volume changes for each specimen were -0.009% and -0.018% . For the second set of duplicate samples, the values were -0.134% and -0.141% . This limited testing indicated that the measurements are repeatable and consistent when taken under same temperature conditions. Based on these test results, an assumption was made that the measurements could be assumed consistent to within $\pm 0.01\%$ of the volume. Therefore, a decision was made to take only one measurement for each specimen type.

A concern regarding volume change was that the use of CRM in asphalt mixtures might lead to a rebound phenomenon, with an increase in volume during the cooling stage. Figures 7.1.1 (a) through 7.1.1 (d) show the volume change results for all the mixtures tested in this study sorted by the aggregate gradation and source. The results indicate that for almost all mixtures, including the control mixtures with no rubber, there is a reduction in volume, rather than swelling.

It appears from the data collected that this concern about swelling of the rubber mixtures due to rebound of the rubber is unfounded. Contrary to prior expectations, the measurements from the specimens show a contraction in volume, which translates to an increase in density in the compacted mix. The changes in volume are in the range of -0.003% to -0.486% of the volume of fresh specimens, which translates to absolute volume changes of between 64 mm^3 and $10,320\text{ mm}^3$.

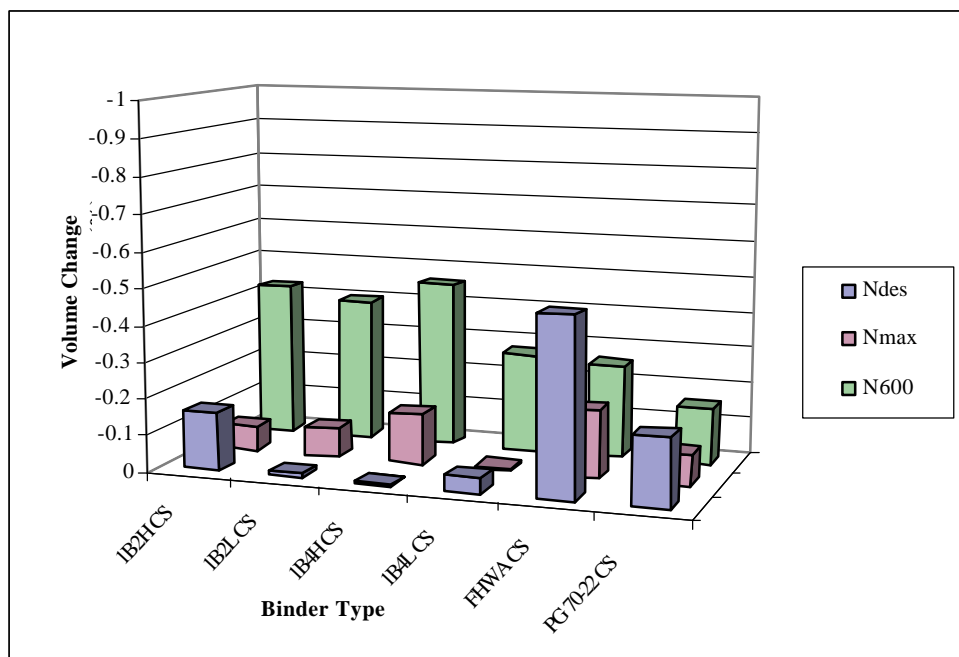


Figure 7.1.1 (a) Volume Change – Coarse Gradation Gravel Specimens

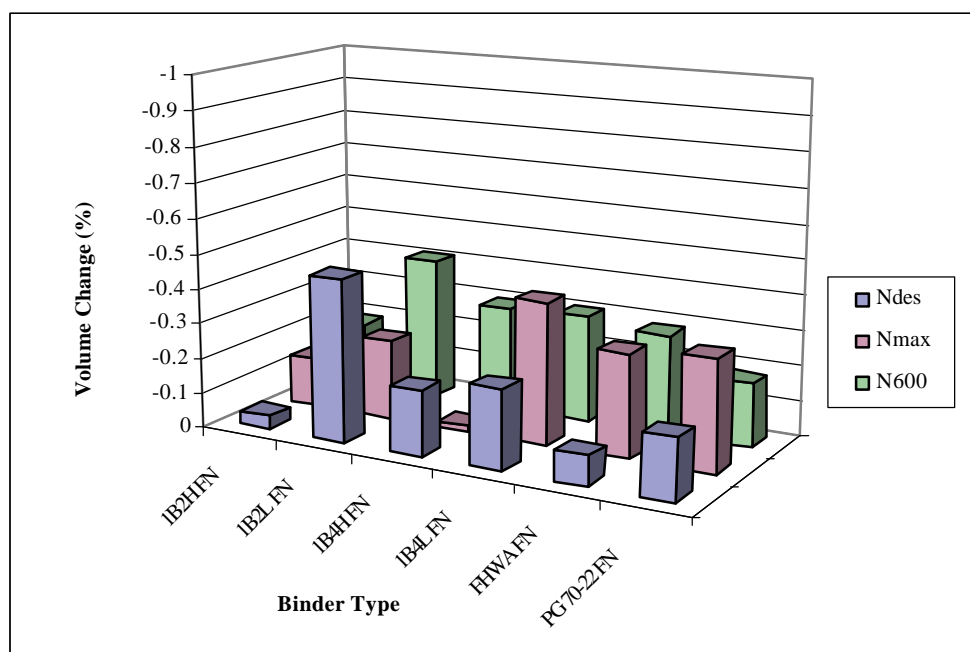


Figure 7.1.1 (b) Volume Change – Fine Gradation Gravel Specimens

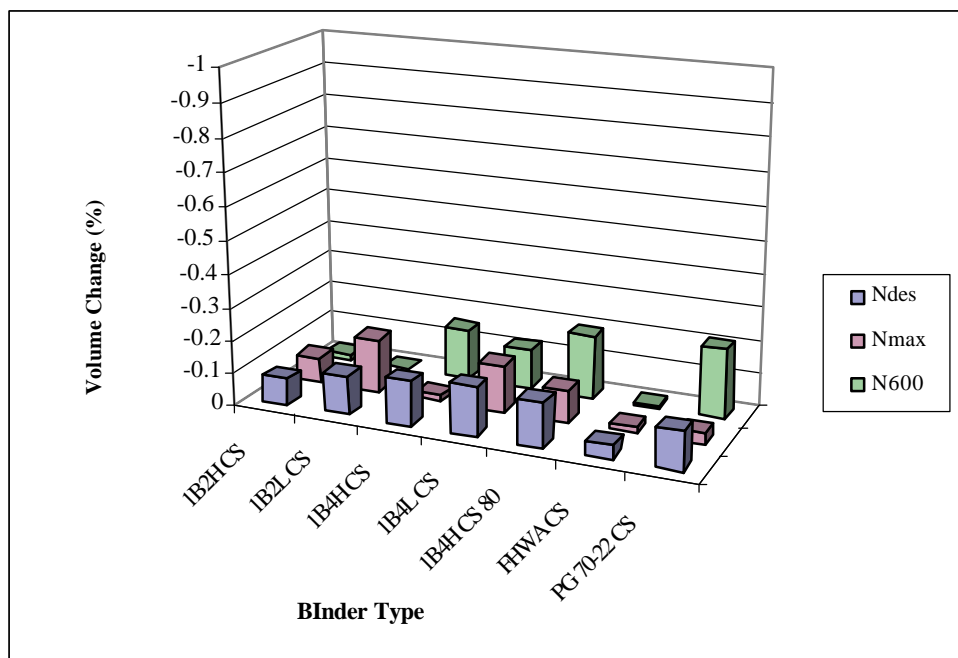


Figure 7.1.1 (c) Volume Change – Coarse Gradation Crushed Aggregate Specimens

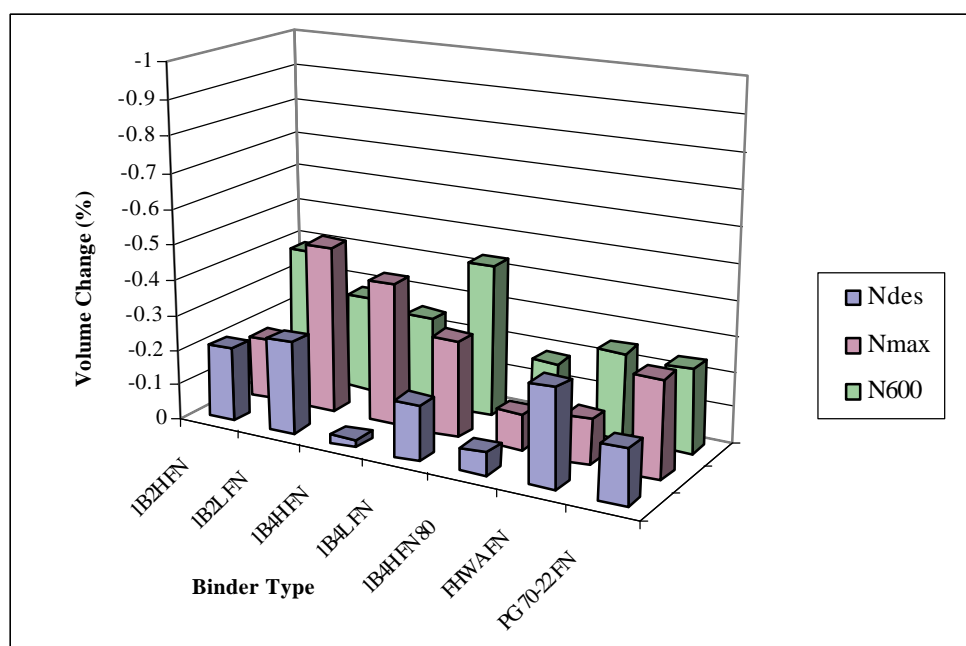


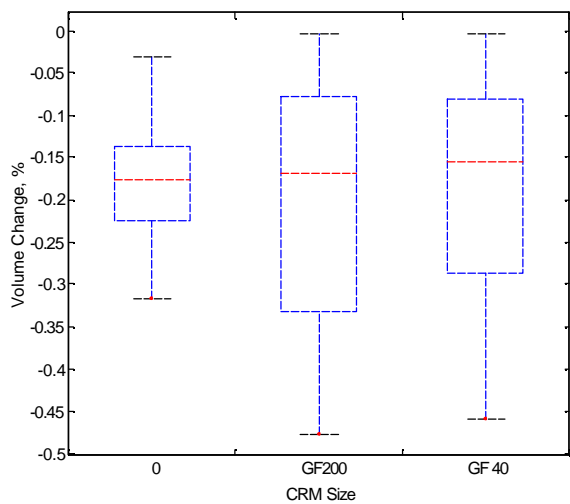
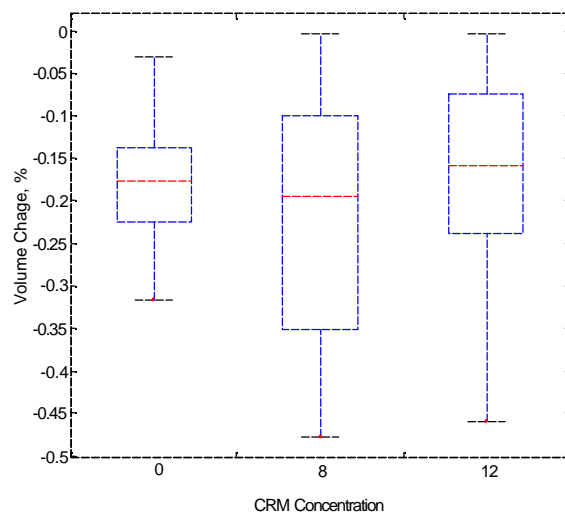
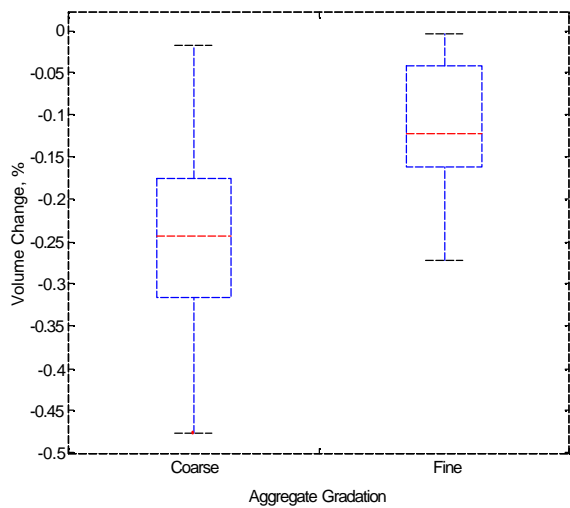
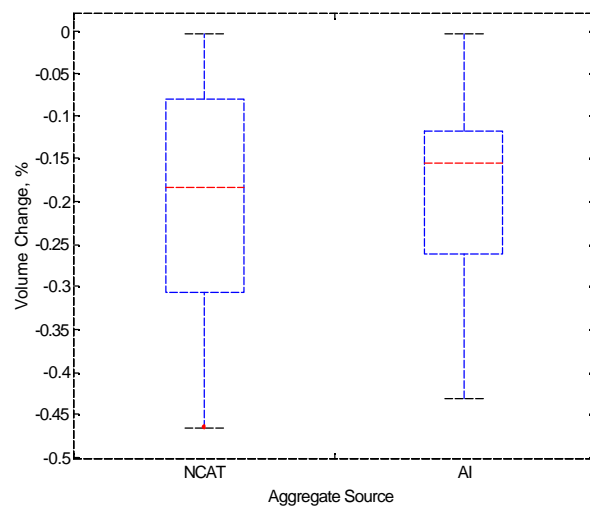
Figure 7.1.1 (d) Volume Change – Fine Gradation Crushed Aggregate Specimens

To quantify the volume changes and determine if certain rubber or aggregate characteristics would affect the volume reduction a statistical analysis was conducted.

Figures 7.1.2 a-d show the box plots for the volume change data, organized according to the four control variables. Figure 7.1.2 (a) shows the box plot with CRM size as the independent variable. The means of the data for each CRM size are not significantly different, suggesting that the rubber size does not contribute significantly to the variation in volume change. Figure 7.1.2 (b) compares the data based on the CRM concentration levels. The means here also do not differ by a significant amount, indicating that CRM concentration is also not a significant factor. Figure 7.1.2 (c) shows the plots for the two levels of aggregate gradation. In this case, it is clear that the means for fine aggregate and coarse aggregate mixes differ significantly. Therefore, aggregate gradation can be considered to have a significant effect on the volume change in the mixtures. Figure 7.1.2 (d) shows the comparison between NCAT and AI aggregates. These box plots do not show significant difference in the means of the volume changes averaged based on aggregate source.

In summary, it appears that the possibility of mixture swelling due to rubber rebound is not strong and cannot be supported by measurements in the laboratory. In fact the measurements show that there is volume reduction for all mixtures, which could be attributed to shrinkage of asphalt due to cooling.

The reduction in volume is relatively small and varies within a narrow range. It is also apparent from the data that neither crumb rubber size nor concentration affects the volume reduction. Aggregate gradation is the only factor that is found to slightly affect volume reduction. Coarse aggregates show higher volume reduction.

**(a) CRM Size****(b) CRM Concentration****(c) Aggregate Gradation****(d) Aggregate Source****Figures 7.1.2 Boxplots of Volume Change**

CHAPTER 8: ANALYSIS OF DENSIFICATION CURVES

The air voids content, as a percentage of total volume, at specifically selected stages during compaction were targeted in the analysis. These selected stages include the 2 gyrations, 8 gyrations (Nini), 100 gyrations (Ndes), 160 gyrations (Nmax), 600 gyrations. The frictional resistance and the importance of the peak point are discussed in a later section in this report.

During compaction, N2 (2 gyrations) to Nini is assumed to represent the compaction that occurs during the laydown process. The pavement is typically open to traffic at a compaction level similar to a level between Nini and Ndes. The densification between Ndes and Nmax is an indication of the performance of the pavement in service. Ndes is the point when the initial (2-3 years) volume of the predicted traffic has passed on the pavement, and Nmax occurs at the point when the pavement mixture achieves a density that should never be exceeded. The final two points of analysis, at N600 (600 gyrations) and maximum frictional resistance, were selected to indicate the terminal condition of the pavement, and the point at which the pavement begins to deteriorate respectively.

Table 8.0.1 shows the air voids in the mixes at the selected stages of compaction. In the table, CS indicates coarse aggregate gradation, and FN indicates fine aggregate gradation.

The mixture designs were provided by the research group of the NCHRP 9-10 project. These designs were not changed to avoid confounding the effects of the rubber characteristics. For the analysis of the densification of the mixes during compaction, the differential air voids relative to the unmodified mixtures are calculated and charted. The differential air voids are calculated by taking the difference between the air voids of each mix and the air voids in the control mix of the same aggregate blend. Since the Superpave

Gyratory Compactor has a variability of 1% in the air voids in compacted mixes, it is assumed that differentials of less than 1% are not significant. The following sections summarize the results and the findings for the effect of the controlled variables.

Table 8.0.1 Air Void Content of Specimen During Compaction

	Binder	Va N2	Va N8	Va N100	Va N160	Va N600	Va @ Max FR
AI	1B2H CS	20.54	16.33	6.16	4.36	0.79	5.65
	1B2H FN	17.55	13.37	3.10	2.02	0.16	10.67
	1B2L CS	20.70	15.69	5.80	4.23	1.18	3.38
	1B2L FN	16.57	11.93	2.82	1.98	0.87	8.70
	1B4H CS	20.26	15.81	5.25	3.73	1.42	7.70
	1B4H FN	19.40	15.03	5.08	3.70	0.79	0.88
	1B4L CS	18.38	13.93	3.99	2.65	0.20	6.07
	1B4L FN	16.90	12.57	2.87	1.63	0.44	5.46
	PG 70-22 CS	19.43	14.75	3.84	3.06	0.55	8.41
	PG 70-22 FN	14.21	9.42	2.15	1.79	1.65	9.50
NCAT	1B2H CS	15.40	12.11	5.43	4.51	2.57	5.74
	1B2H FN	14.28	11.48	6.19	5.58	4.19	4.26
	1B2L CS	16.66	12.70	6.56	4.60	2.61	5.08
	1B2L FN	14.76	10.89	5.74	4.52	2.75	2.12
	1B4H CS	16.23	12.94	6.07	4.96	2.85	10.47
	1B4H FN	15.39	12.60	7.42	6.53	5.16	5.16
	1B4L CS	16.20	12.75	5.56	4.63	2.53	7.67
	1B4L FN	16.08	12.19	6.50	5.80	4.00	6.94
	PG 70-22 CS	15.83	12.23	4.43	3.30	1.45	5.65
	PG 70-22 FN	13.65	10.80	5.17	4.40	2.21	5.67

8.1 Initial Packing of Mixtures

Figure 8.1.1 depicts the differential of the air voids at N=2. Although this is not a Superpave requirement, it is used here to show the effects of the control variables on the initial packing of the mixtures.

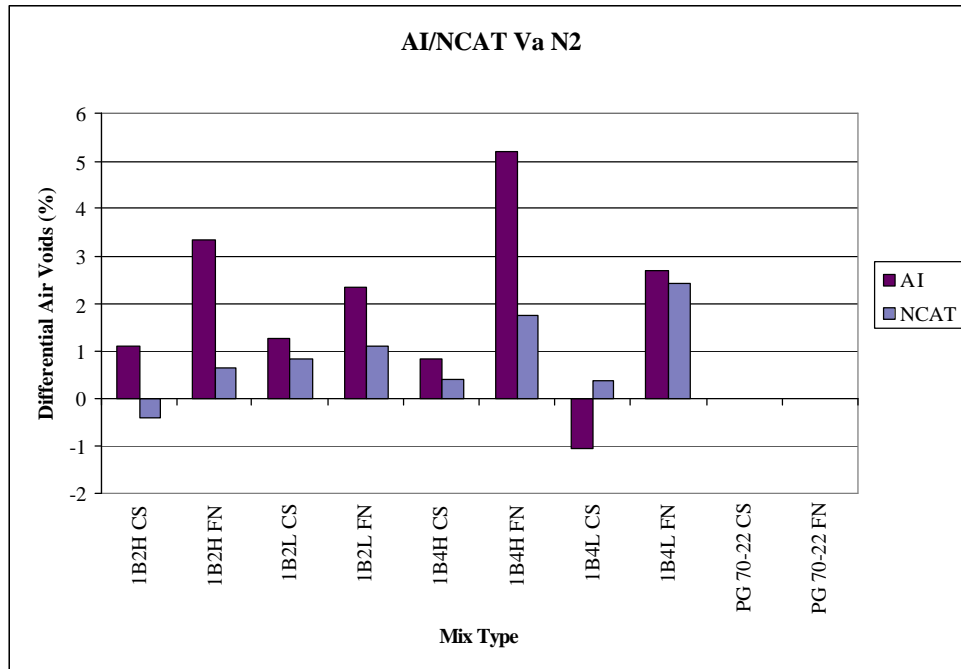


Figure 8.1.1 Differential Air Voids of Mixes at N=2

The data in the figure shows that the inclusion of CRM generally reduces the packing and results in higher initial voids, particularly for fine gradation mixes. Regarding the control variables, the following trends are observed:

- For all combinations of crumb rubber, the effect of CRM is greater on the air voids of the fine aggregate gradation than the coarse gradation.
- The CRM size and concentration show important effects. High concentration is resulting in high air voids, particularly for the fine gradation. Larger size rubber also results in higher air voids for the fine mixtures.
- The CRM has a greater effect on the air voids of AI limestone mixes than they do on the air voids of NCAT gravel mixes.

- For NCAT mixes, the addition of crumb rubber modifier has an effect on the fine aggregate mixes, but not on the coarse aggregate mixes. The effect is significant in almost all AI mixes.

The average increase in the air voids of the CRM mixes at $N=2$ is approximately 2.0 %, which is not significant compared to the actual air voids in the mixes of approximately 15 %. For certain combinations, however, the increase is as high as 4 %, which is significant. It is, therefore concluded that rubber will affect the initial packing of the mixtures and it could therefore require additional compactive effort.

8.2 Air Voids at Ninitial (N=8)

The air voids content at Ninitial is used in the Superpave Gyratory Compactor to represent the mixture capability to compact under the roller during construction processes. Figure 8.2.1 shows a comparison of the differential air voids (increase in voids of mixture as a result of including rubber relative to the mixtures with no rubber) at Nini.

Similar to the voids at $N=2$, it is observed that inclusion of the CRM affects the voids content and that the specific characteristics of the aggregates and the rubber play an important role. The following trends are observed from the data:

- The effect of CRM on the voids of coarse aggregate mixes is negligible in all cases. The effect of the voids of fine aggregate mixtures is much more important and can reach 5% difference in the voids content.
- The effect of crumb rubber is different between mixes with AI aggregates and NCAT aggregates. Crumb rubber has a more pronounced effect on the air voids of mixes with AI aggregates compared to NCAT aggregates.

- Concentration of CRM has an important effect with the high concentration in all cases resulting in more increase in air voids.
- The size of the CRM also plays an important role. For the fine aggregate gradation, the larger size aggregate results in higher voids content. It appears that size is less important than concentration.

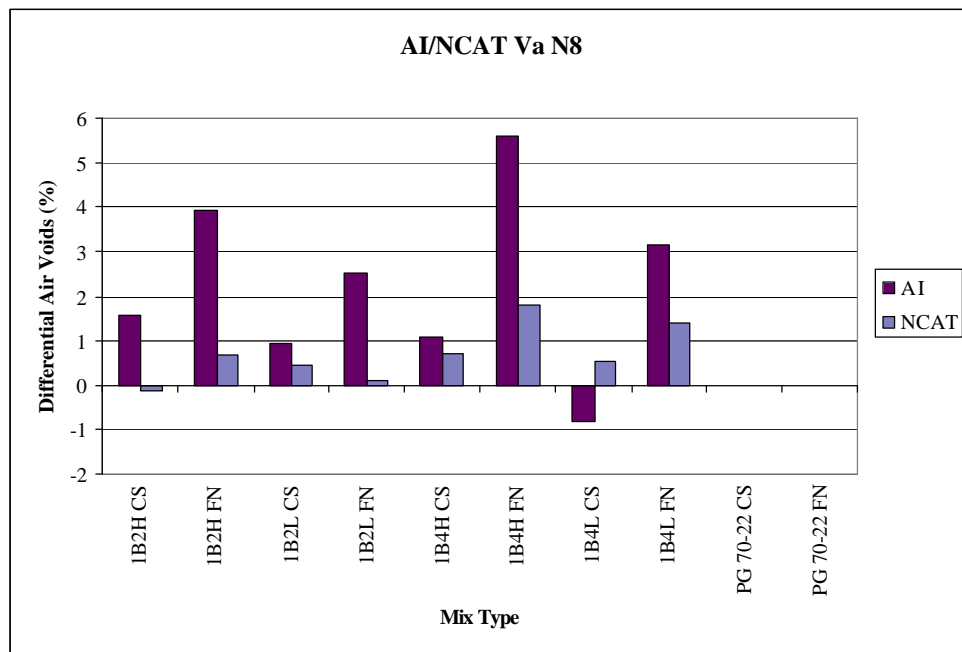


Figure 8.2.1 Differential Air Voids of Mixes at Nini

8.3 Air Voids at Ndesign (N=100)

The amount of air voids at Ndesign is used to represent the densification of the pavement after a predicted amount of traffic has passed on it. Ndesign is one of two indicators of the pavement's performance during service. Figure 8.3.1 shows the air voids in the compacted mixes, relative to the unmodified mixes, after 100 gyrations in the gyratory compactor. The

results show that the CRM will increase the voids content for all mixes by a margin of 0.2 % to 3% at Ndes. The increase in air voids was obtained by taking the difference between the air voids in the unmodified mixes and the CRM mixes. The trends observed for the effect of the control variables are similar to the trends observed for Nini with some exceptions:

- The effects on coarse aggregate mixes are more pronounced at Ndes compared to the Nini. In 2 cases, the change in voids of the coarse aggregate mixtures is higher than the fine mixtures. The trend seen for the Nini where the effect is mainly on fine gradation is not observed at Ndes. It appears that both gradations can be equally affected by the CRM.
- The effects on NCAT gravel mixtures are more significant and in case of large rubber particles, the effect is comparable to the AI limestone aggregates. This is a variation from the trends seen at Nini.
- The concentration of the rubber shows an important effect. From the figure, it is observed that both the AI and NCAT mixes show greater effects from the crumb rubber when higher concentrations are applied. This trend is similar to the results at Nini.
- The effect of CRM size is more complex than the other factors. It can be noted that crumb rubber size has opposite trends for mixes from different sources. AI mixes show a decrease in effect when the crumb rubber particles are larger in most case, while NCAT mixes show an increase in effect when the particles are larger. It appears that there are strong interactions with gradation and also with concentration. The interactive effects are important and can result in major changes in voids.

Among the NCAT mixes, those with larger crumb rubber particles at higher concentration clearly show greater effects due to the rubber modification.

In summary, the CRM will change voids at Ndes that require changes in compaction effort, binder content, or gradation. It is expected that it would be difficult to predict what the effect of size and concentration would be because of the interactive effects.

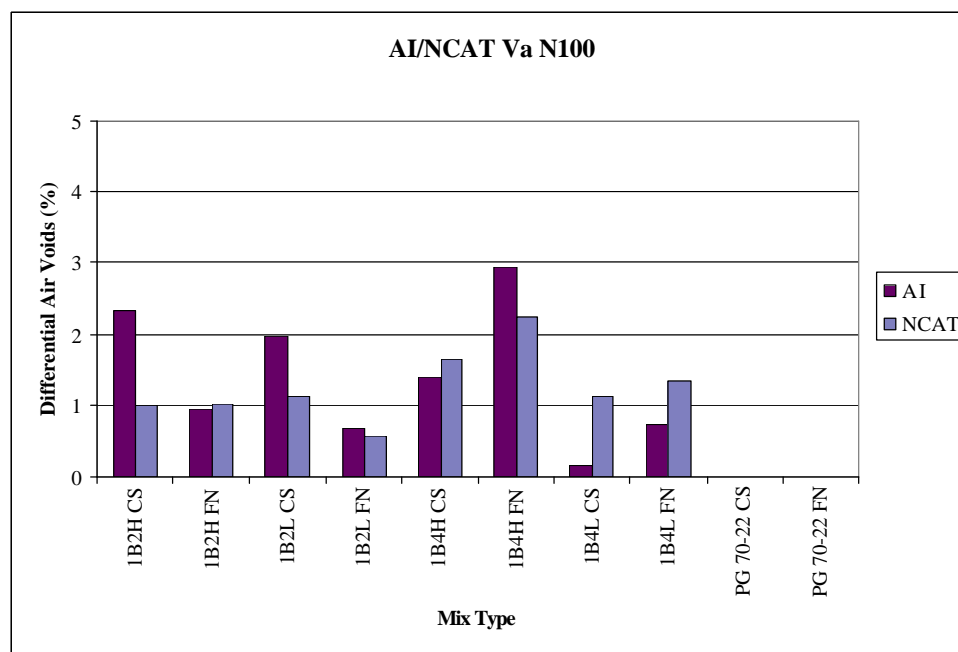


Figure 8.3.1 Differential Air Voids of Mixes at N=100 (Ndes)

8.4 Air Voids at Nmaximum (N=160)

Nmax is another point that is used as an indicator of the performance of the pavement over time. A mixture compacted to Nmax should result in an air void that is the maximum allowable in the field. It sets a limit to prevent over-densification of the pavement mix during its service life. The chart in Figure 8.4.1 shows the differential air voids of mixes at N=160. A study of the figure indicates the following trends:

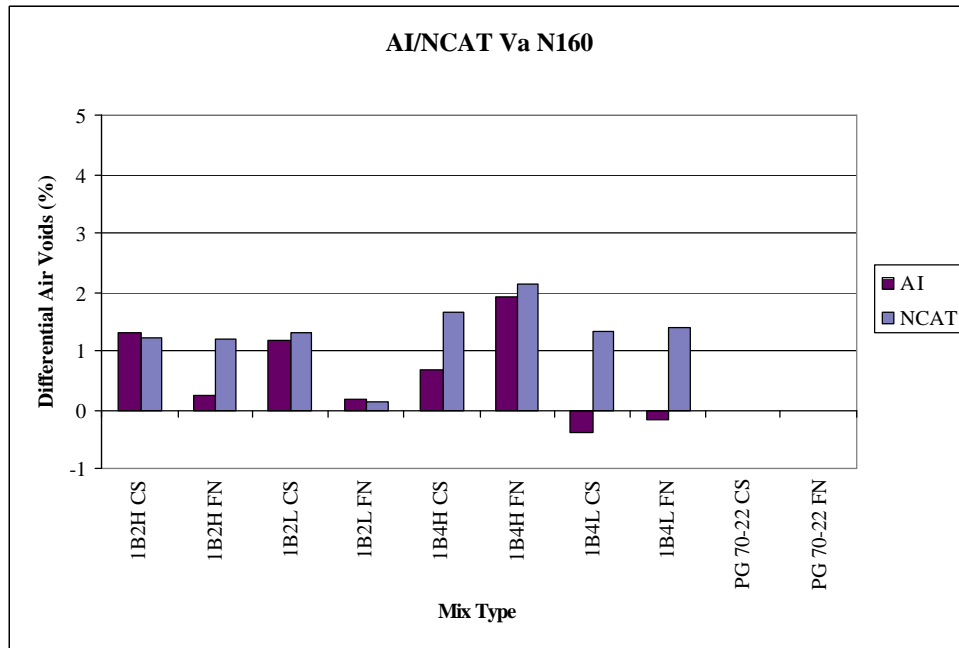


Figure 8.4.1 Differential Air Voids of Mixes at N=160 (Nmax)

- At Nmax, the CRM has a greater effect on NCAT gravel mixes than on AI limestone mixes. The effect is however dependent on the other factors. The exception of NCAT mixes are those that included a smaller size crumb rubber particle at a lower concentration, with a fine graded aggregate blend. In the case of the AI aggregates, the majority of mixes do not show a significant change with the exception of fine gradation at large CRM size.
- The results indicate that the aggregate gradation is an important factor. The effect of gradation is, however, complicated by the interactive effects of the rubber size and concentration. No single trend could be defined as the gradation varies with each specific combination.

Rubber size and concentration have a combined effect on the increase in the air voids. Larger crumb rubber particles appear to result in an increase in voids for the high concentration, but not necessarily so for the low concentration. The effects are also dependent on the aggregate source.

8.5 Terminal Density of Mixtures

As with $N=2$, $N=600$ is not a Superpave specified gyration number. It is used in this research to show the effects of the variables on the density of mixtures when it reaches its terminal stage of service. The differential air voids, between the CRM mixes and the mixes without the crumb rubber, for $N=600$ are shown in Figure 8.5.1. The following trends are observed:

- The data shows that the addition of crumb rubber modifier has more of an effect on NCAT mixtures than it does on AI mixtures. A majority of the NCAT mixtures indicate significant effects from the crumb rubber modifier, while only two AI mixes show significant effects.
- It can be noted that for NCAT fine graded mixtures, the effect is more significant when the concentration of crumb rubber modifier is higher. It appears that a larger crumb rubber size results in greater effect as well.
- The chart also shows that crumb rubber generally has a greater effect in mixtures with fine gradation aggregates than mixes with coarse gradation aggregates, regardless of crumb rubber concentration and size, or aggregate source.
- For the fine graded mixtures, the addition of CRM consistently caused an increase in air voids in the NCAT mixtures, while consistently causing a decrease in air voids in the AI mixtures.

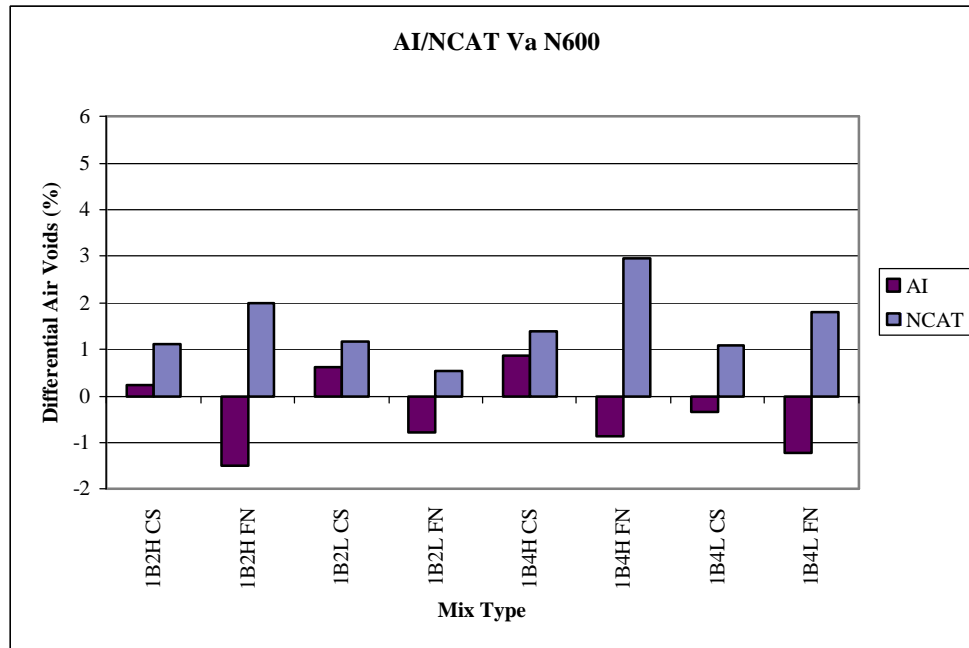


Figure 8.5.1 Differential Air Voids of Mixtures at N=600

8.6 Summary of the Effect of CRM on Air Voids Content

The analysis of the voids content results indicates that the effect of CRM are highly dependent on the densification stage of the mixture and the aggregate characteristics. They indicate that it would be very difficult to predict the effects based on knowledge of the type of the aggregate and the gradation. More importantly, they show that increasing the concentration and changing the size can result in different effects on voids depending on gradation and angularity of the aggregates. Because of the complexity of the effects, statistical analysis was conducted in an effort to sort the interactive effects and simplify the trends.

8.7 Statistical Analysis Air Void Results

The statistical analysis for the data was performed using the SAS statistical package. The independent variables used in all the analyses were the crumb rubber size, crumb rubber concentration, aggregate gradation, and aggregate source.

Based on the analysis, it is not possible to obtain one model that can be applied to all the stages of compaction. Therefore, separate models were analyzed for each set of data. The results from the analysis are shown in Tables 8.7.1-8.7.5. The tables report the sums of squares for the full model, which includes all interactions, as well as the model that includes only the main effects. Three models for estimating the air voids are shown at the bottom of the table for each stage of pavement densification. The first model only considers the aggregate related variables, ie. aggregate gradation and aggregate source. The second model includes one of the crumb rubber variables, and the third model includes all four variables. The models may or may not include the interaction effects of the variables considered.

Table 8.7.1 Statistical Model for Air Voids at N=2

Analysis of Variance					
Source of Variation	d.f.	Sum of Square	Mean Square	F-Ratio	Sig. Level
MAIN EFFECTS					
A: CRM Size	1	0.023846	0.023846	0.03	0.8727
B: CRM Concentration	1	1.331268	1.331268	1.46	0.2273
C: Aggregate Gradation	1	60.365234	60.365234	66.34	<0.0001
D: Aggregate Source	1	72.122502	72.122502	79.25	<0.0001
INTERACTIONS					
AB	1	2.284573	2.284573	2.51	0.1252
AC	1	2.015020	2.015020	2.21	0.1488
AD	1	1.540598	1.540598	1.69	0.2046
BC	1	0.267775	0.267775	0.29	0.5921
BD	1	2.869040	2.869040	3.15	0.0875
CD	1	7.713509	7.713509	8.48	0.0073
RESIDUAL	29	23.7753784	0.9144376		
TOTAL	39	216.2829975	R ² = 0.891		
REDUCED MODEL					
MAIN EFFECTS					
A: CRM Size	1	0.0152433	0.0152433	0.01	0.9169
B: CRM Concentration	1	1.275773	1.275773	0.92	0.3430
C: Aggregate Gradation	1	58.852192	58.852192	42.65	<0.0001
D: Aggregate Source	1	88.905732	88.905732	64.44	<0.0001
RESIDUAL	35	53.2870719	1.5672668		
TOTAL	39	216.2829975	R ² = 0.783		
Models for Estimating Air Voids		Std Error of Y est.		Std. Error of Coeff.	R ² Adjusted
Va = 18.41911 + 5.46225G – 1.94356Sc – 1.97963(G*Sc)		1.15933		1.16400 0.53267 0.73507	0.758
Va = 17.59686 + 0.11563C + 5.27536G – 1.99496Sc – 1.88619(G*Sc)		1.04417		0.03776 1.05016 0.44006 0.66276	0.803
Va = 17.59085+ 0.02217Sz + 0.11010C + 5.26998G – 1.99643Sc – 1.88349(G*Sc)		1.05913		0.16436 0.05609 1.06596 0.48706 0.67255	0.798
Sz = CRM Size (GF 40, 200) C = CRM Concentration (8, 12%) G = Aggregate Gradation (Fine=1, Coarse = 2) Sc = Aggregate Source (Crushed Stoned = 1, Crushed Gravel = 2)					

Table 8.7.2 Statistical Model for Air Voids at N=8

Analysis of Variance					
Source of Variation	d.f.	Sum of Square	Mean Square	F-Ratio	Sig. Level
MAIN EFFECTS					
A: CRM Size	1	0.065219	0.065219	0.07	0.7995
B: CRM Concentration	1	2.521401	2.521401	2.54	0.1227
C: Aggregate Gradation	1	45.627294	45.627294	46.05	<0.0001
D: Aggregate Source	1	17.470701	17.470701	17.62	0.0003
INTERACTIONS					
AB	1	1.281498	1.281498	1.29	0.2658
AC	1	2.033934	2.033934	2.05	0.1638
AD	1	1.042494	1.042494	1.05	0.3145
BC	1	0.084547	0.084547	0.09	0.7725
BD	1	4.557897	4.557897	4.60	0.0415
CD	1	12.608810	12.608810	12.73	0.0014
RESIDUAL	29	27.6912937	1.0650498		
TOTAL	39	146.4812975	R ² = 0.824		
REDUCED MODEL					
MAIN EFFECTS					
A: CRM Size	1	0.079016	0.079016	0.05	0.8263
B: CRM Concentration	1	2.632443	2.632443	1.63	0.2105
C: Aggregate Gradation	1	42.466919	42.466919	26.90	<0.0001
D: Aggregate Source	1	24.637933	24.637933	15.25	0.0004
RESIDUAL	35	55.8323827	1.6421289		
TOTAL	39	146.4812975	R ² = 0.625		
Models for Estimating Air Voids		Std Error of Y est.		Std. Error of Coeff.	R ² Adjusted
Va = 12.24423 + 5.94030G – 0.24767Sc – 2.51515(G*Sc)		1.24903		1.25406 0.57389 0.79195	0.585
Va = 11.23396 + 0.14206C + 5.71068G – 0.31081Sc – 2.40034(G*Sc)		1.07868		0.03901 1.08486 0.49592 0.68466	0.690
Va = 8.74158 + 0.30074Sz + 0.38543C + 6.80167G + 0.92466Sc – 0.52448(Sz*G) – 0.16544(C*Sc) – 2.31646(G*Sc)		0.96702		0.18465 0.11692 1.08657 0.70257 0.20553 0.07002 0.61475	0.751
Sz = CRM Size (GF 40, 200) C = CRM Concentration (8, 12%) G = Aggregate Gradation (Fine=1, Coarse = 2) Sc = Aggregate Source (Crushed Stoned = 1, Crushed Gravel = 2)					

The voids contents at N2 and N8 (Nini) represent the densification of the pavement during the construction stages. The tables show that the most significant factors during this stage of the pavement life are the aggregate gradation and aggregate source. The concentration-source and gradation-source interactions are also significant. The interesting finding is that the CRM size and concentration are not important.

The voids contents at N100 (Ndes) and N160 (Nmax) represent the performance period of the pavement life, during which the predicted traffic passes over the pavement and the minimum allowable air void is reached. At this stage, the tables indicate that the aggregate source is the most significant main effect. The interactions between size and concentration, size and gradation, concentration and source, and gradation and source are also significant. This indicates that the specific characteristics of the rubber have an important effect but the effect is highly mixture type specific.

The statistical analysis indicates that during the terminal stage the rubber existence is important but the specific characteristics of the rubber size and concentration are not highly important.

Table 8.7.3 Statistical Model for Air Voids at N=100

Analysis of Variance						
Source of Variation	d.f.	Sum of Square	Mean Square	F-Ratio	Sig. Level	
MAIN EFFECTS						
A: CRM Size	1	0.229827	0.229827	0.05	0.8218	
B: CRM Concentration	1	0.894856	0.894856	2.02	0.1675	
C: Aggregate Gradation	1	3.368010	3.368010	7.59	0.0106	
D: Aggregate Source	1	35.059565	35.059565	78.99	<0.0001	
INTERACTIONS						
AB	1	2.736720	2.736720	6.17	0.0198	
AC	1	2.868984	2.868984	6.46	0.0173	
AD	1	0.794764	0.794764	1.79	0.1924	
BC	1	0.0033685	0.0033685	0.01	0.9312	
BD	1	1.877635	1.877635	4.23	0.0499	
CD	1	22.100638	22.100638	49.80	<0.0001	
RESIDUAL	29	11.73845530	0.45147905			
TOTAL	39	100.7411500	R ² = 0.885			
REDUCED MODEL						
MAIN EFFECTS						
A: CRM Size	1	0.000157	0.000157	0.00	0.9912	
B: CRM Concentration	1	1.248632	1.248632	0.98	0.3296	
C: Aggregate Gradation	1	4.2383	4.2383	3.46	0.0714	
D: Aggregate Source	1	38.728586	38.728586	30.35	<0.0001	
RESIDUAL	35	39.76043430	1.16942454			
TOTAL	39	100.7411500	R ² = 0.569			
Models for Estimating Air Voids		Std Error of Y est.		Std. Error of Coeff.		R ² Adjusted
Va = -0.80656 + 5.48465G + 3.63878Sc – 3.17232(G*Sc)		0.95825		0.96211 0.44028 0.60758		0.672
Va = -1.72664 + 0.12939C + 5.27554G + 3.58127Sc – 3.06777(G*Sc)		0.76071		0.02751 0.76507 0.34974 0.48284		0.776
Va = -1.74058 + 0.03129Sz + 0.12791C + 5.27822G + 3.58201Sc – 0.00212(Sz*C) – 3.06911(G*Sc)		0.78316		0.23866 0.05048 0.79220 0.36083 0.02678 0.49892		0.763
Sz = CRM Size (GF 40, 200) C = CRM Concentration (8, 12%) G = Aggregate Gradation (Fine=1, Coarse = 2) Sc = Aggregate Source (Crushed Stoned = 1, Crushed Gravel = 2)						

Table 8.7.4 Statistical Model for Air Voids at N=160

Analysis of Variance					
Source of Variation	d.f.	Sum of Square	Mean Square	F-Ratio	Sig. Level
MAIN EFFECTS					
A: CRM Size	1	0.094439	0.094439	0.26	0.6175
B: CRM Concentration	1	0.436279	0.436279	1.18	0.2872
C: Aggregate Gradation	1	0.520734	0.520734	1.41	0.2460
D: Aggregate Source	1	41.987992	41.987992	113.60	<0.0001
INTERACTIONS					
AB	1	2.527356	2.527356	6.84	0.0147
AC	1	1.725457	1.725457	4.67	0.0401
AD	1	0.555973	0.555973	1.50	0.2310
BC	1	0.003571	0.003571	0.01	0.9224
BD	1	1.535381	1.535381	4.15	0.0518
CD	1	19.224373	19.224373	52.01	<0.0001
RESIDUAL	29	2.50545781	0.31318223		
TOTAL	39	98.89009750	R ² = 0.903		
REDUCED MODEL					
MAIN EFFECTS					
A: CRM Size	1	0.0203954	0.0203954	0.02	0.8937
B: CRM Concentration	1	0.691318	0.691318	0.61	0.4385
C: Aggregate Gradation	1	0.826127	0.826127	0.73	0.3974
D: Aggregate Source	1	51.397025	51.397025	45.70	<0.0001
RESIDUAL	35	9.90938338	0.61933646		
TOTAL	39	98.89009750	R ² = 0.613		
Models for Estimating Air Voids		Std Error of Y est.		Std. Error of Coeff.	R ² Adjusted
Va = -1.87867 + 4.71203G + 3.80533Sc – 2.92052(G*Sc)		0.84585		0.84927 0.38864 0.53621	0.718
Va = -1.86998 + 0.00642C + 4.60289G + 3.28641Sc + 0.06111(C*Sc) – 2.86594(G*Sc)		0.72081		0.08253 0.72618 0.52362 0.05213 0.45800	0.795
Va = -1.87739 + 0.00719Sz + 0.01156G + 3.28867Sc – 0.00234(Sz*C) + 0.06116(C*Sc) – 2.87080G*Sc)		0.74279		0.22636 0.09359 0.75276 0.53992 0.02540 0.05372 0.47373	0.782
Sz = CRM Size (GF 40, 200) C = CRM Concentration (8, 12%) G = Aggregate Gradation (Fine=1, Coarse = 2) Sc = Aggregate Source (Crushed Stoned = 1, Crushed Gravel = 2)					

Table 8.7.5 Statistical Model for Air Voids at N=600

Analysis of Variance					
Source of Variation	d.f.	Sum of Square	Mean Square	F-Ratio	Sig. Level
MAIN EFFECTS					
A: CRM Size	1	0.051756	0.051756	0.13	0.7239
B: CRM Concentration	1	0.113906	0.113906	0.29	0.6021
C: Aggregate Gradation	1	2.353364	2.353364	6.09	0.0389
D: Aggregate Source	1	31.439604	31.439604	81.31	<0.0001
INTERACTIONS					
AB	1	2.197806	2.197806	5.68	0.0443
AC	1	0.805506	0.805506	2.06	0.1869
AD	1	0.023256	0.023256	0.06	0.8124
BC	1	0.024806	0.024806	0.06	0.8064
BD	1	0.327756	0.327756	0.85	0.3841
CD	1	2.810588	2.810588	7.27	0.0272
RESIDUAL	11	0.2846344	0.1423172		
TOTAL	21	59.61125909	R ² = 0.948		
REDUCED MODEL					
MAIN EFFECTS					
A: CRM Size	1	0.051756	0.051756	0.06	0.8106
B: CRM Concentration	1	0.113906	0.113906	0.13	0.7220
C: Aggregate Gradation	1	1.879314	1.879314	2.16	0.1607
D: Aggregate Source	1	37.497513	37.497513	43.16	<0.0001
RESIDUAL	17	42.1479262	2.8098617		
TOTAL	21	59.61125909	R ² = 0.767		
Models for Estimating Air Voids		Std Error of Y est.		Std. Error of Coeff.	R ² Adjusted
Va = -1.70806 – 0.58455G + 2.75117Sc		0.93039		0.39672 0.39837	0.6951
Va = -1.47236 – 0.15940C + 1.48333G + 2.20635Sc + 0.15731(C*Sc) – 1.42167(G*Sc)		0.75268		0.10265 0.99094 0.69345 0.06962 0.64455	0.800
Va = -1.47801 + 0.19769Sz – 0.16384C + 1.48333G + 2.16963Sc – 0.01735(Sz*C) + 0.16084(C*Sc) – 1.42167(G*Sc)		0.79469		0.33621 0.12314 1.04625 0.73481 0.03774 0.07375 0.68053	0.778
Sz = CRM Size (GF 40, 200) C = CRM Concentration (8, 12%) G = Aggregate Gradation (Fine=1, Coarse = 2) Sc = Aggregate Source (Crushed Stoned = 1, Crushed Gravel = 2)					

CHAPTER 9: ANALYSIS OF FRICTIONAL RESISTANCE

As previously mentioned in Section 2.3, frictional resistance of mixtures during compaction is measured using the Gyratory Load Cell Plate Assembly (GLPA).

During compaction, 50 readings are taken from each load cell per gyration. These readings are acquired using a program created using the LabVIEW software. Once the readings have been recorded, the frictional resistance of a mix can be calculated, and an EXCEL spreadsheet with the data and charts is produced utilizing a program written in MATLAB.

Figure 9.0.1 shows a typical chart, which includes both the densification and frictional resistance of the mix, generated using the readings and the software programs. From the chart, the development of the amount of frictional resistance in a mixture can be observed. For the mixes that were compacted in this project, the amount of frictional resistance increases until a certain point during the compaction, this point being different from mix to mix, and then declines. Some mixes achieve higher frictional resistance than others at the same point of compaction, and the decline in frictional resistance is also more rapid in some mixes compared to others.

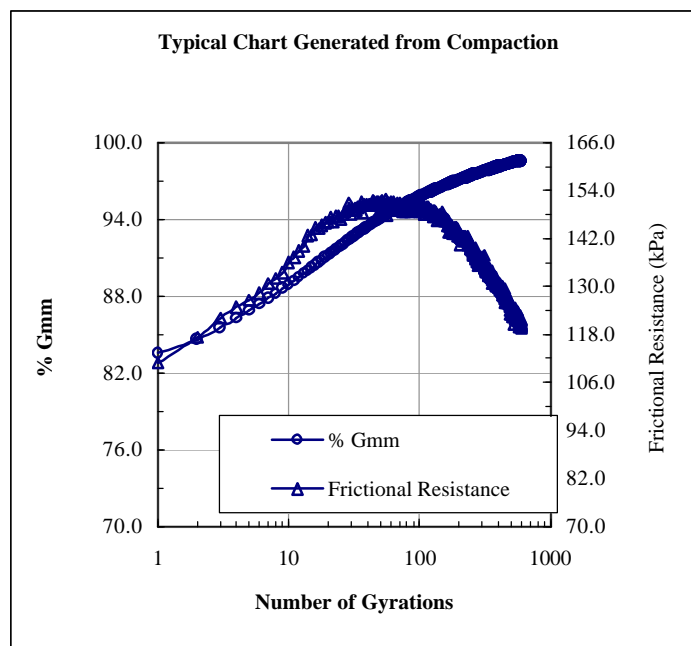


Figure 9.0.1 Typical Chart Generated from Gyratory Load Cell Plate Assembly

To discuss the differences between mixtures, the frictional resistance values at selected stages during the compaction of mixtures are extracted from the spreadsheet. These selected points are the same as those that were used in the analysis of air void data, which are N2 (2 gyrations), Nini (N=8), Ndes (N=100), Nmax (N=160), N600 (600 gyrations), and the point of maximum frictional resistance.

Table 9.0.1 shows the frictional resistance of the various mixtures at those selected points of compaction. The range in values is between a low at 75 kPa and a high of 165 kPa. The following sections represent highlights of differences between mixtures and the relationships to the mixture or rubber characteristics.

Table 9.0.1 Frictional Resistance (units are kPa) of Specimens During Compaction

	Binder	FR N2	FR N8	FR N100	FR N160	FR 600	Max FR
AI	1B2H CS	98.28	124.55	153.05	152.08	138.69	157.51
	1B2H FN	106.12	122.93	94.87	92.03	83.45	127.99
	1B2L CS	98.88	127.30	151.38	157.39	144.61	162.22
	1B2L FN	114.21	134.73	116.13	93.29	77.21	148.48
	1B4H CS	100.77	123.65	138.51	124.48	78.65	139.21
	1B4H FN	105.20	127.14	125.72	114.22	100.54	135.82
	1B4L CS	105.35	122.25	119.91	109.90	102.41	147.48
	1B4L FN	102.77	124.03	128.48	113.34	74.32	141.34
	PG 70-22 CS	105.39	129.94	150.04	144.20	102.39	162.70
	PG 70-22 FN	103.19	112.12	157.10	144.35	122.33	158.64
NCAT	1B2H CS	113.25	128.57	139.45	139.13	117.97	141.27
	1B2H FN	116.55	130.34	138.84	136.78	126.48	140.49
	1B2L CS	118.77	133.93	149.32	142.91	125.02	153.81
	1B2L FN	117.84	133.53	136.48	133.61	127.61	142.06
	1B4H CS	120.10	137.81	141.65	137.31	128.77	149.12
	1B4H FN	117.70	135.66	149.57	145.46	142.30	155.31
	1B4L CS	116.16	132.90	143.11	137.21	129.63	148.59
	1B4L FN	120.30	137.43	151.69	149.41	146.28	153.38
	PG 70-22 CS	116.10	131.24	135.42	131.05	119.64	151.83
	PG 70-22 FN	126.28	145.23	146.34	141.91	139.61	150.84

9.1 Initial Resistance to Deformation

Figure 9.1.1 shows the frictional resistance of the mixes at the end of 2 gyrations in the gyratory compactor. The 2 gyration measurement is not a Superpave requirement, and it is used to show the effects of the control variables on the resistance of the mixture to deformation at the initial moment of the compaction operation.

At 2 gyrations, the results as shown in Figure 9.1.1 clearly indicate that the effect of aggregate source is significant, with the NCAT mixtures demonstrating greater resistance to deformation than the AI mixtures. The results also show that aggregate gradation may have an effect, particularly for AI mixes with GF 200 crumb rubber particles in the binder. Apart from the aggregate related variables, the results do not show significant influence from the variables related to crumb rubber modifiers. Also, the control mixtures that do not contain

rubber show the same range of FR values. It can be therefore concluded that rubber characteristics and the addition of crumb rubber do not have an important impact on frictional resistance of mixture at N=2.

Figures 9.1.2 (a)-(d) show the boxplots from statistical analysis of the data at N=2. They illustrate the averages of all mixtures with comparisons made with respect to each control variable. These figures help to show other patterns that may not be obvious from the bar charts. Figure 9.1.2 (b) suggests that frictional resistance in asphalt mixtures decrease with an increased concentration of crumb rubber modifiers in the binder, though the differences in the values are not significantly different at approximately 3%. Figure 9.1.2 (c) shows that aggregate gradation is a significant effect, and Figure 9.1.2 (d) confirms the indication from Figure 9.1.1 that aggregate source is the most important effect at N=2.

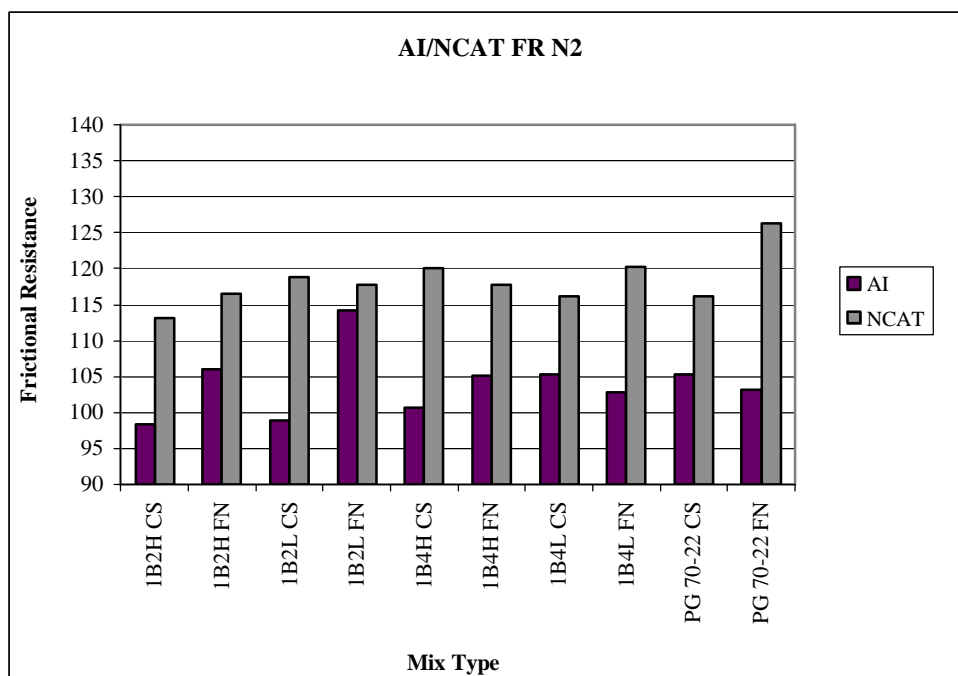
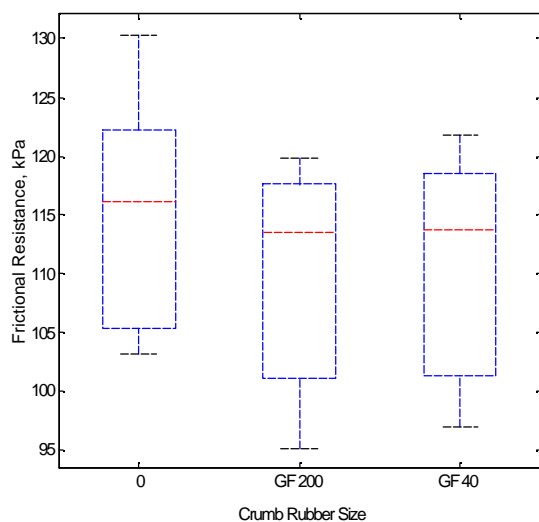
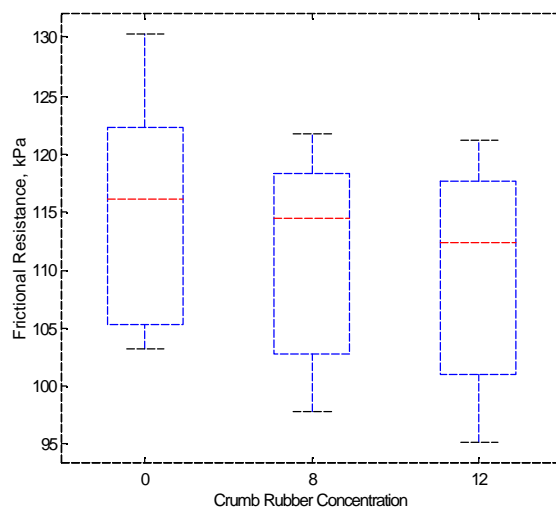
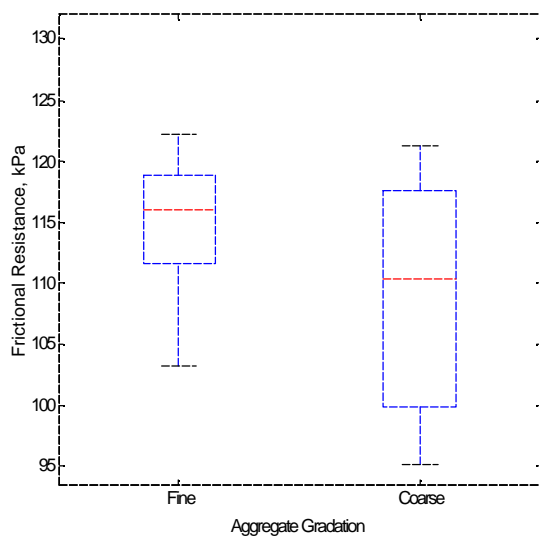
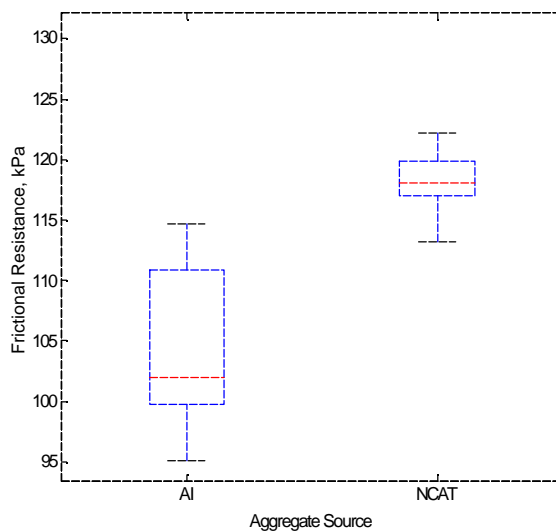


Figure 9.1.1 Frictional Resistance of Mixes at N=2

**(a) CRM Size****(b) CRM Concentration****(c) Aggregate Gradation****(d) Aggregate Source****Figures 9.1.2 Boxplots of Frictional Resistance at N = 2**

9.2 Frictional Resistance of Mixes at Nini (N=8)

Figure 9.2.1 shows the frictional resistance of asphalt mixtures to compaction at 8 gyrations, which is Nini. This would represent the response of the pavement under the compactive efforts of the roller during pavement construction. Figures 9.2.2 (a) – (d) show the boxplots obtained from statistical analysis of the frictional resistance data at Nini.

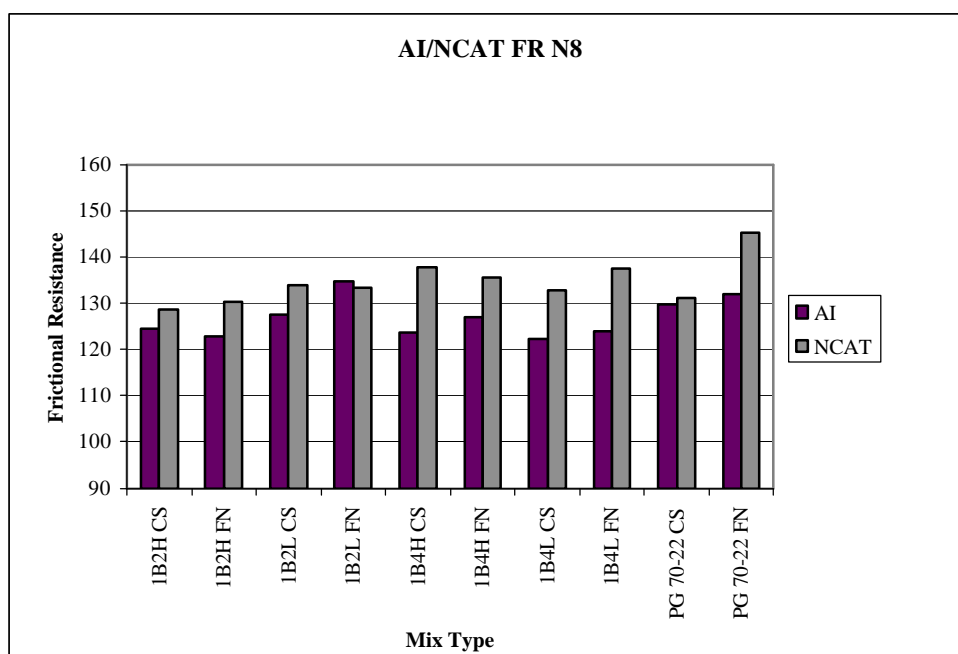
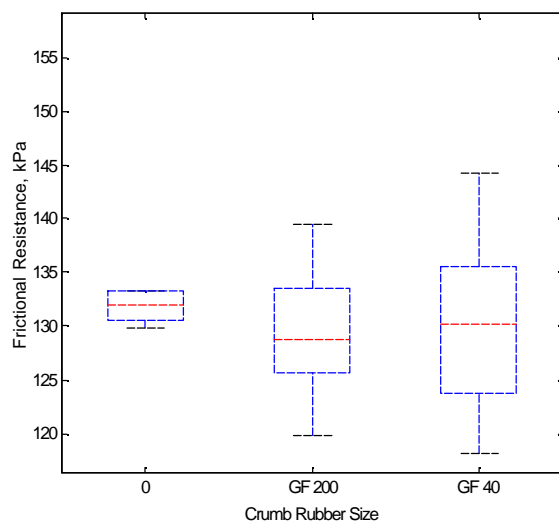
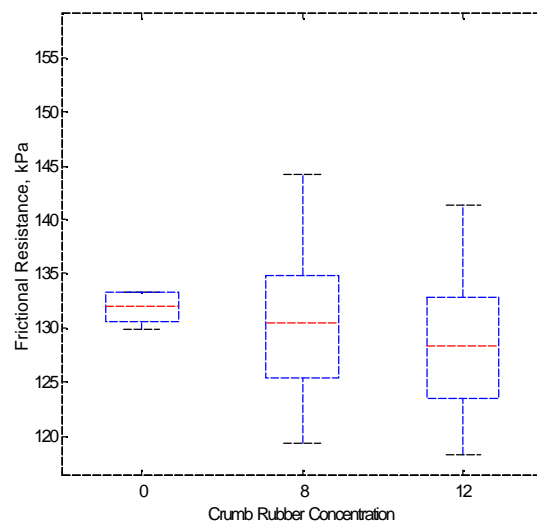
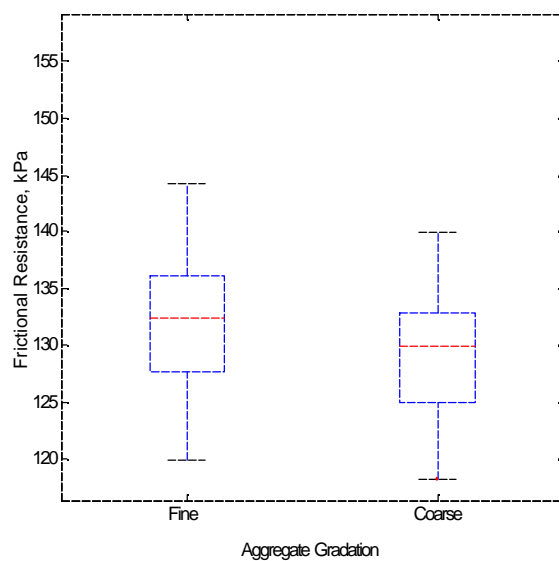
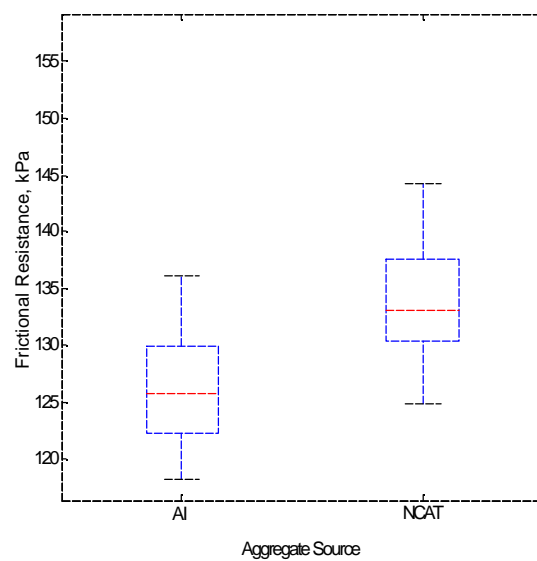


Figure 9.2.1 Frictional Resistance of Mixes at Nini (N=8)

**(a) CRM Size****(b) CRM Concentration****(c) Aggregate Gradation****(d) Aggregate Source****Figures 9.2.2 Boxplots of Frictional Resistance at N = 8**

From the figures, it can be observed that the inclusion of crumb rubber and crumb rubber characteristics have similar effects on frictional resistance of mixtures at $N=8$, as shown in the mixtures at $N=2$. The boxplots once again show that frictional resistance decreases with an increase in the concentration of crumb rubber in the binder, but as with the case at $N=2$, the differences are not significant.

In comparing the effects of aggregate characteristics on the frictional resistance of mixtures at $N=8$, the trends are also similar to those seen at $N=2$, as there are proportionate increases in the levels of frictional resistance from $N=2$ to $N=8$. The average frictional resistance shows that the changes are slightly gentler for fine mixes than for coarse mixes.

9.3 Statistical Analysis for Construction Stage of Compaction

Table 9.3.1 Statistical Model for Frictional Resistance at N=2

Analysis of Variance					
Source of Variation	d.f.	Sum of Square	Mean Square	F-Ratio	Sig. Level
MAIN EFFECTS					
A: CRM Size	1	6.467727	6.467727	0.32	0.5777
B: CRM Concentration	1	22.434900	22.434900	1.10	0.3033
C: Aggregate Gradation	1	279.913866	279.913866	13.76	0.0010
D: Aggregate Source	1	1695.110690	1695.110690	83.33	<.0001
INTERACTIONS					
AB	1	37.625232	37.625232	1.85	0.1855
AC	1	25.993989	25.993989	1.28	0.2686
AD	1	8.753895	8.753895	0.43	0.5176
BC	1	2.479385	2.479385	0.12	0.7298
BD	1	0.804271	0.804271	0.04	0.8439
CD	1	53.205212	53.205212	2.62	0.1179
RESIDUAL	29	528.879705	20.341527		
TOTAL	39	2957.19288	R ² = 0.821		
REDUCED MODEL					
MAIN EFFECTS					
A: CRM Size	1	6.116398	6.116398	0.31	0.5839
B: CRM Concentration	1	23.571553	23.571553	1.18	0.2853
C: Aggregate Gradation	1	260.274128	260.274128	13.01	0.0010
D: Aggregate Source	1	1846.801104	1846.801104	92.34	<.0001
RESIDUAL	35	680.000537	20.000016		
TOTAL	39	2957.192878	R ² = 0.770		
Models for Estimating Frictional Resistance		Std Error of Y est.		Std. Error of Coeff.	
FR = 93.71504 - 5.23256G + 13.60187Sc		4.541		1.43944 1.43765	
FR = 96.13452 – 0.31184C – 5.10720G + 13.60814Sc		4.372		0.15794 1.38763 1.38444	
FR = 95.97121 + 0.44588Sz - 0.42317C - 5.13414G + 13.60679Sc		4.408		0.68370 0.23344 1.39945 1.39563	
Sz = CRM Size (GF 40, 200) C = CRM Concentration (8, 12%) G = Aggregate Gradation (Fine=1, Coarse = 2) Sc = Aggregate Source (Crushed Stoned = 1, Crushed Gravel = 2)					

Table 9.3.2 Statistical Model for Frictional Resistance at N=8

Analysis of Variance					
Source of Variation	d.f.	Sum of Square	Mean Square	F-Ratio	Sig. Level
MAIN EFFECTS					
A: CRM Size	1	3.4681052	3.4681052	0.09	0.7686
B: CRM Concentration	1	28.1454171	28.1454171	0.72	0.4048
C: Aggregate Gradation	1	109.7810691	109.7810691	2.80	0.1064
D: Aggregate Source	1	548.7537381	548.7537381	13.96	0.0009
INTERACTIONS					
AB	1	123.8045209	123.8045209	3.15	0.0874
AC	1	2.2687667	2.3687667	0.06	0.8079
AD	1	107.293462	107.2933463	2.73	0.1103
BC	1	7.5719864	7.5719854	0.19	0.6641
BD	1	2.2727584	2.2727584	0.06	0.8117
CD	1	2.7481774	2.7481774	0.07	0.7934
RESIDUAL	29	1020.418464	39.246864		
TOTAL	39	2170.971998	R ² = 0.530		
REDUCED MODEL					
MAIN EFFECTS					
A: CRM Size	1	4.7681608	4.7681608	0.13	0.7254
B: CRM Concentration	1	25.3171913	25.3171913	0.67	0.4201
C: Aggregate Gradation	1	92.0343572	92.0343572	2.42	0.1290
D: Aggregate Source	1	598.6308763	598.6308763	15.75	0.0004
RESIDUAL	35	1292.482178	38.014182		
TOTAL	39	2170.971998	R ² = 0.405		
Models for Estimating Frictional Resistance		Std Error of Y est.	Std. Error of Coeff.	R ² Adjusted	
FR = 120.77795 - 3.19075G + 7.373996Sc		6.2507	1.98162 1.97914	0.298	
FR = 124.19207 – 0.44003C – 3.01386G + 7.74881Sc		6.0029	0.21684 1.90504 1.90067	0.353	
FR = 124.08135 + 0.30229Sz – 0.51551C – 3.03212G + 7.74789Sc		6.0791	0.94294 0.32195 1.93008 1.92481	0.336	
Sz = CRM Size (GF 40, 200) C = CRM Concentration (8, 12%) G = Aggregate Gradation (Fine=1, Coarse = 2) Sc = Aggregate Source (Crushed Stoned = 1, Crushed Gravel = 2)					

At the construction stage of the pavement compaction, which is represented by N2 and Nini (N=8), the effects that appear to be most significant are the aggregate source. This deduction can be drawn from the results reported in Tables 9.3.1 and 9.3.2, and is consistent with the observations made from the charts in Sections 9.1 and 9.2.

Based on the results at N=2 and N=8, it appears that

- Neither crumb rubber size nor concentration greatly affects a mixture's frictional resistance to compaction efforts during the construction process.
- An increase in crumb rubber concentration results in a gentle decrease in frictional resistance.
- During construction compaction, aggregate source plays a very significant role in the frictional resistance of the mixture.
- Aggregate gradation causes a significant difference in frictional resistance of mixes at N=2, but decreases in effect at N=8.

The statistical analyses from Table 9.3.1 and 9.3.2 help to identify the effects that are significant in estimating the frictional resistance of mixtures during the construction processes. At this stage of pavement life, of the models that were considered in this analysis, the one that best fits the data is the second model, which includes one crumb rubber variable. The crumb rubber variable suitable for the estimation of frictional resistance at this stage of pavement life is the concentration. However, from the analysis results shown in the tables, it can also be noted that the R^2 value of the model for frictional resistance at Nini is extremely low. This accentuates the difficulty in explaining the behaviour of mixtures during the compaction process, and confirms the need to look further into how mixtures, particularly crumb rubber modified mixtures, respond to compaction.

9.4 Frictional Resistance at Ndesign (N=100)

Ndes (N=100) is one of two stages that is used in Superpave as an indication of the pavement performance during its service life. The frictional resistance results at Ndes are shown in Figure 9.4.1. Boxplots from the statistical analyses of frictional resistance at Ndes are shown in Figures 9.4.2 (a) – (d).

Unlike the responses at N=2 and Nini, the effects of the control variables on the frictional resistance of mixtures are more complex at Ndes. Some of the control effects may not directly impact the level of frictional resistance when considered on their own, but when they are interacted with other effects, they indicate influences.

The results from the bar chart show that in most cases, the inclusion of crumb rubber particles have opposite effects on NCAT and AI mixtures. For AI mixtures, this decreases the frictional resistance by as much as 40 %, the greater differences occurring in fine aggregate mixes. For NCAT mixes, on the other hand, the frictional resistance of the mix is increased by the addition of crumb rubber, with the effect up to 10 %. It is also observed that in most AI mixtures, an increase in crumb rubber particle size results in a decrease in frictional resistance if the mix uses coarse aggregates, and an increase in frictional resistance if the mix uses fine aggregates.

From Figure 9.4.1, it can also be noted that AI mixes demonstrate higher frictional resistance compared to NCAT mixes for the control mixes. However, this relationship is reversed in almost all cases when crumb rubber modifiers are added. The exceptions are the two coarse gradation mixes with GF 200 crumb rubber modifier.

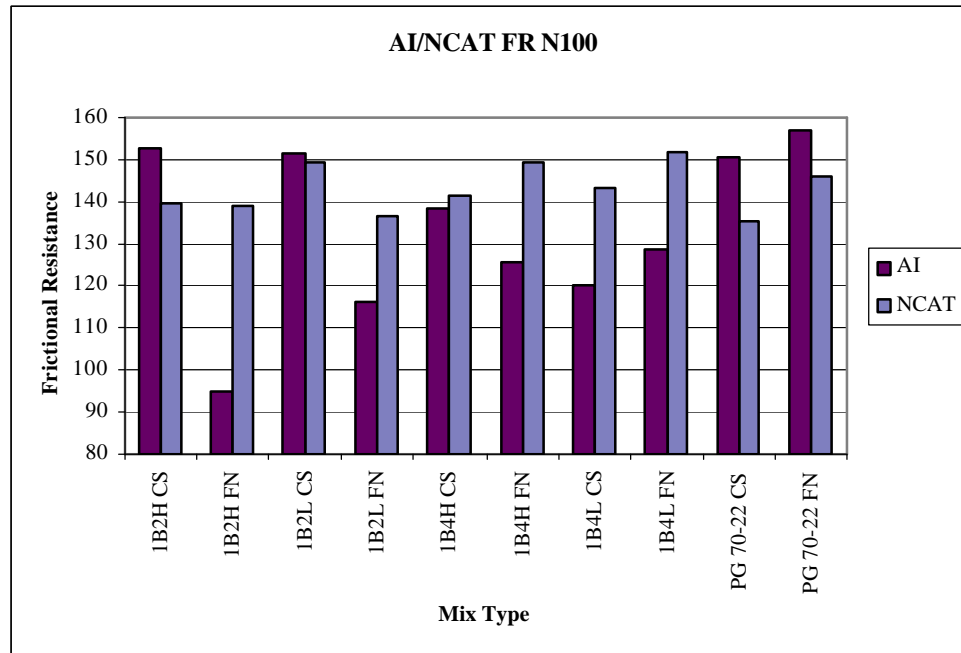
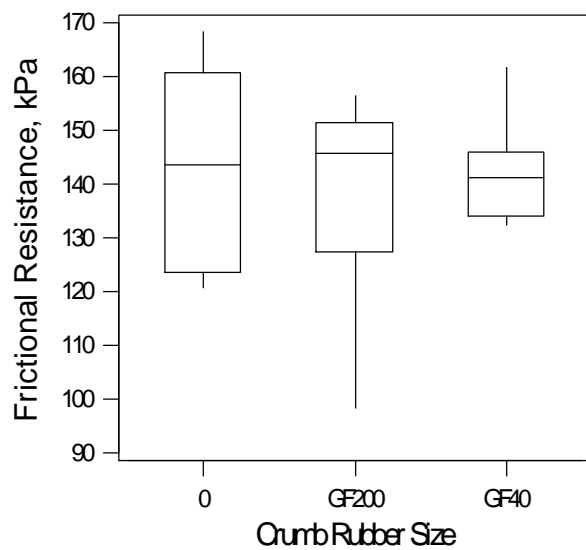
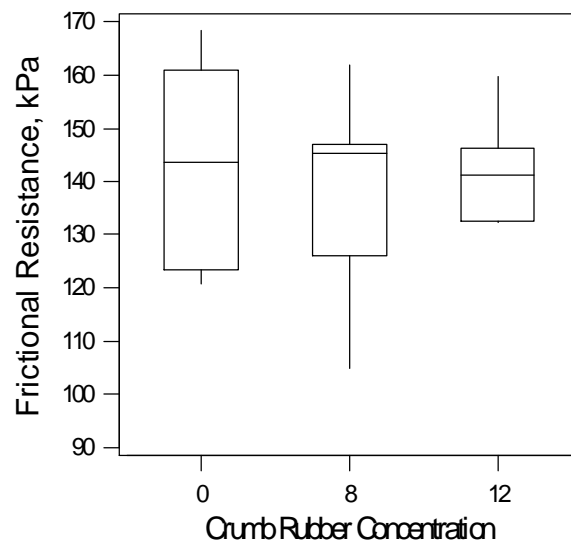
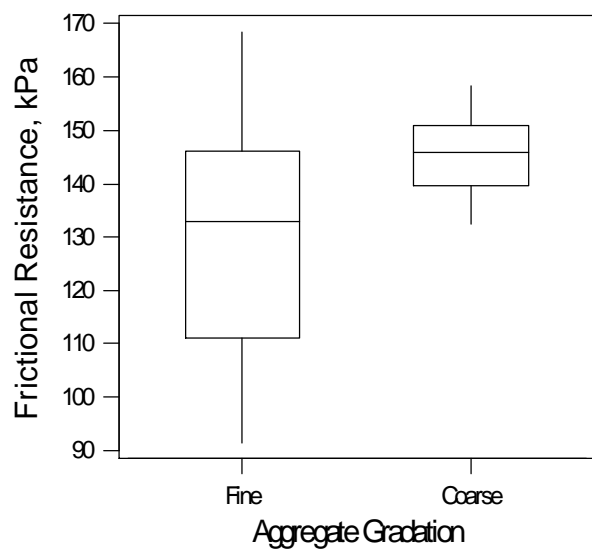
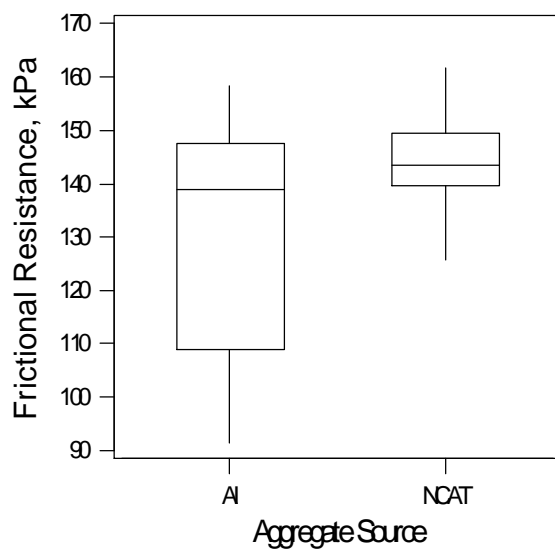


Figure 9.4.1 Frictional Resistance of Mixes at Ndes (N=100)

Apart from the contribution of crumb rubber modifier, aggregate gradation also makes a difference in the frictional resistance of the mixtures, but only in AI mixes. In those cases, fine aggregate mixes generally show lower frictional resistance than coarse aggregate mixes. In NCAT mixes, the differences in the frictional resistance are less than 10%, and not enough to be considered significant.

The results from the frictional resistance of the mixtures at N=100 indicate that all the control variables play a role in influencing the frictional resistance of the mixture, especially in AI mixes, and therefore the performance of pavements during its service life.

**(a) CRM Size****(b) CRM Concentration****(c) Aggregate Gradation****(d) Aggregate Source****Figures 9.4.2 Boxplots of Frictional Resistance at N = 100**

A study of the boxplots reveal the influences of the control variables when all other variables are disregarded. Those plots show that all the variables have an effect on the frictional resistance of mixtures except for aggregate source. Increases in crumb rubber particle size result in decreases in frictional resistance. The same trend is observed when the crumb rubber concentration is increased. The plots for aggregate gradation indicate the same trend as observed from the bar chart, which is that the fine aggregate mixes demonstrate lower frictional resistance than the coarse aggregate mixes.

9.5 Frictional Resistance at N_{maximum} (N=160)

N_{max} (N=160), is the other performance indicator, along with N_{des}, which was discussed in the previous section. The frictional resistance for different mixes at this point in the compaction is charted in Figure 9.5.1.

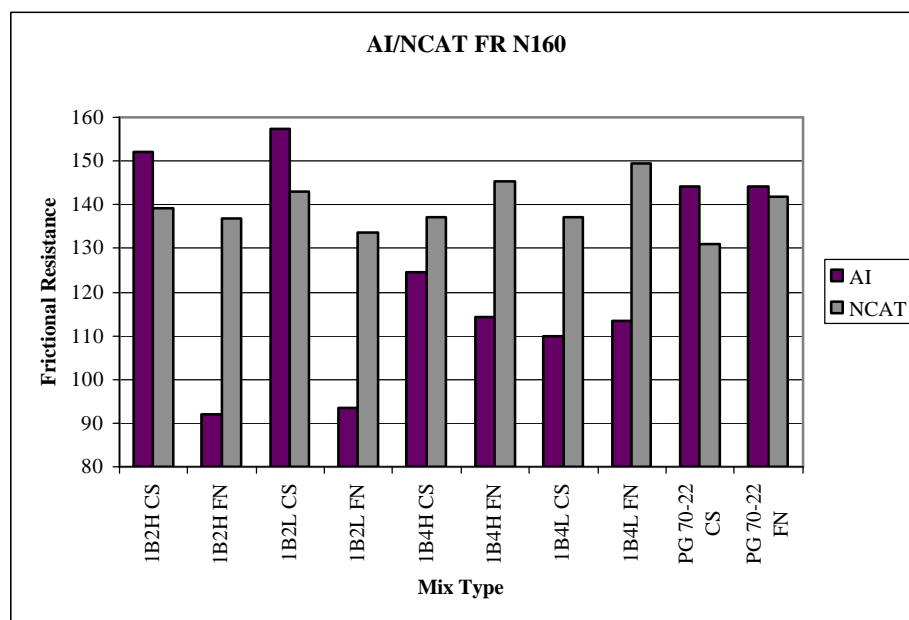
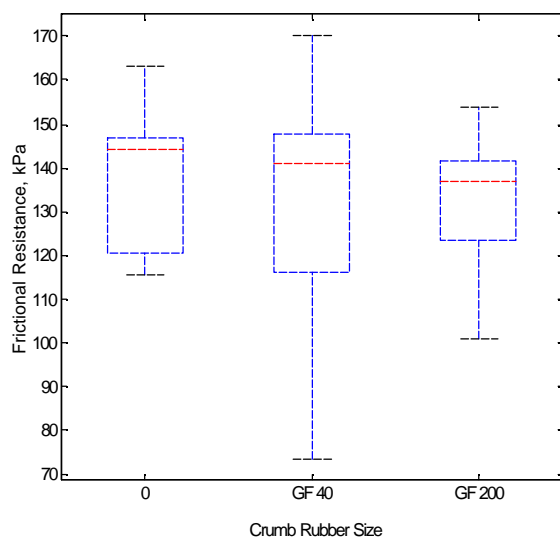


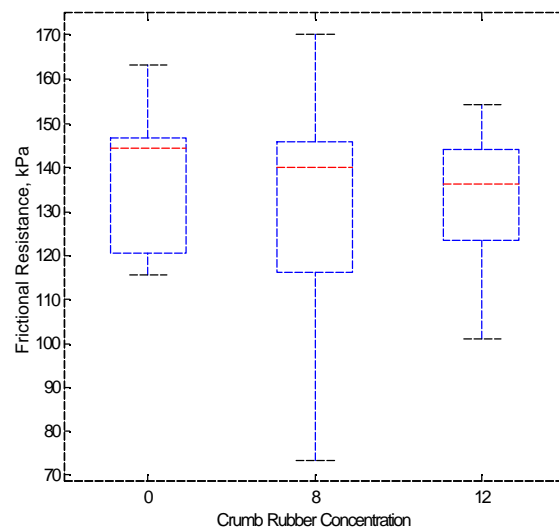
Figure 9.5.1 Frictional Resistance of Mixes at N_{max} (N=160)

In most parts, the trends observed at this stage of compaction are similar to those previously found in the results for Ndes. The mixtures with NCAT aggregate continue to indicate little effect from the variation in control variables. The mixtures with AI aggregates display the same trends as they did at Ndes. Additionally, it is observed that the differences in frictional resistance due to changes in the size of crumb rubber particles added to the binder is larger compared to the same comparisons at Ndes. Similar to the results at N=100, there is a difference between mixes compacted using gravel versus limestone aggregates, regardless of CRM size and concentration or aggregate gradation. This difference is observed to have increased at N=160. It may be deduced from these observations that over the service life of the pavement, the level of resistance to deformation becomes more sensitive to the effects of crumb rubber particle size and aggregate source.

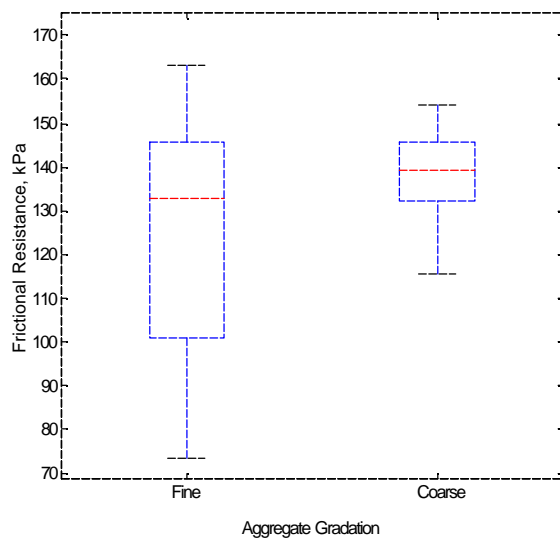
Parallel to the observations for the results at Ndes, the boxplots shown in Figures 9.5.2 (a) – (d) show the same trends with the exception of the boxplot comparing results based on aggregate sources. In the comparison of results due to the effects of aggregate sources, the results at Ndes show that there is no difference due to aggregate sources if other factors are disregarded, while the results at Nmax show that NCAT mixes demonstrate higher frictional resistance.



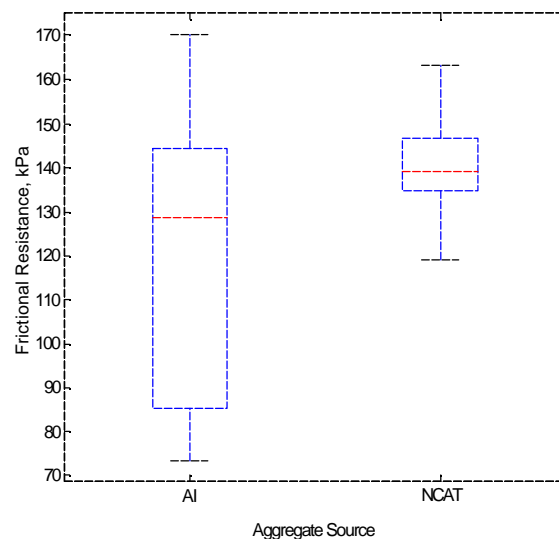
(a) CRM Size



(b) CRM Concentration



(c) Aggregate Gradation



(d) Aggregate Source

Figures 9.5.2 Boxplots of Frictional Resistance at N = 160

9.6 Statistical Analysis for Performance Stage of Compaction

Tables 9.6.1 and 9.6.2 show the results of the statistical analysis performed on the frictional resistance data for mixtures at N_{des} and N_{max} , the performance stage of the pavement life.

From the tables, it can be seen that the notable effects for modeling the frictional resistance during this stage are the aggregate gradation and source main effects, and the crumb rubber size-aggregate gradation and aggregate gradation-source interaction effects. This agrees with the observations that were made from the Figures 9.4.1 and 9.5.1 in Section 9.4 and 9.5.

The tables also show that the models with either one or two crumb rubber variables fit equally well. In the second model, unlike during the construction stage, the crumb rubber variable that results in a better fit is crumb rubber size.

Table 9.6.1 Statistical Model for Frictional Resistance at N=100

Analysis of Variance					
Source of Variation	d.f.	Sum of Square	Mean Square	F-Ratio	Sig. Level
MAIN EFFECTS					
A: CRM Size	1	0.002402	0.002402	0.00	0.9979
B: CRM Concentration	1	87.395413	87.395413	0.25	0.6139
C: Aggregate Gradation	1	5496.298667	5496.298667	16.40	0.0004
D: Aggregate Source	1	6305.437595	6305.437595	18.81	0.0002
INTERACTIONS					
AB	1	49.778235	49.778235	0.15	0.7031
AC	1	1331.419842	1331.419842	3.97	0.0568
AD	1	164.264929	164.264929	0.49	0.4901
BC	1	350.972338	350.972338	1.08	0.3089
BD	1	17.500126	17.500126	0.05	0.8210
CD	1	5080.168531	5080.168531	15.16	0.0006
RESIDUAL	29	8714.16218	335.16008		
TOTAL	39	29487.77444	R ² = 0.7044		
REDUCED MODEL					
MAIN EFFECTS					
A: CRM Size	1	3.165969	3.165969	0.01	0.9398
B: CRM Concentration	1	57.488660	57.488660	0.11	0.7477
C: Aggregate Gradation	1	4245.790348	4245.790348	7.77	0.0086
D: Aggregate Source	1	5047.676469	5047.676469	9.22	0.0045
RESIDUAL	35	18588.84527	546.73074		
TOTAL	39	29487.77444	R ² = 0.370		
Models for Estimating Frictional Resistance		Std Error of Y est.	Std. Error of Coeff.	R ² Adjusted	
FR = 50.97133 + 90.49039G + 46.80533Sc – 46.27070 (G*Sc)		20.5364	20.61917 9.43581 13.02109	0.442	
FR = 31.55492 + 9.49716Sz + 115.54373G + 45.11695Sc – 11.59196(Sz*G) – 44.88701(G*Sc)		18.1430	2.80100 20.37625 8.35098 3.85101 11.53075	0.565	
FR = 29.37139 + 7.83289Sz + 0.78554C + 115.43853G + 45.06369Sc– 11.62483(Sz*G) – 44.79496(G*Sc)		18.2339	3.48010 0.96576 20.47892 8.39310 3.87053 11.57907	0.560	
Sz = CRM Size (GF 40, 200) C = CRM Concentration (8, 12%) G = Aggregate Gradation (Fine=1, Coarse = 2) Sc = Aggregate Source (Crushed Stoned = 1, Crushed Gravel = 2)					

Table 9.6.2 Statistical Model for Frictional Resistance at N=160

Analysis of Variance					
Source of Variation	d.f.	Sum of Square	Mean Square	F-Ratio	Sig. Level
MAIN EFFECTS					
A: CRM Size	1	86.117714	86.117714	0.21	0.6515
B: CRM Concentration	1	35.637598	35.637598	0.09	0.7711
C: Aggregate Gradation	1	6193.424328	6193.424328	15.02	0.0006
D: Aggregate Source	1	9730.026657	9730.026657	23.59	<0.0001
INTERACTIONS					
AB	1	25.802377	25.802377	0.06	0.8045
AC	1	2299.124090	2299.124090	5.57	0.0260
AD	1	360.078675	360.078675	0.87	0.3587
BC	1	104.173402	104.173402	0.25	0.6195
BD	1	25.406356	25.406356	0.06	0.8000
CD	1	6969.050506	6969.050506	16.87	0.0004
RESIDUAL	29	10723.31148	412.43506		
TOTAL	39	38132.61459	R ² = 0.719		
REDUCED MODEL					
MAIN EFFECTS					
A: CRM Size	1	60.727206	60.727206	0.09	0.7658
B: CRM Concentration	1	19.896948	19.896948	0.03	0.8646
C: Aggregate Gradation	1	5347.037923	5347.037923	7.94	0.0080
D: Aggregate Source	1	8215.603159	8215.603159	12.20	0.0013
RESIDUAL	35	22903.88537	673.64369		
TOTAL	39	38132.61459	R ² = 0.399		
Models for Estimating Frictional Resistance		Std Error of Y est.		Std. Error of Coeff.	R ² Adjusted
FR = 27.03400 + 104.02791G + 56.88600Sc – 5366245(G*Sc)		22.3201		22.41010 10.25538 14.15308	0.491
FR = 8.76381 + 8.92650Sz + 128.79387G + 55.29729Sc – 11.34675(Sz*G) + 52.42433(G*Sc)		20.5157		3.16731 23.04112 9.44310 4.35463 13.02740	0.570
FR = 5.21588 + 6.23229Sz + 1.27639C + 128.62294G + 55.21075Sc – 11.40018(Sz*G) – 52.27476(G*Sc)		20.3973		3.89298 1.08035 22.90860 9.38889 4.32974 12.95284	0.575
Sz = CRM Size (GF 40, 200) C = CRM Concentration (8, 12%) G = Aggregate Gradation (Fine=1, Coarse = 2) Sc = Aggregate Source (Crushed Stoned = 1, Crushed Gravel = 2)					

9.7 Frictional Resistance at N=600

In this research, compaction was performed past the Superpave specified number of gyrations, up to 600 gyrations. For the purpose of this research, N=600 was considered as the terminal pavement condition, at which point the pavement is considered to require reconstruction. Figure 9.7.1 illustrates the results obtained from the compaction of mixtures up to N=600.

These results once again present similar trends to those observed at Ndes and Nmax. The effect of changing aggregate source results in the same trends of responses in the mixtures, suggesting that aggregate source is an important factor affecting the frictional resistance during mixture compaction. Exceptions to those observations are noted as follows:

- Unlike the results at Ndes and Nmax, the control mixes at N=600 also show that NCAT mixes demonstrate greater frictional resistance than AI mixes.
- The relative differences between NCAT and AI mixtures are increased yet again, reinforcing the idea of increased sensitivity to aggregate source variation with increased pavement age.
- The variation in aggregate gradation result in differing effects on the frictional resistance of mixtures.
 - For NCAT mixtures containing GF 200 (smaller) crumb rubber particles, there is no significant effect from varying aggregate gradation, while mixtures including GF 40 crumb rubber particles show increased frictional resistance with a finer aggregate gradation.
 - For AI mixtures, a finer aggregate gradation used in the mixtures

generally results in a lower frictional resistance.

The boxplots, Figures 9.7.2 (a) – (d), show trends based on the individual control variable, while holding all other variables as constant. These figures show that the aggregate characteristics are very significant effects in determining the frictional resistance of mixtures at the terminal point of its service life. Figure 9.7.2 (c) shows that there is a noticeable difference in the frictional resistance of fine aggregate mixes and coarse aggregate mixes. However, this trend is opposite of those that were noticed in the cases at N_{des} and N_{max} . At $N=600$, there is a drastic decrease in frictional resistance if coarse gradation aggregates were used in the mix, while at N_{des} and N_{max} , using coarse aggregates instead of fine aggregates would increase the frictional resistance. The difference in aggregate source, on the other hand, caused the same response, except that the change was more pronounced at $N=600$.

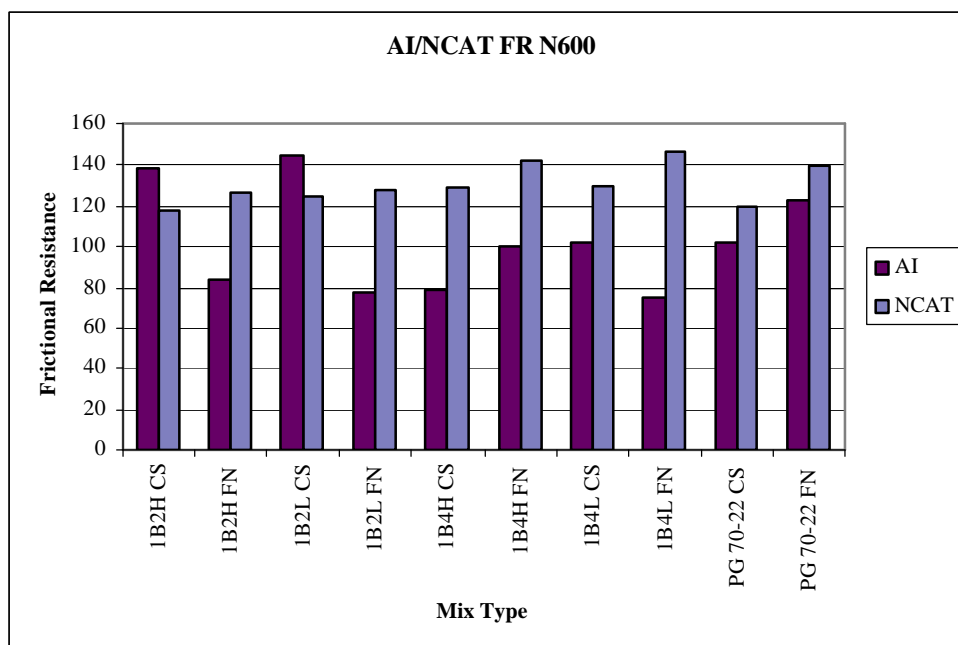
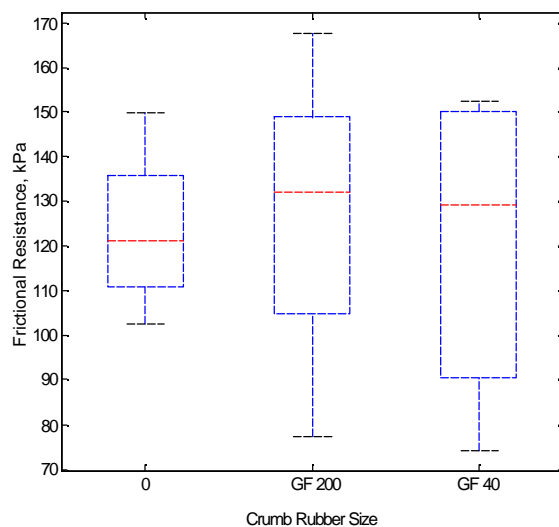
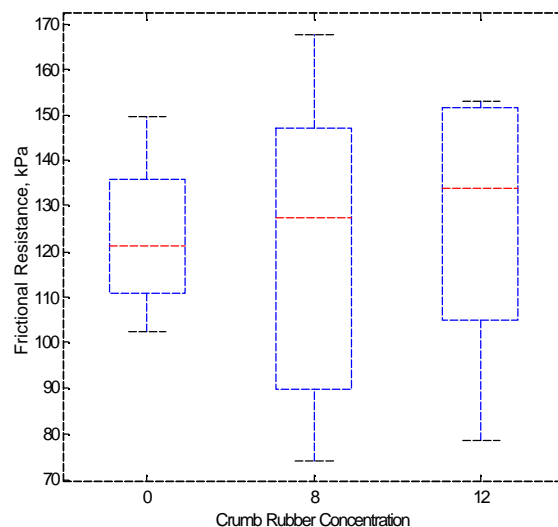
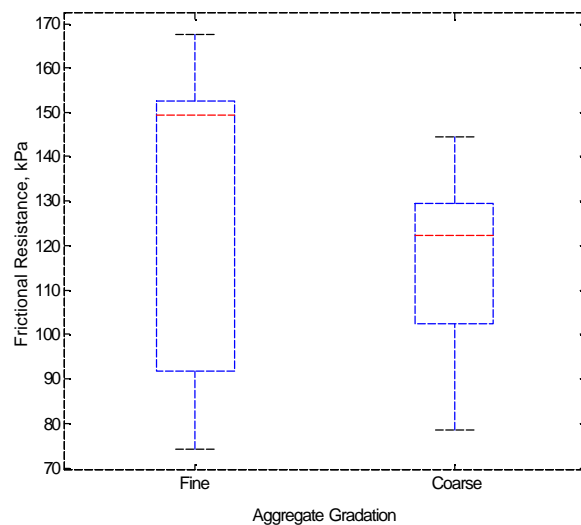
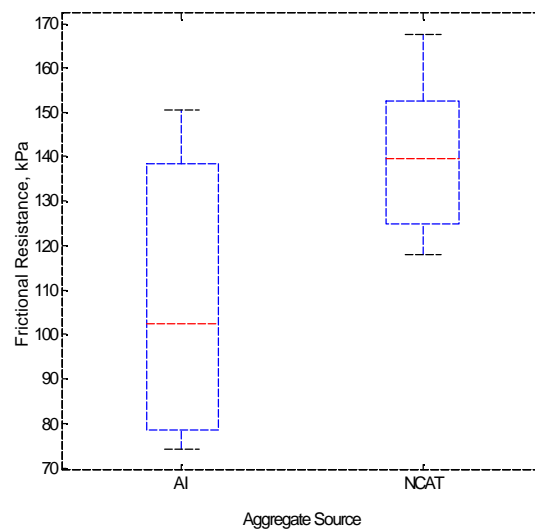


Figure 9.7.1 Frictional Resistance in Mixes at $N=600$

**(a) CRM Size****(b) CRM Concentration****(c) Aggregate Gradation****(d) Aggregate Source****Figures 9.7.2 Boxplots of Frictional Resistance at N = 600**

9.8 Maximum Frictional Resistance

In the analysis for this research, the point at which maximum frictional resistance is exerted by a mixture is considered as the point at which the mixture begins to experience failure. The results from the compaction of mixtures at this point are shown in Figure 9.8.1.

It is obvious from the figure that the trends at Max FR are not as clear as those at points previously discussed. This may be because the maximum level of frictional resistance occurs at different points during the pavement's life for different pavement mixes.

The responses in the frictional resistance to the changes in the control variables differed for NCAT mixes and AI mixes. The results show that the effect of crumb rubber modifier in the mixtures is significant at maximum frictional resistance only in some AI mixtures. For NCAT mixtures, the addition of crumb rubber affected the frictional resistance between 1.3 and 6.9 %, which is considered to be insignificant. The effects are more pronounced in AI mixtures, the range of change in frictional resistance with the inclusion of crumb rubber particles being from 0.3 to 19.3 %. The extent of the effect of crumb rubber modifier on the maximum frictional resistance also depends on other factors:

- A change in crumb rubber concentration does not result in a significant change in the maximum frictional resistance if the larger crumb rubber particle size is included.
- If the smaller crumb rubber particle is included in the mixture, a decrease in concentration would lead to an increase in the maximum frictional resistance, but if the larger crumb rubber particle is included, the changes in frictional resistance is not significant.
- An increase in crumb rubber particle size leads to a decrease in maximum frictional resistance if coarse aggregates are used in the mix, but if fine aggregates are used in

the mix, a change in crumb rubber particle size has no effect on the frictional resistance.

A study of the boxplots in Figures 9.8.2 (a) – (d) indicate that there is a trend when crumb rubber characteristics are varied. An increase in crumb rubber size or crumb rubber concentration would decrease the frictional resistance of the mixture. However, these changes do not appear to be significant when considered relative to the magnitude of the frictional resistance. The variation of aggregate characteristics also do not cause any significant deviations in frictional resistance.

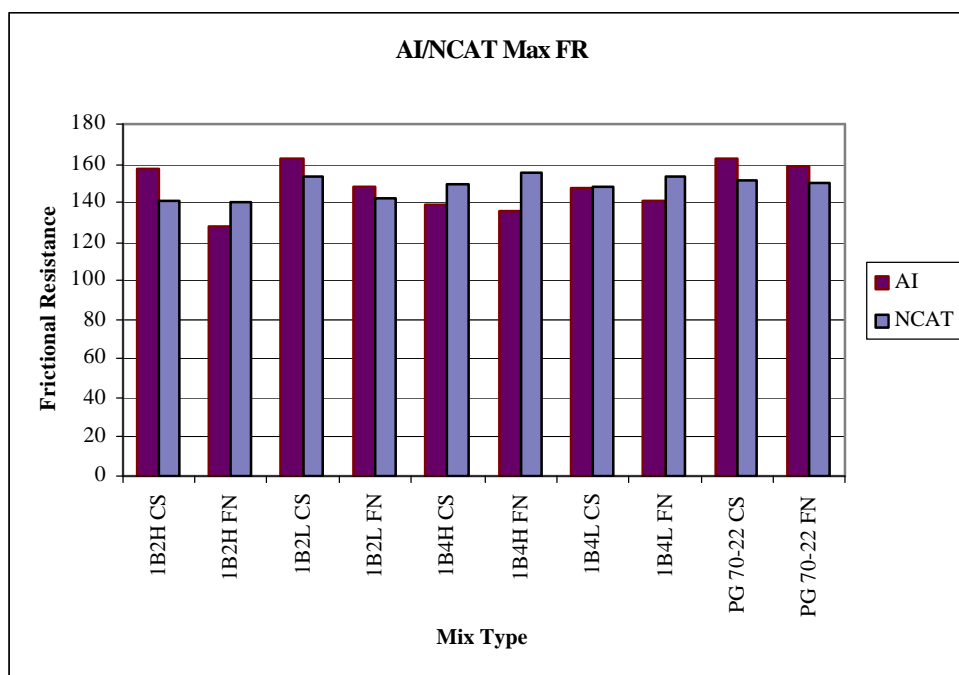
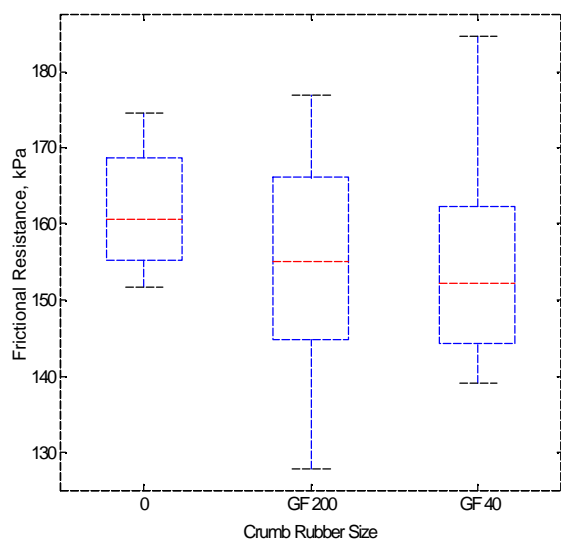
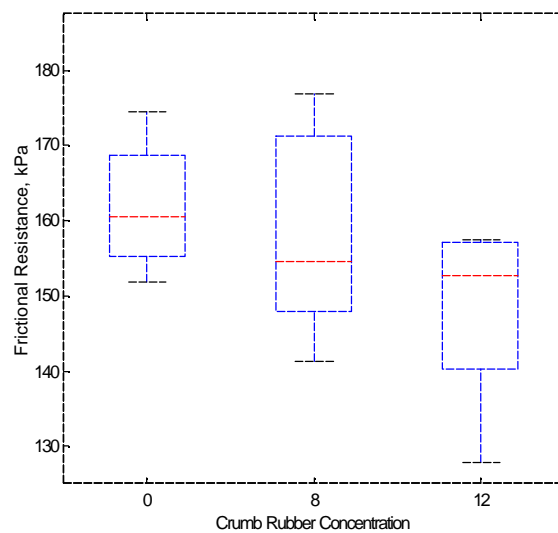


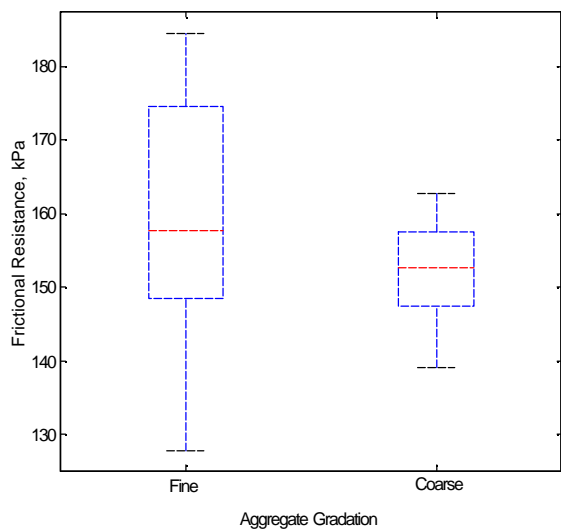
Figure 9.8.1 Maximum Frictional Resistance



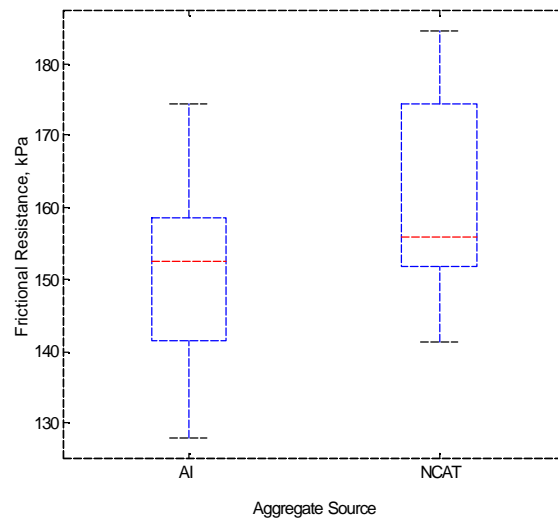
(a) CRM Size



(b) CRM Concentration



(c) Aggregate Gradation



(d) Aggregate Source

Figures 9.8.2 Boxplots of Maximum Frictional Resistance

9.9 Statistical Analysis for Failure Stage of Compaction

Table 9.9.1 Statistical Model for Frictional Resistance at N=600

Analysis of Variance					
Source of Variation	d.f.	Sum of Square	Mean Square	F-Ratio	Sig. Level
MAIN EFFECTS					
A: CRM Size	1	157.75360	157.75360	0.25	0.6323
B: CRM Concentration	1	109.51622	109.51622	0.17	0.6895
C: Aggregate Gradation	1	1950.24003	1950.24003	3.06	0.1185
D: Aggregate Source	1	13440.47041	13440.47041	21.07	0.0018
INTERACTIONS					
AB	1	281.56840	281.56840	0.44	0.5251
AC	1	952.03103	952.03103	1.49	0.2566
AD	1	115.56250	115.56250	0.18	0.6816
BC	1	856.14760	856.14760	1.34	0.2800
BD	1	408.64623	408.64623	0.64	0.4466
CD	1	1398.38430	1398.38430	2.19	0.1770
RESIDUAL	11	5102.46008	637.80751		
TOTAL	21	36110.18426	R ² = 0.859		
REDUCED MODEL					
MAIN EFFECTS					
A: CRM Size	1	157.75360	157.75360	0.19	0.6677
B: CRM Concentration	1	109.51622	109.51622	0.13	0.7203
C: Aggregate Gradation	1	1292.24237	1292.24237	1.57	0.2287
D: Aggregate Source	1	11598.74630	11598.74630	14.06	0.0017
RESIDUAL	17	13196.60036	824.78752		
TOTAL	21	36110.18426	R ² = 0.635		
Models for Estimating Frictional Resistance		Std Error of Y est.		Std. Error of Coeff.	R ² Adjusted
FR = 43.16842 – 15.32818G + 51.90233Sc		32.5449		13.87718 13.93488	0.384
FR = 23.93509 + 3.60625C – 15.32818G + 47.09400Sc		27.63157		1.24742 11.78214 11.94747	0.556
FR = 23.99585 – 0.29112Sz + 3.68219C – 15.32818G + 47.10919Sc		28.43081		6.20282 2.06536 12.12294 12.29730	0.530
Sz = CRM Size (GF 40, 200) C = CRM Concentration (8, 12%) G = Aggregate Gradation (Fine=1, Coarse = 2) Sc = Aggregate Source (Crushed Stoned = 1, Crushed Gravel = 2)					

Table 9.9.2 Statistical Model for Frictional Resistance when FR is Maximum

Analysis of Variance					
Source of Variation	d.f.	Sum of Square	Mean Square	F-Ratio	Sig. Level
MAIN EFFECTS					
A: CRM Size	1	13.266802	13.266802	0.15	0.7386
B: CRM Concentration	1	97.674525	97.674525	1.08	0.4078
C: Aggregate Gradation	1	15.941133	15.941133	0.18	0.7154
D: Aggregate Source	1	38.398021	38.398021	0.42	0.5815
E: Gyration Number	1	90.687085	90.687085	1.00	0.4221
INTERACTIONS					
AB	1	0.919161	0.919161	0.01	0.9289
AC	1	3.770907	3.770907	0.04	0.8571
AD	1	20.186318	20.186318	0.22	0.6831
AE	1	13.569119	13.569119	0.15	0.7358
BC	1	26.212288	26.212288	0.29	0.6442
BD	1	0.362551	0.362551	0.00	0.9553
BE	1	0.020682	0.020682	0.00	0.9893
CD	1	2.484608	2.484608	0.03	0.8836
CE	1	12.511314	12.511314	0.14	0.7456
DE	1	2.356561	2.356561	0.02	0.8866
RESIDUAL	6	180.877940	90.438970		
TOTAL	21	5017.874182	R ² = 0.964		
REDUCED MODEL					
MAIN EFFECTS					
A: CRM Size	1	23.140586	23.140586	0.15	0.6999
B: CRM Concentration	1	570.205391	570.205391	3.80	0.0701
C: Aggregate Gradation	1	206.54816	206.54816	1.38	0.2588
D: Aggregate Source	1	333.504781	333.504781	2.22	0.1566
E: Gyration Number	1	1640.312582	1640.312582	10.94	0.0048
RESIDUAL	16	2248.845801	149.923053		
TOTAL	21	5017.874182	R ² = 0.552		
Models for Estimating Frictional Resistance		Std Error of Y est.	Std. Error of Coeff.	R ² Adjusted	
FR = 111.24413 + 47.62465G + 26.23278Sc + 0.02220Gy – 31.21928(G*Sc)		10.34269	14.05457 7.08309 0.01286 9.61247	0.552	
FR = 111.93270 – 0.34898Sz + 47.37737G + 26.13730Sc + 0.02312Gy – 30.95388(G*Sc)		10.64215	1.50568 14.50216 7.30049 0.01380 9.95777	0.526	
FR = 136.60796 + 2.82111Sz – 1.71555C + 6.58062G + 8.56086Sc + 0.05094Gy		12.31915	2.71212 0.96582 5.77418 5.51699 0.01578	0.365	
Sz = CRM Size (GF 40, 200) C = CRM Concentration (8, 12%) G = Aggregate Gradation (Fine=1, Coarse = 2) Sc = Aggregate Source (Crushed Stoned = 1, Crushed Gravel = 2) Gy = Number of Gyration					

The frictional resistance at N600 and the maximum resistance represent the response of a mixture material when it is on the course of deterioration and failure. As the maximum frictional resistance occurs at different points during the compaction of the mixtures, the gyration number at which it occurred was considered as a variable when maximum frictional resistance was evaluated.

The analysis of frictional resistance at N=600 and at maximum value indicate that different variables are significant in determining the response of a mixture to deformation, even though they are both being considered as the failure stage of pavement life. At 600 gyrations, aggregate source is a significant factor, while crumb rubber concentration and the gyration number is important in estimating the maximum frictional resistance.

Although two different models are required to estimate the frictional resistance at N=600 and the maximum frictional resistance, both analyses identify aggregate source and gradation as variables necessary for predicting the response of the mixture to compaction. The model that best estimates the frictional resistance at N=600 involves crumb rubber concentration, aggregate gradation, and aggregate source, while the model that provides the best fit for estimating the maximum frictional resistance considers the aggregate gradation and source, the number of gyration at which this point occurs, and the interaction effect between the aggregate gradation and source.

9.10 Summary of the Effect of Crumb Rubber on Frictional Resistance

Based on the analysis of frictional resistance, crumb rubber has an effect on the frictional resistance of a pavement mixture under deformation, especially once the pavement is put into service. However, the effects cannot be generalized, and is dependent on the stage

in the pavement life, and other components of the mixture material. At the beginning of the service life, it appears that crumb rubber effects are not significant. The impact of crumb rubber modifiers becomes more noticeable as a part of an interaction effect as the mixtures pass through the performance phase. When they arrive at the failure stage, crumb rubber is once again not a major role player when it comes to determining frictional resistance.

CHAPTER 10: SUMMARY OF FINDINGS OF PART II

For this research, the focus was on the effects of crumb rubber modifiers on compacted asphalt mixtures. Studies were conducted to look into the densification characteristics and possible rebound effects of compacted mixtures. In addition, the frictional resistance of mixtures during compaction as a result of varying crumb rubber particle size and concentration in the asphalt binders used was evaluated. The effects of different aggregate sources and gradation were also considered. Statistical analyses were performed to identify the factors that had significant effects on the densification and frictional resistance of mixtures. The following sections give a summary of the findings.

10.1 Rebound Effects of Crumb Rubber Modified Mixes

- Prior expectations that the presence of crumb rubber modifiers in asphalt mixtures may lead to swelling due to rebound of the rubber were not supported by lab measurements. Lab tests show that there is a volume reduction in compacted mixes after cooling. The reduction in volume can be attributed to the shrinkage of asphalt due to cooling.
- Statistical analysis of the rebound effects show that
 - Crumb rubber particle size does not significantly affect the amount of volume change in a compacted mix.
 - Crumb rubber concentration is not a significant contributor to the change in volume of a mix.
 - Aggregate gradation are found to have significant effect on the volume change in a mixture.

- Aggregate source is not a significant factor in the amount of volume change in a mix.

10.2 Crumb Rubber Effects on Densification Characteristics of Asphalt Mixtures

The compaction of asphalt mixtures was separated into three stages to represent the pavement construction and service life. The three stages are the construction, performance, and terminal stages. These stages are represented by gyration numbers: 2 and 8 gyrations for construction, 100 and 160 for performance, and 600 for failure. Analyses of the results for air void content were considered according to those stages.

10.2.1 During the Construction Stage

- The inclusion of crumb rubber modifiers affects the voids content by reducing the packing of mixture. The effect is also dependent on the specific characteristics of the crumb rubber and aggregates in the mix.
- The effect of crumb rubber is different between AI limestone mixes and NCAT gravel mixes. The effect is more pronounced in AI mixes than it is in NCAT mixes.
- The effect of crumb rubber is also influenced by the aggregate gradation of the mix. Mixes with fine aggregates are more likely to be affected by the inclusion of crumb rubber.
- Statistical analysis show that crumb rubber size and concentration is not highly important in estimating the densification of mixtures at this stage of the pavement's service life.

10.2.2 During the Performance Stage of the Pavement Life

- The effect of crumb rubber on the densification of mixtures during the performance stage is more complex than at the construction stage, as the effect is dependent on multiple interacting factors.
- The effect of aggregate gradation differed for the two numbers of gyrations considered in mixture performance (N=100 and N=160). The effect is significantly dependent on crumb rubber size and concentration.
- NCAT mixes are more susceptible to the effects of crumb rubber modifiers than AI mixes, especially for mixes with larger crumb rubber particles.
- Crumb rubber size and concentration have a combined effect on the densification of mixtures. Mixes with higher crumb rubber concentration and larger crumb rubber particles indicate greater effects due to the modification.
- In order to estimate the void content of a mixture during this stage, it is necessary to have information on all the control variables, as the interactive effects are significant factors in the estimation.

10.2.3 At the Terminal Stage of Pavement Life

- The results show that NCAT mixes demonstrate greater response to addition of crumb rubber than AI mixtures.
- Crumb rubber has a greater effect on mixtures with fine gradation aggregates than mixes with coarse gradation aggregates.

- A combination of NCAT fine graded mixes with high crumb rubber concentration or large crumb rubber size also results in greater change in voids content.

10.3 Crumb Rubber Effects on the Frictional Resistance of Mixtures

The results for frictional resistance were analyzed in a similar manner to those for air void content. The compaction was separated into the construction, performance, and failure stages. The construction stage was represented by results of mixes at 2 and 8 gyrations during compaction, performance stage was represented by results at 100 and 160 gyrations, and the failure stage was represented by the results at 600 gyrations and the maximum value.

10.3.1 During the Construction Stage

- The frictional resistance is not greatly affected by either aggregate gradation, crumb rubber size or rubber concentration at the initial compaction stage,
- Aggregate source is the only important factor. The effect from aggregate source is more significant at N=2 and not as important at N=8. The significance of N=2 is not well known.

10.3.2 During the Performance Stage

- The analysis indicates that the inclusion of crumb rubber does create a difference in the frictional resistance of mixtures, but the effect is also influenced by other control variables.
- Aggregate source has a role in the frictional resistance of mixtures, with NCAT mixtures showing greater frictional resistance to deformation than AI mixtures.

- Mixtures with AI aggregates appear to respond to variations in crumb rubber particle size and concentration and aggregate gradation more than mixtures with NCAT aggregates.
- Crumb rubber induces opposite effects in AI and NCAT mixtures. The frictional resistance in AI mixes decreases with the addition of crumb rubber, while in NCAT mixes, an increase is observed.
- Aggregate gradation is a significant factor affecting the frictional resistance in AI mixes, but not in NCAT mixes.
- The results seem to indicate that as the pavement goes further through its service life, the frictional resistance of a mixture becomes more sensitive to the effects of crumb rubber particle size and aggregate source.

10.3.3 During the Failure Stage of the Pavement's Service Life

- Aggregate source plays a role in the frictional resistance, with NCAT mixtures showing higher frictional resistance, but only at N=600. At maximum frictional resistance, there is no clear trend indicating the effect of aggregate source.
- The role of aggregate gradation on the frictional resistance varies, and is dependent on aggregate source and crumb rubber size.
- The role of crumb rubber size and concentration is highly interactive.

10.4 Limitations of Research and Suggested Future Work

This research was performed primarily to investigate the effects that crumb rubber modifiers have on the performance of asphalt mixtures. There is no Superpave specification

currently in place to test mixtures which use crumb rubber particles. The results that were found from this research cannot be taken as universal since the combination of control variables used, which are crumb rubber size and concentration, and aggregate type and gradation, was not a wide and comprehensive range.

This research also used a new device, the gyratory load cell plate assembly, which measures a property – frictional resistance – which was previously not considered. The feasibility of this device and practicality of the results produced by this device are still being investigated. It should be recommended that the capabilities of the device be further examined and applied towards a wider range of crumb rubber modified mixtures.

Finally, the statistical models developed during this research were only used to identify the effects, which are influential in determining the desired properties, based on assumptions of linear regression. They should not be used to estimate the absolute performance of the materials.

CHAPTER 11: SUMMARY OF PROJECT

11.1 Overall Summary

The addition of CRM affects the properties and behavior of CRM modified binders and mixtures in a variety of ways. The effects can be summarized as follows:

- *Effect on viscosity:* It is found that the addition of CRM has a significant effect on the viscosity of asphalt binder. CRM modified binders are affected by the concentration and size of CRM, as well as the shear rate applied during viscosity testing.
- *Particulate additive test:* The results indicate that the size of the CRM particles have a significant effect on the volume of residue present in the asphalt binder.
- *Mechanical working dependency:* The addition of CRM increases the dependency of asphalt binders on mechanical working. G^* ratio, which is the relative change in G^* between 50 cycles and 5000 cycles, and δ ratio, which is the relative change in phase angle between 50 and 5000 cycles, are indicators used to determine mechanical working dependency. It is found that the dependency of CRM binders on mechanical working is affected by asphalt binder type and the strain applied during the test.
- *Strain dependency:* CRM binders are found to be highly strain dependent. The dependency on strain is affected by the temperature, asphalt binder type, and CRM size.
- *Frequency testing:* The critical temperatures calculated from the results of frequency sweep tests are found to be sensitive to binder type, CRM concentration, level of aging, and the frequency of oscillation used in the testing.
- *Creep and direct tension testing:* The creep response of CRM binders was found to be sensitive to temperature, time of loading, binder type, and the size and concentration of the CRM. The critical temperature for creep stiffness and creep rate was found to

decrease with increasing loading time. The failure stress and strain, determined using the DTT, were found to reduce with increased CRM size and increase with increased CRM concentration.

- *Storage stability:* The LAST tests indicate that CRM binders possess the potential for separation and degradation during storage. It is found that CRM size and concentration are factors that affect the potential for separation of the additives in the asphalt during storage, but not the potential for degradation. Agitation of the binder reduces the potential for separation, but does not affect the likelihood for degradation.
- *Rebound effects of CRM mixtures:* Lab measurements do not support prior expectations that the presence of CRM may lead to swelling due to rebound of the rubber. The compacted mixtures were observed to experience volume reduction upon cooling.
- *Densification during construction stage:* The addition of CRM affects the voids content by reducing the packing of the mixture. The effect is more pronounced in limestone mixes than in gravel mixes. The effect of CRM is also influenced by the aggregate gradation of the mixtures.
- *Densification during performance stage:* The effect of CRM on asphalt mixtures is more complex during the performance stage, and dependent on multiple interacting effects. It is necessary to have information on all control variables to estimate the void content of a mixture during this stage.
- *Densification during terminal stage:* The use of CRM affects gravel mixes more than limestone mixtures, and the effects are more significant for mixes with fine gradation aggregates versus mixtures with coarse gradation aggregates.

- *Frictional resistance during construction stage:* The frictional resistance during the initial construction stage is not greatly affected by aggregate gradation, CRM size or concentration. The aggregate source is the only important factor.
- *Frictional resistance during performance stage:* The inclusion of CRM is found to create a difference in the frictional resistance of mixtures, but the effect is also influenced by aggregate variables such as aggregate source and aggregate gradation.
- *Frictional resistance during terminal stage:* The effects of CRM size and concentration are highly interactive. Aggregate source and gradation also play a role in the frictional resistance, but the effects vary.

11.2 Summary of Construction Applications

Based on findings of the research, the addition of crumb rubber modifiers in the asphalt binder, and subsequently in the asphalt mixtures, changes the properties of the material, which in turn could affect the use of the material in the field.

The addition of CRM increases the viscosity of the asphalt binder, an unfavorable effect. This makes the pumping, mixing, and compaction using the material more difficult. On the other hand, the increased viscosity does reduce the potential for reflective cracking, stripping, and rutting. The addition of CRM contributes favorably to the rutting resistance of the modified binder and mixtures. It also enhances the material's ability to resist tensile stresses (thermal cracking) at low temperatures, as well as improving the binder's durability and helping delay the effects of oxidation and aging.

The research results show that there is no need for concern for the rebound of CRM modified mixtures after compaction, since there is no significant contribution of the CRM to volume change.

During the compaction of asphalt mixtures, the addition of CRM does affect the void contents and packing of the mixture, but the effects are often coupled with other factors, such as aggregate source and aggregate gradation. The CRM modification does not, however, create significant effects in the sheer resistance of the mixture to compaction. Therefore, the use of CRM in mixture should not be a great concern where the frictional resistance is being considered.

REFERENCES

1. R.G. Hicks “The Use of Crumb Rubber Modifier in Asphalt Pavement : A National Research Program 1995.
2. Summary of Texas Department of Transportation Reseach Projects, September 1995.
3. Bahia U. Hussain “Effect of Crumb Rubber Modifiers (CRM) on Performance-Related Properties of Asphalt Binders” Proceeding of Asphalt Paving Technology – 1994.
[Madapati et al, 1996]
4. Andres Rangel “Rheological Evaluation of Asphalt Binders Modified with Solid Additives 1998.
5. The Asphalt Research Group Department of Civil & Environmental Engineering The University of Wisconsin – Madison, “Characterization of Simple and Complex Crumb Rubber Modified Binders” 1998.
6. H.B. Bahia, H. Zhai, “Storage Stability of Modified Binders Using the Newly Developed LAST Procedures.” , International Journal of Road Materials and Pavement Design. 1999
7. Michael A. Heitzman, P.E. “ State of the Practice – Design and Construction of Asphalt Paving Materials with Crumb Rubber Modifier”
8. Mt. St Helens Project “Association of Asphalt Paving Technologists, Evaluation of Rubber-Modified Asphalt Performance”.
9. Proceedings of National Seminar on Asphalt Rubber, Design Methods for Hot-Mixed Asphalt-Rubber Concrete Paving Materials, October. 1989

10. Douglas I. Hanson and Gregory M. Duncan “Characterization of Crumb Rubber-Modified Binder Using Strategic Highway Research Program Technology”
Transportation Research Record, v. 1488, 1995
11. Heizman, M. Specification Guidelines “Crumb Rubber Modifier Workshop Notes”
FHWA U.S. Department of Transportation, Feb. 1993.
12. Robert B. McGennis “Evaluation of Physical Properties of Fine Crumb Rubber-Modified Asphalt Binders” Transportation Research Record, v. 1488, 1995.
13. Oregon State University “Crumb Rubber Modifier in Asphalt Pavement – Interim Reprot” 1997.
14. Bahia U. Hussain “Critical Properties of Modified Binders: Summary of Results From NCHRP 9-10 Project ”1999.
15. D.A. Anderson, D. W. Christensen, H. U. Bahia, R. Dongre, M.G. Sharma and J.J. Button, “Binder Characterization and Evaluation, Volume 3: Physical Characterization, SHRP-A-369 Report, The Strategic Highway Research Program, National Research Council, Washington, D.C., 1994.
16. Bahia U. Hussain, W. Hlslop “Classification of Asphalt Binders into Simplex and Complex Binders” Journal of the Association of Asphalt Paving Technology, v 67,1998.
17. Bahia U. Hussain, Davies Robert “Role of Crumb Rubber Content and Type in Changing Critical Properties of Asphalt Binders” Journal of the Association of Asphalt Paving Technology, v 64, 1995.
18. H.B. Bahia, H. Zhai, and A. Rangel, The LAST, The PAT, and the Modified RTFO :
New Test Methods for Better Characterization of Modified Asphalt Binders, submitted for presentation at the 1998 Annual Transportation Research Board Meeting.

19. H.B. Bahia, D.A. Anderson, and D Christensen, "The Bending Beam Rheometer : A Simple device for Measuring Low Temperature Rheology of Asphalt" H.B. Bahia, Journal of the Association of Asphalt Paving Technology, v 62, 1993.
20. H.B. Bahia, D.I. Hanson, et al., Quarterly Report for NCHRP 9-10, Dec., 1996
21. D.A. Anderson, and T.W. Kennedy, "Development of SHRP Binder Specification", Journal of the Association of Asphalt Paving Technology, v 62, 1993.
22. D.A. Anderson, and D.W. Christensien, and H.U. Bahia, "Properties of Asphalt Cement and the Development of Performance-Related Specification , Journal of the Association of Asphalt Paving Technology, v 60, 1991.
23. G.N. King, H.W., King, O. Harders, P. Chavenot, "Influence of Asphalt Grade and Polymer Concentration on the High Temperature Performance of Polymer Modified Asphalt, Asphalt Paving Technology, v 60, 1992
24. H.B. Bahia, Dario Perdomo, and Pamela Turner, "Applicability of Superpave Binder Testing Protocols to Modified Binders", Transportation Research Record 1586, 1997
25. Bahia, H.U., and D.A. Anderson, The New Proposed Rheological Properties : "Why Are They Required and How They Compare to Conventional Properties ", Transportation Research Record 1488, 1995
26. Mei Ling, Christine W., Curtis, Douglas I. Hanson, and Jamens N. Hool, "Quantitative Analysis of Polymers and Crumb Rubber in Hot-Mix Asphalts", Transportation Research Record 1586, 1996
27. Guler, Murat, and Bahia, H.U, "Development of a Device for Measuring Shear Resistance of HMA in the Gyratory Compactor", Transportation Research Board Preprint, 2000

28. Troy, Kenneth, Sebaaly, Peter E., and Epps, Jon A., “ Evaluation Systems for Crumb Rubber Binders and Mixtures”, Transportation Research Record 1530, 1996
29. Gowda, Gary V., Hall, Kevin D., and Elliott, Robert P., “ Arkansas Experience with Crumb Rubber Modified Mixes Using Marshall and Strategic Highway Research Program Level I Design Methods, Transportation Research Record 1530, 1996
30. Rebela, Sekhar R. and Estakhri, Cindy K., “Laboratory Evaluation of Crumb Rubber Modified Mixtures Designed Using TxDOT Mixture Design Method”, Transportation Research Record 1515, 1995
31. Malpass, Glen A. and Khosla, N. Paul, “ Use of Ground Tire Rubber in Asphalt Concrete Pavements – A Design and Performance Evaluation”, Transportation Research Record 1515, 1995